

Microenvironmental parameters in head and neck tumours

*Patterns and quantitative analysis of vasculature, hypoxia
and proliferation*

Karien I.E.M. Wijffels

Print: Printpartners Ipskamp
Layout: Diny Helsper

ISBN: 978-90-9024123-4

© K.I.E.M. Wijffels

Microenvironmental parameters in head and neck tumours;

Patterns and quantitative analysis of vasculature, hypoxia and proliferation

Thesis Radboud University Nijmegen Medical Centre, Nijmegen.

All rights reserved. No part of this publication may be reproduced in any form or by any means, electronically, mechanically, by print or otherwise without written permission of the copyright owner.

Microenvironmental parameters in head and neck tumours

*Patterns and quantitative analysis of vasculature, hypoxia
and proliferation*

Een wetenschappelijke proeve
op het gebied van de Medische Wetenschappen

PROEFSCHRIFT

ter verkrijging van de graad van doctor
aan de Radboud Universiteit Nijmegen op gezag van de rector magnificus,
prof. mr S.C.J.J. Kortmann, volgens besluit van het College van Decanen in het
openbaar te verdedigen op
maandag 25 mei 2009
om 13.30 uur precies

door

Karien Irène Eugénie Marie Wijffels
geboren op 6 september 1970
te Nijmegen

Promotores: Prof. dr. J.H.A.M. Kaanders
Prof. dr. A.J. van der Kogel
Prof. dr. H.A.M. Marres

Manuscriptcommissie:

Prof. dr. M.A.W. Merkx (voorzitter)
Prof. dr. K. Haustermans (Leuven)
Prof. dr. P.J. Slootweg

This study was financially supported by Cancer Society Grant KUN 98-1814.

Contents

	Abbreviations	6
Chapter 1	General introduction	7
Chapter 2	Vascular architecture and hypoxic profiles in human head and neck squamous cell carcinomas. K.I.E.M. Wijffels, J.H.A.M. Kaanders, P.F.J.W. Rijken, J. Bussink, F.J.A. van den Hoogen, H.A.M. Marres, P.C.M. de Wilde, J.A. Raleigh, A.J. van der Kogel. <i>British Journal of cancer</i> 2000;83(5): 674-683	17
Chapter 3	Pimonidazole binding and tumour vascularity predict for treatment outcome in head and neck cancer. J.H.A.M. Kaanders, K.I.E.M. Wijffels, H.A.M. Marres, A.S.E. Ljungkvist, L.A.M. Pop, F.J.A. van den Hoogen, P.C.M. de Wilde, J. Bussink, J.A. Raleigh, A.J. van der Kogel <i>Cancer research</i> 2002;62(23):7066-7074	37
Chapter 4	The prognostic value of endogenous hypoxia-related markers for head and neck squamous cell carcinomas treated with ARCON. R.A. Jonathan, K.I.E.M. Wijffels, W. Peeters, P.C.M. de Wilde, H.A.M. Marres, M.A.W. Merks, E. Oosterwijk, A.J. van der Kogel, J.H.A.M. Kaanders <i>Radiother.Oncol.</i> 2006;79(3): 288-297	59
Chapter 5	Patterns of proliferation related to vasculature in human head and neck carcinomas before and after transplantation in nude mice. K.I.E.M. Wijffels, J.H.A.M. Kaanders, H.A.M. Marres, J. Bussink, H.P.W. Peters, P.F.J.W. Rijken, F.J.A. van den Hoogen, P.C.M. de Wilde, A.J. van der Kogel. <i>Int.J. Radiation Oncology Biol. Phys.</i> 2001;51(5):1346-1353	81
Chapter 6	Tumour cell proliferation under hypoxic conditions in human head and neck squamous cell carcinomas. K.I.E.M. Wijffels, H.A.M. Marres, J.P.W. Peters, P.F.J.W. Rijken, A.J. van der Kogel, J.H.A.M. Kaanders <i>Oral Oncology</i> 2008; 44(4):335-344	97
Chapter 7	Absence of hypoxia in malignant salivary gland tumours; preliminary results. K.I.E.M. Wijffels, I.J. Hoogsteen, J. Lok, P.F.J.W. Rijken, H.A.M. Marres, P.C.M. de Wilde, A.J. van der Kogel, J.H.A.M. Kaanders <i>Int.J. Radiation Oncology Biol. Phys.</i> 2008; accepted	119
Chapter 8	General discussion	137
Chapter 9	Summary / Samenvatting	147
	Dankwoord	157
	Curriculum Vitae	159

Abbreviations

ARCON:	accelerated radiotherapy with carbogen and nicotinamide
BrdUrd:	bromodeoxyuridine
CA-IX:	carbonic anhydrase IX
CD-34:	cluster of differentiation 34, endothelial marker
EF-5:	2-(2-nitro-1H-imidazole-1-yl)-N-(2,2,3,3,3-pentafluoropropyl)acetamide
EGFR:	epidermal growth factor receptor
9F1:	a rat monoclonal to mouse endothelium (CD-146)
FITC:	fluorescein isothiocyanate
FId _{pimo} :	fraction of IdUrd-labelled cells positive for pimonidazole
Glut:	glucose transporter
HF:	hypoxic fraction
HIF-1:	hypoxia-inducible factor 1
HNSCC:	head and neck squamous cell carcinoma
IdUrd:	iododeoxyuridine
LI:	labelling index
LIH:	labelling index in hypoxia
MLD:	monoclonal liquid diluent
PAL-E:	pathologie anatomie Leiden-endothel
PBS:	phosphate buffered saline
PCNA:	proliferating cell nuclear antigen
PET:	positron emission tomography
Pimonidazole:	1-[(2-hydroxy-3-piperidinyl)propyl]-2-nitroimidazole hydrochloride
PLD:	polyclonal liquid diluent
RVA:	relative vascular area
TPZ:	tirapazamine (3-amino-1,2,4-benzotriazine 1,4-dioxide)
VD:	vascular density
VHL:	von Hippel Lindau
TRITC:	tetramethyl rhodamine isothiocyanate

Chapter 1

General Introduction

Introduction

Head and neck cancers are tumours originating from the lips, oral cavity, pharynx, nose and sinuses, larynx and the salivary glands. More than 500.000 new patients with head and neck squamous cell carcinomas are diagnosed each year worldwide.¹ In the Netherlands the incidence is approximately 2300 per year and increasing with 3-4% per year. This is due to increasing effects of alcohol and nicotine abuse.^{2,3} Primary parotid gland malignant tumours are relatively rare and represent 1-3% of all head and neck malignancies.⁴ The treatment of head and neck carcinomas consists of surgical resection, radiation therapy, chemotherapy or a combination of these treatment modalities. During the past decade there has been a notable shift from surgery to organ preservation strategies. At the University Medical Centre St Radboud the number of patients with a T3-4 laryngeal carcinoma treated by a surgical resection of the larynx has decreased from 50% (1988-1991) to less than 10% (2000-2003)³ in favour of radiotherapy. The consequence of laryngectomy is a permanent stoma, loss of the natural voice and sometimes impaired swallowing function, the latter in particular if laryngectomy is followed by postoperative radiotherapy. In addition, the tracheostoma increases the risk of upper airway infections. The most important advantage of radiotherapy is that the larynx, and therefore also the natural speech, can be preserved. Good tumour control rates are obtained with primary radiotherapy, especially in early stage disease. For advanced tumours there is still a need to improve the effectiveness of radiotherapy.

There has been much work attempting to understand the causes of radiotherapy failure. Important factors determining the treatment outcome of radiotherapy are hypoxia and proliferation. Many efforts have been made to overcome these problems in order to enhance the cure rate after radiotherapy for head and neck carcinomas.

Hypoxia

The relevance of blood flow for the outcome of radiation treatments was already described by Schwartz in 1909.⁵ He noticed that skin reactions were less severe when the radium applicator was firmly pressed to the skin. It was Cramer in 1935⁶ who gave the first suggestion of an “oxygen effect”. He suggested that the radiosensitive tumours had a better blood supply and, consequently, were better oxygenated. Later, Gray et al. established the importance of tumour oxygenation for radiotherapy.⁷ Clinically relevant hypoxia is detected in approximately 50% of all solid tumours irrespective of their size and histological features.⁸ Two types of

tumour hypoxia can be distinguished: perfusion-limited and diffusion-limited hypoxia. Perfusion-limited or acute hypoxia is often transient and may be due to severe structural and functional abnormalities of the tumour microvessels.⁹ These abnormalities cause disturbances in the blood supply leading to temporal shutdown of vessels, gradients of oxygen and nutrients and even reversal of blood flow.⁹⁻¹¹ Hypoxia can also be caused by an increase in diffusion distances, resulting in diffusion-limited hypoxia, leaving cells chronically deprived of oxygen and other nutrients.^{9,12} In most tumours, both types co-exist and contribute to greater or lesser extent.

Several methods have been developed over the years in an attempt to visualize and quantify hypoxia within a tumour. Initial evidence for hypoxia in human tumours came from work measuring oxygen status using polarographic electrodes.¹³ Unfortunately, the use of this invasive technique is limited to accessible tumours and careful needle positioning.

Exogenous and endogenous hypoxia markers detectable by immunohistochemistry require no additional intervention beyond the initial pre-treatment biopsy and may be suitable for widespread clinical use. Clinically relevant exogenous markers are the 2-nitroimidazoles pimonidazole and EF5 which require intravenous administration before tissue sampling.^{14,15} In viable cells with oxygen partial pressures ≤ 10 mm Hg the 2-nitroimidazoles are reductively activated and form protein adducts which can then be visualized by immunohistochemistry. Clinical experience with these compounds exists in head and neck carcinomas¹⁶, cervical cancer¹⁴, bladder cancer¹⁷, prostate cancer¹⁸ and soft tissue sarcoma.¹⁹ Endogenous hypoxia-related markers include Hypoxia Inducible Factor-1 α (HIF-1 α), Carbonic Anhydrase IX (CA-IX) and the glucose transporters (gluts).

The transcription factor Hypoxia Inducible Factor consists of several subunits that include HIF-1 α , HIF-2 α and HIF-3 α . Of the three HIF- α subunits HIF-1 α functions as master regulator of oxygen homeostasis, HIF-2 α is predominantly expressed in endothelial cells and iPAS, a variant of HIF-3 α , is expressed in the cornea, cerebellum and cerebrum.²⁰

Hypoxia leads to inactivation of the von Hippel-Lindau (VHL) gene which subsequently leads to stabilisation of the HIF-1 α subunits and activation.²¹ Once activated, HIF-1 α plays an important role in tumour growth, angiogenesis, pH regulation, cell proliferation and glucose metabolism.^{20,22-24}

CA-IX is up-regulated by HIF-1 α in order to control acid-base homeostasis. Hypoxia increases glycolysis and lactate production, resulting in acidosis. CA-IX catalyzes the hydration of extracellular carbon dioxide to carbonic acid thereby maintaining a stable intracellular pH. Most studies, except in renal cancer show

that CA-IX upregulation is associated with tumour aggressiveness.²⁵ *In vitro* studies indicate that CA-IX is upregulated from oxygen partial pressures of ≤ 20 mm Hg and lower.²⁶

The glucose transporters are also controlled via the HIF-1 pathway. They mediate glucose uptake and facilitate anaerobic glycolysis. Glut-1 and Glut-3 have been examined in many tumour types including head and neck carcinomas. Glut-1 expression is mainly found at a distance from perfused vessels, corresponding with areas of diffusion-limited hypoxia.²²

Non-invasive methods for detecting hypoxia include positron emission tomography (PET) and dynamic contrast-enhanced magnetic resonance imaging (DCE-MRI). Important advantages of these methods are that they visualize the whole tumour and because of their repetitive capacity they are ideally suited for treatment monitoring and early response assessment. PET tracers for hypoxia include [18F]-misonidazole (¹⁸F-MISO), [18F]-azomycin arabinoside (¹⁸F-AZA), ⁶⁰Cu (II)-diacetyl-bis(*N*⁴-methylthiosemicarbazone) (⁶⁰Cu-ATSM), [18F]-fluoro-erythronitroimidazole (¹⁸FETNIM), and [18F]-2-(2-nitroimidazol-1-yl)-N-(3,3,3-trifluoropropyl)-acetamide (¹⁸F-EF3). These radiopharmaceuticals differ in their kinetics and binding characteristics and it is not yet clear which is to be preferred for clinical use. Rischin et al. compared ¹⁸F-MISO-PET and ¹⁸F-AZA-PET in patients with head and neck squamous cell carcinomas and found a similar distribution of tumour hypoxia for both tracers. However, less background tracer accumulation occurred with ¹⁸F-AZA-PET.²⁷

DCE-MRI is used both experimentally and clinically to monitor the functionality of the tumour vasculature after administration of the contrast agent Gadolinium-DTPA. Due to the high spatial resolution of MRI heterogeneities in blood flow, vascular volume and permeability of blood vessels within a tumour can be detected. Other magnetic resonance based methods include: blood oxygen level-dependent magnetic resonance imaging (BOLD MRI); ¹⁹F MRI using perfluorocarbon probes; electron paramagnetic resonance imaging (EPRI) and proton-electron double resonance imaging (PEDRI). Finally, optical methods as near-infrared spectroscopy (NIRS) and phosphorescence imaging are used. The latter were reviewed with all their advantages and disadvantages by Vikram et al.²⁸

Proliferation

A second important cause for radiation treatment failure is cellular repopulation. Shortening the overall radiotherapy treatment time (accelerated fractionation) can counteract this phenomenon and improve outcome.²⁹

Different markers have been used for assessment of proliferation. These include the endogenous markers Ki-67, proliferating nuclear antigen (PCNA) and members of the cyclin group. Clinically available exogenous markers are the thymidine analogues bromodeoxyuridine (BrdUrd) and iododeoxyuridine (IdUrd) which need to be administered intravenously. The latter have a short half-life and are rapidly incorporated in the DNA, thus being specific S-phase markers.³⁰

Although not proliferation specific, EGFR signalling is an important stimulator of cell growth as well as other biological processes. EGFR overexpression is common in head and neck squamous cell carcinomas and is associated with poor locoregional control.³¹ Two clinical studies in head and neck cancer demonstrated improved locoregional control rates with a schedule of accelerated radiotherapy in tumours with high EGFR-expression levels but not in tumours with low EGFR-expression.^{32,33} This strongly suggests that the EGFR-signalling pathway controls the proliferative response of tumours to fractionated radiotherapy.³² Additionally, the use of the anti-EGFR monoclonal antibody cetuximab in combination with radiotherapy has been shown to be superior to radiation alone.³⁴

Outline of the thesis

The purpose of this investigation was to characterize human head and neck cancers in terms of their proliferative activity and oxygenation status using endogenous and exogenous immunohistochemical markers. A second aim was to analyze microenvironmental patterns of proliferation and hypoxia in relation to each other and to the tumour vasculature. The ultimate aim was to explore the potential of this immunohistochemistry-based characterization as a predictive tool that allows selection of patients for treatment strategies that counteract proliferation and hypoxic radioresistance.

The biopsy material used for this investigation was obtained from patients with stage II-IV squamous cell carcinomas of the head and neck that were treated with primary radiotherapy. Part of these patients were treated by a new strategy that combines Accelerated fractionated Radiotherapy with administration of CarbOgen and Nicotinamide (ARCON). Accelerated radiotherapy counteracts radioresistance by tumour cell repopulation. Carbogen is a gas mixture composed of oxygen 95-98% and carbon dioxide 5-2% and reduces diffusion limited hypoxia whereas nicotinamide, a derivative of vitamin B3, reduces the intermittent closure

of blood vessels and thus acute hypoxia. We aimed to deliver proof of principle that microenvironmental profiling based on immunohistochemical markers can predict responsiveness to ARCON. In addition, a small cohort of patients who underwent surgery for a salivary gland tumour was studied as there was no previous knowledge on the clinical relevance of hypoxia in this tumour type.

Chapter 2 describes the result of hypoxia and vasculature staining in 21 head and neck squamous cell carcinomas. We use the exogenous bioreductive marker pimonidazole which has been shown to be a robust marker of hypoxia. We demonstrate that we are able to visualize and quantify this marker noticing large intra- and intertumour variations. Also, we demonstrate that different architectural patterns of hypoxia exist with different spatial relationships with tumour vasculature. We make a first attempt to categorize tumours based on their hypoxic profile.

In *chapter 3* we compare outcome in patients treated with radiotherapy alone against patients treated with ARCON and associate this with measurements of hypoxic fraction and vascular density in the respective biopsies. Forty-three biopsies of head and neck carcinomas are stained for hypoxia by pimonidazole and CA-IX and for blood vessels. Staining patterns of pimonidazole and CA-IX are compared and co-localization is quantified. Hypoxic fraction, vascular density and relative vascular area are calculated and related to locoregional control and disease free survival.

In *chapter 4*, we investigate the prognostic value of the endogenous hypoxia-related markers CA-IX, Glut-1 and Glut-3 in biopsy material of 58 patients with head and neck carcinomas treated with ARCON. We study the expression patterns of these proteins using semi-quantitative scoring and relate this with clinical characteristics and outcome parameters such as locoregional control, freedom of distant metastasis and overall survival.

Proliferation is another important biologic determinant for radiation outcome and may be of special interest if examined in conjunction with tumour hypoxia. In *chapter 5* we study proliferation patterns in 50 head and neck tumours before and after transplantation in nude mice. The purpose is to quantitatively categorize human tumours according to proliferation patterns. A second aim is to examine whether these characteristics are retained after xeno-transplantation, an issue that is relevant when these tumour lines are used for preclinical studies. We stain both human tumour samples and xeno-transplanted tumours for the endogenous proliferation marker Ki-67 and for vasculature. We categorize the tumours according to distinct patterns of proliferation and quantify the number of vascular structures and proliferation and compare results of pre- and post-transplantation

samples. We also investigate if these parameters are predictive for the probability of growth after xeno-transplantation.

As both hypoxia and proliferation are relevant for outcome after radiotherapy, there might be a subpopulation of tumour cells with particular relevance for radiotherapy responsiveness, i.e. cells that retain proliferative capacity under hypoxic conditions. In *chapter 6* we investigate the magnitude of that cell population by dual staining for pimonidazole and the exogenous proliferation marker IdUrd. Thirty-nine biopsies of head and neck cancer patients are examined for co-localisation of these markers and associations with outcome parameters are sought.

Finally, *chapter 7* describes the results of multiple immunohistochemical analysis for hypoxia, proliferation and vasculature in salivary gland carcinomas. To investigate the potential relevance of hypoxia in this tumour type we perform immunohistochemistry for a panel of hypoxia-related markers including pimonidazole, CA-IX, Glut-1, Glut-3 and HIF1- α in 8 salivary gland carcinomas. In addition, staining is done for IdUrd and the epidermal growth factor receptor (EGFR).

References

1. Le Tourneau C, Faivre S, Siu LL. Molecular targeted therapy of head and neck cancer: review and clinical development challenges. *Eur J Cancer* 2007;43:2457-2466.
2. [www.ikcnet.nl/>>nederlandse kankerregistratie](http://www.ikcnet.nl/>>nederlandse_kankerregistratie).
3. www.ru.nl/oraties Marres.
4. Kane WJ, McCaffrey TV, Olsen KD, *et al.* Primary parotid malignancies. A clinical and pathologic review. *Arch Otolaryngol Head Neck Surg* 1991;117:307-315.
5. Schwartz G. Über desensibilisierung gegen röntgen und radiumstrahlen. *Munchener medizinischen wochenschrift* 1909;24:1-2.
6. Cramer W. The therapeutic action of radium on spontaneous mammary carcinomata of the mouse. *Annual report of the imperial cancer research fund report* 1935;11:127-146.
7. Gray LH, Conger AD, Ebert M, *et al.* The concentration of oxygen dissolved in tissues at the time of irradiation as a factor in radiotherapy. *Br J Radiol* 1953;26:638-648.
8. Vaupel P, Mayer A, Hockel M. Tumor hypoxia and malignant progression. *Methods Enzymol* 2004;381:335-354.
9. Vaupel P, Thews O, Hoeckel M. Treatment resistance of solid tumors: role of hypoxia and anemia. *Med Oncol* 2001;18:243-259.
10. Vaupel P, Kallinowski F, Okunieff P. Blood flow, oxygen and nutrient supply, and metabolic microenvironment of human tumors: a review. *Cancer Res* 1989;49:6449-6465.
11. Dewhirst MW, Ong ET, Braun RD, *et al.* Quantification of longitudinal tissue pO₂ gradients in window chamber tumours: impact on tumour hypoxia. *Br J Cancer* 1999;79:1717-1722.
12. Harris AL. Hypoxia--a key regulatory factor in tumour growth. *Nat Rev Cancer* 2002;2:38-47.
13. Gatenby RA, Kessler HB, Rosenblum JS, *et al.* Oxygen distribution in squamous cell carcinoma metastases and its relationship to outcome of radiation therapy. *Int J Radiat Oncol Biol Phys* 1988;14:831-838.
14. Evans SM, Hahn S, Pook DR, *et al.* Detection of hypoxia in human squamous cell carcinoma by EF5 binding. *Cancer Res* 2000;60:2018-2024.
15. Raleigh JA, Calkins-Adams DP, Rinker LH, *et al.* Hypoxia and vascular endothelial growth factor expression in human squamous cell carcinomas using pimonidazole as a hypoxia marker. *Cancer Res* 1998;58:3765-3768.
16. Kaanders JH, Wijffels KI, Marres HA, *et al.* Pimonidazole binding and tumor vascularity predict for treatment outcome in head and neck cancer. *Cancer Res* 2002;62:7066-7074.
17. Hoskin PJ, Sibtain A, Daley FM, *et al.* The immunohistochemical assessment of hypoxia, vascularity and proliferation in bladder carcinoma. *Radiother Oncol* 2004;72:159-168.
18. Carnell DM, Smith RE, Daley FM, *et al.* An immunohistochemical assessment of hypoxia in prostate carcinoma using pimonidazole: implications for radioresistance. *Int J Radiat Oncol Biol Phys* 2006;65:91-99.
19. Evans SM, Fraker D, Hahn SM, *et al.* EF5 binding and clinical outcome in human soft tissue sarcomas. *Int J Radiat Oncol Biol Phys* 2006;64:922-927.
20. Liao D, Johnson RS. Hypoxia: a key regulator of angiogenesis in cancer. *Cancer Metastasis Rev* 2007;26:281-290.
21. Maxwell PH, Wiesener MS, Chang GW, *et al.* The tumour suppressor protein VHL targets hypoxia-inducible factors for oxygen-dependent proteolysis. *Nature* 1999;399:271-275.
22. Hoogsteen IJ, Marres HA, Bussink J, *et al.* Tumor microenvironment in head and neck squamous cell carcinomas: predictive value and clinical relevance of hypoxic markers. A review. *Head Neck* 2007;29:591-604.
23. Moeller BJ, Richardson RA, Dewhirst MW. Hypoxia and radiotherapy: opportunities for improved outcomes in cancer treatment. *Cancer Metastasis Rev* 2007;26:241-248.
24. Kim JW, Gao P, Dang CV. Effects of hypoxia on tumor metabolism. *Cancer Metastasis Rev* 2007;26:291-298.
25. Vaupel P, Mayer A. Hypoxia in cancer: significance and impact on clinical outcome. *Cancer Metastasis Rev* 2007;26:225-239.
26. Lal A, Peters H, St Croix B, *et al.* Transcriptional response to hypoxia in human tumors. *J Natl Cancer Inst* 2001;93:1337-1343.
27. Rischin D, Fisher R, Peters L, *et al.* Hypoxia in head and neck cancer: studies with hypoxic positron emission tomography imaging and hypoxic cytotoxins. *Int J Radiat Oncol Biol Phys* 2007;69:S61-63.
28. Vikram DS, Zweier JL, Kuppusamy P. Methods for noninvasive imaging of tissue hypoxia. *Antioxid Redox Signal* 2007;9:1745-1756.

29. Bourhis J, Overgaard J, Audry H, *et al.* Hyperfractionated or accelerated radiotherapy in head and neck cancer: a meta-analysis. *Lancet* 2006;368:843-854.
30. Begg AC, Haustermans K, Hart AA, *et al.* The value of pretreatment cell kinetic parameters as predictors for radiotherapy outcome in head and neck cancer: a multicenter analysis. *Radiother Oncol* 1999;50:13-23.
31. Ang KK, Berkey BA, Tu X, *et al.* Impact of epidermal growth factor receptor expression on survival and pattern of relapse in patients with advanced head and neck carcinoma. *Cancer Res* 2002;62:7350-7356.
32. Bentzen SM, Atasoy BM, Daley FM, *et al.* Epidermal growth factor receptor expression in pretreatment biopsies from head and neck squamous cell carcinoma as a predictive factor for a benefit from accelerated radiation therapy in a randomized controlled trial. *J Clin Oncol* 2005;23:5560-5567.
33. Eriksen JG, Steiniche T, Overgaard J. The influence of epidermal growth factor receptor and tumor differentiation on the response to accelerated radiotherapy of squamous cell carcinomas of the head and neck in the randomized DAHANCA 6 and 7 study. *Radiother Oncol* 2005;74:93-100.
34. Bonner JA, Harari PM, Giralt J, *et al.* Radiotherapy plus cetuximab for squamous-cell carcinoma of the head and neck. *N Engl J Med* 2006;354:567-578.

Chapter 2

Vascular architecture and hypoxic profiles in human head and neck squamous cell carcinomas

K.I.E.M. Wijffels

J.H.A.M. Kaanders

P.F.J.W. Rijken

J. Bussink

F.J.A. van den Hoogen

H.A.M. Marres

P.C.M. de Wilde

J.A. Raleigh

A.J. van der Kogel

Abstract

Tumour oxygenation and vasculature are determinants for radiation treatment outcome and prognosis in patients with squamous cell carcinomas of the head and neck. In this study we visualized and quantified these factors which may provide a predictive tool for new treatments.

Twenty-one patients with stage III-IV squamous cell carcinomas of the head and neck were intravenously injected with pimonidazole, a bioreductive hypoxic marker. Tumour biopsies were taken 2 h later. Frozen tissue sections were stained for vessels and hypoxia by fluorescent immunohistochemistry. Twenty-two sections of biopsies of different head and neck sites were scanned and analyzed with a computerized image analysis system.

The hypoxic fractions varied from 0.02 to 0.29 and were independent from T- and N-classification, localization and differentiation grade. No significant correlation between hypoxic fraction and vascular density was observed. As a first attempt to categorize tumours based on their hypoxic profile, three different hypoxia patterns are described. The first category comprised tumours with large hypoxic, but viable, areas at distances even greater than 200 μm from the vessels. The second category showed a typical band-like distribution of hypoxia at an intermediate distance (50-200 μm) from the vessels with necrosis at greater distances. The third category demonstrated hypoxia already within 50 μm from the vessels, suggestive for acute hypoxia.

This method of multiparameter analysis proved to be clinically feasible. The information on architectural patterns and the differences that exist between tumours can improve our understanding of the tumour micro-environment and may in the future be of assistance with the selection of (oxygenation modifying) treatment strategies.

Introduction

The relevance of blood flow for the outcome of radiation treatments was already described by Schwartz in 1909.¹ He noticed that skin reactions were less severe when the radium applicator was firmly pressed to the skin. It was Cramer in 1935² who gave the first suggestion of an “oxygen effect”. He found that mouse mammary tumours with a well developed stroma and vascular network were more radiosensitive than tumours with a more delicate stromal component. He suggested that the radiosensitive tumours had a better blood supply and, consequently, were better oxygenated. Later, Gray et al.³ established the importance of tumour oxygenation for radiotherapy.

The tumour micro-environment is a key factor in tumour biology and has great impact on clinical radiotherapy as well as other cancer treatments. Single parameters such as polarographic pO₂ measurements and microvascular density have been demonstrated to be prognostic indicators in a variety of tumour types, including carcinomas of the head and neck.⁴⁻⁹ However, considering the complexity of the micro-environmental system, it is unlikely that a single parameter can reliably predict treatment outcome on an individual basis. Multiple parameter analysis will be necessary to acquire a better understanding of the tumour micro-environment and to obtain a “predictive profile” which can guide the clinician in the selection of patients for new treatment strategies.

A computerized image analysis system for multi-parameter analysis has been developed in our institute.¹⁰ The method involves computer controlled microscopic scanning of immunohistochemically stained tissue sections. It allows quantitative and simultaneous analysis of vascular parameters, oxygenation status and proliferation parameters. We have recently published our experience with this method in xenografted human tumours.^{11,12}

We now apply this method also to tumour biopsies from patients with squamous cell carcinomas of the head and neck. Before a biopsy was taken, the patients were injected with Hypoxyprobe-1 (pimonidazole hydrochloride) as a hypoxia marker. Pimonidazole can easily be dissolved in saline, has a low toxicity, and an efficient tumour uptake. So far pimonidazole has proven to be an effective hypoxia marker for human tumours of the cervix and head and neck.¹³⁻¹⁵

In the present study we report the results of the analysis of biopsy material from 21 patients with squamous cell carcinoma of the head and neck.

Materials and Methods

Patients

Patients with primary laryngeal, oropharyngeal (stage III-IV) or hypopharyngeal (stage II-IV) squamous cell carcinomas were entered. Accrual was restricted to patients who were also eligible for our ongoing phase II ARCON-study (Accelerated Radiotherapy with Carbogen and Nicotinamide).¹⁶ Inclusion criteria were: age over 18 years, WHO performance status of 0-2, no severe heart or lung disease, no severe liver or kidney dysfunction, no severe stridor, no distant metastases, and written informed consent. In the period from May 1998 to December 1998, 21 patients were included. Approval from the local ethics committee was obtained.

Markers of hypoxia and proliferation

As hypoxia marker we used pimonidazole hydrochloride (Hypoxyprobe-1, Natural Pharmacia International Inc.). Pimonidazole is a bio-reductive chemical probe with an immuno-recognizable side chain. The addition of the first electron in bio-reductive activation is reversibly inhibited by oxygen with a half maximal pO_2 of inhibition of 3 mm Hg and almost complete inhibition at about 10 mm Hg.¹⁷ Pimonidazole (0.5g/m^2) was dissolved in 100cc NaCl 0.9% and was administered intravenously over 20 minutes, two hours before biopsy (range 1h35 min - 4h05 min, median 1h59 min). A maximum dose of one gram was given to patients with a body surface $> 2\text{ m}^2$. After biopsy the tissue was directly frozen in liquid nitrogen. Sections of $5\text{ }\mu\text{m}$ were cut and mounted on poly-L-lysine coated slides and stored at -80°C until staining.

Immunohistochemical staining

Prior to the staining procedure, sections were fixed in acetone of 4°C for 10 min. Then the sections were rehydrated in phosphate buffered saline (PBS). Next, sections were incubated overnight at 4°C with both anti-pimonidazole (rabbit polyclonal)¹⁸ diluted 1:200 in PBS and PAL-E diluted 1:5 in PBS (Department of Pathology, University Hospital Nijmegen, The Netherlands). The monoclonal antibody PAL-E is a marker for human endothelium, especially useful in frozen tissue sections.¹⁹ After rinsing three times in PBS the staining procedure was followed by a pooled incubation for 1 h at room temperature with fluorescein isothiocyanate (FITC)-conjugated donkey anti-rabbit antibody (Jackson Immuno Research Laboratories, West Grove, PA, USA) 1:100 in PBS for the hypoxia signal, combined with tetramethyl rhodamine isothiocyanate (TRITC)-conjugated goat anti-mouse antibody (Jackson Immuno Research Laboratories, West Grove,

PA, USA) diluted 1:100 in PBS to visualize the vessels. After rinsing in PBS for three times the sections had another pooled incubation for 1 h with the same FITC-conjugated antibody, but now combined with TRITC-conjugated donkey anti-goat antibody (Jackson Immuno Research Laboratories) diluted 1:100 in PBS to amplify the blood vessel signal. Slides were then rinsed and mounted in PBS for scanning of the hypoxia and vessel signals.

Scanning of tumour sections and image processing

For quantitative analysis, the slides were scanned by a computerized image processing system using a high-resolution intensified solid-state video camera on a fluorescence microscope (Zeiss Axioskop). The fluorescence signals were recorded by the camera and subsequently digitized to a binary image on a Macintosh computer. For the vessels (TRITC-signal, 510-560 nm excitation) a 590 nm emission filter was used and for hypoxia (FITC-signal, 450-490 nm excitation) a 520 nm emission filter was used. In order to move a tissue section automatically a motorized scanning stage, coupled to a stage controller, was interfaced with the computer. Each tumour section was scanned two times at 100x magnification. In the first scan only the vascular structures were detected, in the second scan the hypoxic marker was detected. Each scan consisted of 16, 25 or 36 fields (4x4, 5x5 or 6x6, field size 1.22 mm²) depending on the size of the biopsy. Processing all fields of one scanning procedure resulted in a composite binary image. After the scanning procedure the two composite binary images, one showing vascular structures and the other showing hypoxic areas, were superimposed. A detailed description of the scanning method has been given by Rijken et al.¹⁰ With the use of a haematoxylin-eosin staining of a consecutive section the tumour area was delineated. This area was used as a mask in further image analysis excluding non-tumour tissue and large necrotic areas from the analysis. Necrosis can produce an aspecific red stain in the fluorescent images. It is therefore important that these areas be excluded such that they do not disturb the analysis of vascular parameters. Small necrotic areas were not excluded because this could cause loss of information of the directly surrounding viable tissue. The delineation of the tumour area was supervised by a pathologist (P.C.M. de Wilde).

Analysis of hypoxic and vascular parameters

The vascular density was calculated as the number of vascular structures per mm². The relative vascular volume was defined as the PAL-E positive surface divided by the total tumour surface. The hypoxic fraction was defined as the pimonidazole positive surface divided by the total tumour surface. These

parameters were calculated for the complete tumour surface, but also in arbitrary subareas of 0.3 mm² for analysis of the intra-tumour variability.

In order to quantitate the distribution of hypoxia in relation to the vasculature, zones were chosen arbitrarily at increasing distance from the surface of the nearest vessel (0-50 µm, 50-100 µm, 100-150 µm, 150-200 µm, 200-250 µm, and >250 µm). The hypoxic fraction in a zone was calculated as the pimonidazole-stained surface in a zone divided by the tumour surface in that zone.

Statistics

Mean values were compared by the student-t-test. Correlations between various parameters were tested by linear least-squares regression analysis. The statistical analyses were done on a Macintosh computer using Statistica 4.0 software.

Results

Patients

Twenty-three patients entered the study. Two biopsies were not included in the analysis, one biopsy contained no tumour tissue and one patient had a mucoepidermoid carcinoma. Thus biopsies from 21 patients with confirmed squamous cell carcinoma were the subject of this study. The median age of the patients was 58 years (range 47-75). There were 17 men and 4 women. Tumours were localized in the oropharynx (2), in the larynx (9) and in the hypopharynx (9). One patient suffered from two primary tumours, an oropharyngeal and a hypopharyngeal tumour which were both biopsied. Thirteen tumours were moderately differentiated and nine were poorly differentiated. Classification of the tumours according to the TNM staging system (as defined by the UICC, 1997) is shown in Table 1.

None of the patients had any adverse reaction to the pimonidazole administration.

Table 1. TNM-classification of the 22 biopsied tumours

	N0	N1	N2	N3	Total
T1	-	1	1	-	2
T2	1	1	3 *	2	7
T3	2	1	5 *	-	8
T4	-	2	3	-	5
Total	3	5	12	2	22

* Biopsies from one patient with two primary tumours.

Hypoxia and vessel staining

The hypoxic staining gave a reproducible and bright green fluorescent signal in all tissue sections. At increasing distance from the vessels an increasing intensity of the hypoxic staining was found. There was no or very little background staining (Figure 1). At the edges of some tumour sections we observed a strong staining. This so called “edge-effect” was sometimes substantial and, if included in the analysis, could influence the outcome significantly. Three different causative phenomena were identified. First, freezing artefacts occur sometimes at the tissue edges which are caused by the formation of ice crystals with subsequent tissue damage. These freezing artefacts are known to give non-specific staining with immunohistochemical techniques. Secondly, the edges of tissue sections can become pleated while being cut, which enhances the background staining. The third reason is the presence of normal epithelium covering the surface of a biopsy. The differentiated squamous layers can demonstrate considerable hypoxia. The latter is obviously not an artefact but was excluded from the analysis as non-tumour tissue. In the majority of the biopsies no or very little normal epithelium was identified.

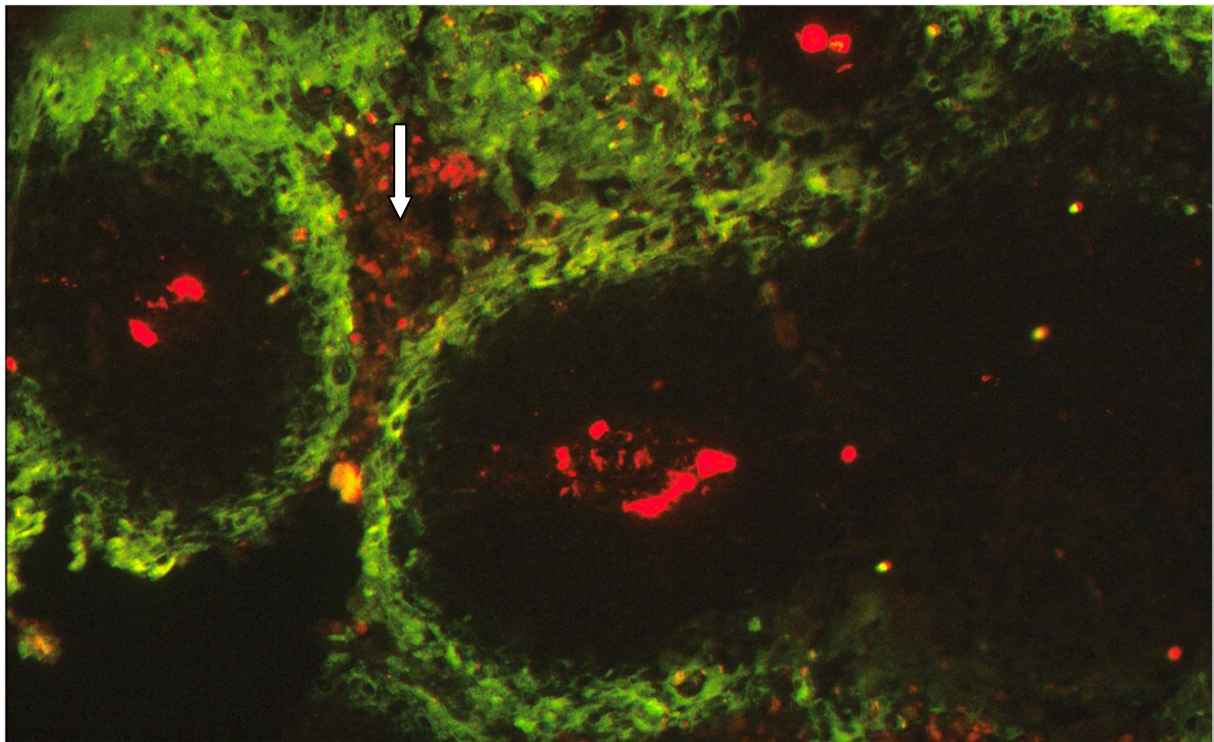


Figure 1. Fluorescence microscopic image of a tumour section (200x magnification) after staining for hypoxia with pimonidazole (green) and vessels with PAL-E (red). Typical tumour cords can be recognized with well oxygenated areas directly adjacent to vessels and hypoxia at greater distance. At even greater distances there is necrosis (white arrow, confirmed in H&E stain).

The red fluorescent vessel staining gave a strong signal in all tumours with hardly any background staining. Some aspecific staining was observed in areas of necrosis, which also can contain remnants of bloodvessels (Figure 1).

Staining patterns

Based on the vascular architecture and the pattern of hypoxic staining we have tried to categorize the tumours into three groups. Category A (N=8) showed increasing amounts of hypoxia with increasing distance from the vessels and large areas of hypoxia at distances greater than 200 μm . They had almost no hypoxia close to the vessels (Figure 2a). Category B (N=4) tumours had a typical band-like pattern of hypoxia at shorter distances from the vessels (between 50 and 200 μm) (Figure 2b). In this category of tumours we found small areas of necrosis at distances > 150-200 μm . This was confirmed in the haematoxylin-eosin staining but these areas were too small to be excluded from the analysis. Category C demonstrated a more diffuse hypoxic pattern with significant amounts of hypoxia in the zones closest to the vessels. The relation to the vasculature was less obvious in this category (N=4) (Figure 2c). Even tumours with similar hypoxic fractions could vary in their hypoxic patterns. Six tumours had small hypoxic fractions of less than 5% and, therefore, could not be properly classified (Figure 2d).

Quantitative analysis

Vascular parameters

The vascular density (VD) of the 22 tumours ranged from 11 mm^{-2} to 67 mm^{-2} with a median value of 42 mm^{-2} . The vascular density was also calculated in arbitrary subareas of 0.3 mm^{-2} . The highest values of these subareas were a factor of 1.5 to 6 higher than the overall values of the various tumours.

The relative vascular volume varied from 1.9 % to 9.0 %, with a median of 3.8 %.

There was no correlation between the vascular parameters and tumour site, T- and N-stage or histological grade.

Hypoxia

Figure 3 presents the hypoxic fractions of the tumours as a cumulative plot. The lowest and highest values were 0.02 and 0.29, respectively, with a median of 0.09. There was an indication that pharyngeal tumours had a higher hypoxic fraction (median 0.10) as compared to the larynx tumours (median 0.05). However, these differences were not statistically significant ($p=0.21$, t-test). There was also no correlation between T- and N-stage or histological grade and the

hypoxic fraction. Hypoxic fractions were also calculated for the subareas in each tumour and cumulative plots were constructed. Figure 4 shows these plots for the three tumours of which the corresponding images are shown in figure 2. The steepest curve with the lowest median value ($=0.03$) corresponds with the tumour that demonstrates hypoxia mainly at large distances from vessels (category A). The plot for the tumour with the more diffuse hypoxic pattern (category C) is less steep with a much higher median value ($=0.26$).

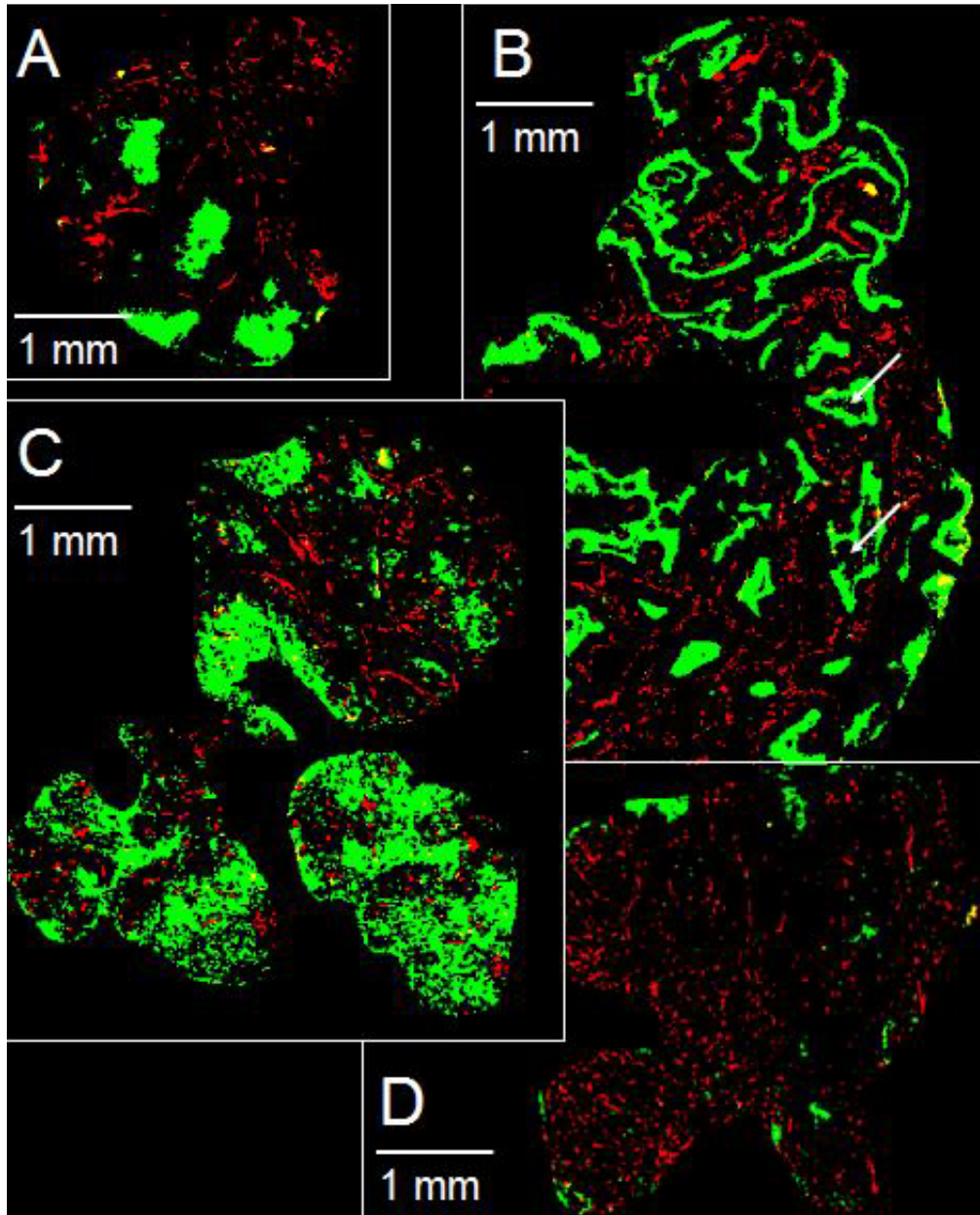


Figure 2. Composite binary images of four different tumours; sccNij50 (A), sccNij70 (B), sccNij49 (C) and sccNij69 (D) showing hypoxia (green) and vessels (red). The tumours represent examples of different hypoxic patterns. Large necrotic areas have been excluded from these binary images. Only in tumour sccNij70 there were areas of necrosis that were too small to be excluded (arrows).

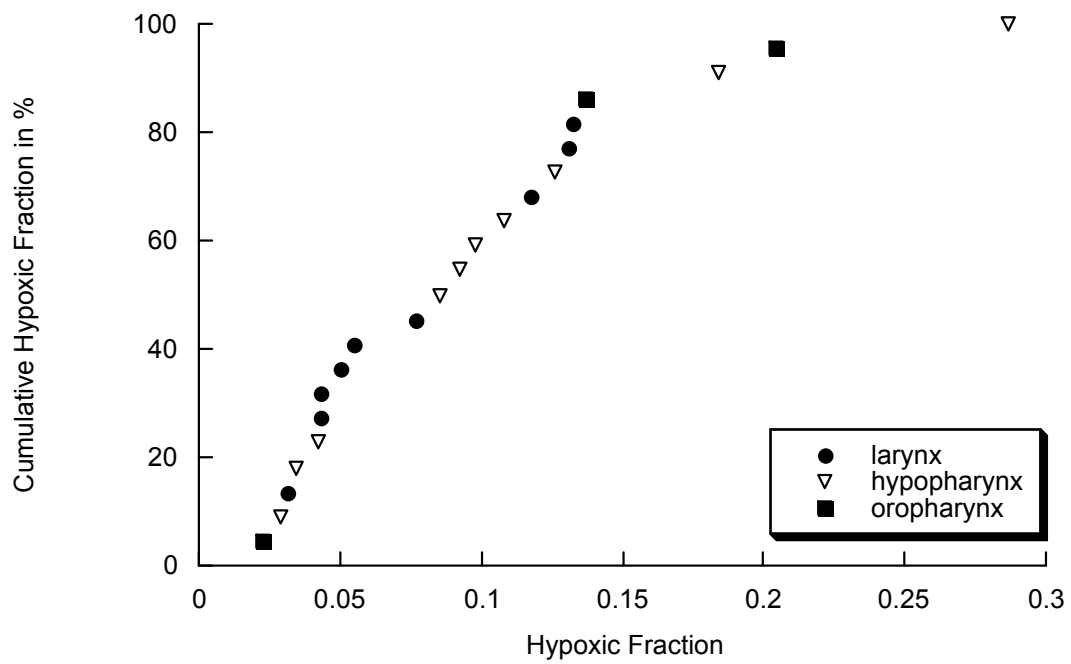


Figure 3. Cumulative plot of hypoxic fractions of 22 tumours originating in three head and neck sites.

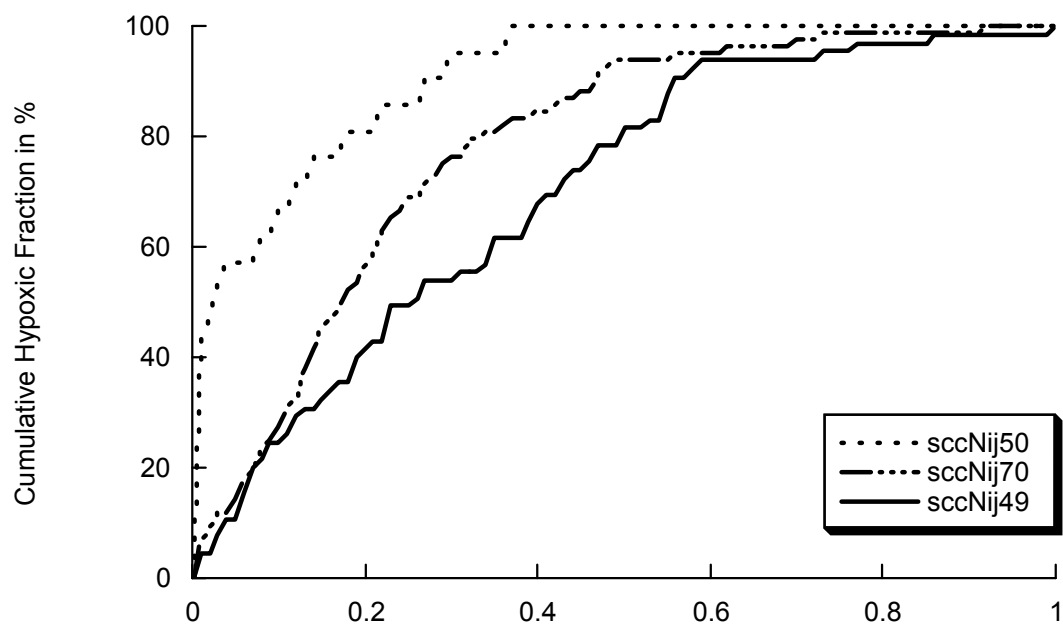


Figure 4. Cumulative plot of the hypoxic fractions of arbitrary subareas in three tumours (sccNij50, sccNij70, sccNij49).

Relation between vasculature and hypoxia

We sought for further correlations between vascular density, relative vascular volume, and hypoxic fraction. There was a significant correlation between relative vascular volume and vascular density ($r=0.56$, $p<0.01$). There was only a weak and non-significant inverse correlation between vascular density and hypoxic fraction ($r=-0.34$, $p=0.13$) (Figure 5).

In all tumours there was an increase of hypoxia with increasing distance from the vessels. As an example, figure 6 shows how the arbitrary zones chosen at increasing distances from the vessels are projected over the binary image of vessels and hypoxia in tumour sccNij50. Figure 7 shows the relative distribution of hypoxia over these zones for the tumours of figure 2A-C.

Discussion

Methods

With the quantitative analysis method used here we successfully visualized and quantitated multiple parameters while maintaining the tissue architecture.¹⁰⁻¹² To obtain a strong signal with lower background staining we used fluorescent labelled antibodies on frozen sections. A disadvantage of the immunohistochemical staining is that only specific structures are stained, i.e. the complete tissue architecture is not visualized. Therefore we used haematoxylin-eosin staining of consecutive sections to contour the tumour area, excluding non-tumour tissue and areas of necrosis. Both the hypoxia and the vessel stainings gave strong signals with very low background staining in all slides. Edge artefacts were easily recognized with the aid of the haematoxylin-eosin stained sections and were excluded from the analysis.

Vascular parameters

There is an abundance of literature on morphometric vascular tumour parameters, in particular microvascular density, and their prognostic value. For squamous cell carcinomas of the head and neck, as for other tumour types such as carcinoma of the breast, conflicting results have been reported. Some investigators found a correlation between vascular density and metastatic potential²⁰⁻²³, whereas others did not.^{5,6,24-28} In this study no correlation was found between vascular density and N-stage, even when the 75th percentile value or the highest value of the subareas was used. The latter analysis was done to approximate the so called “hot spot counting” method which is often used by others.^{20,22-24,27}

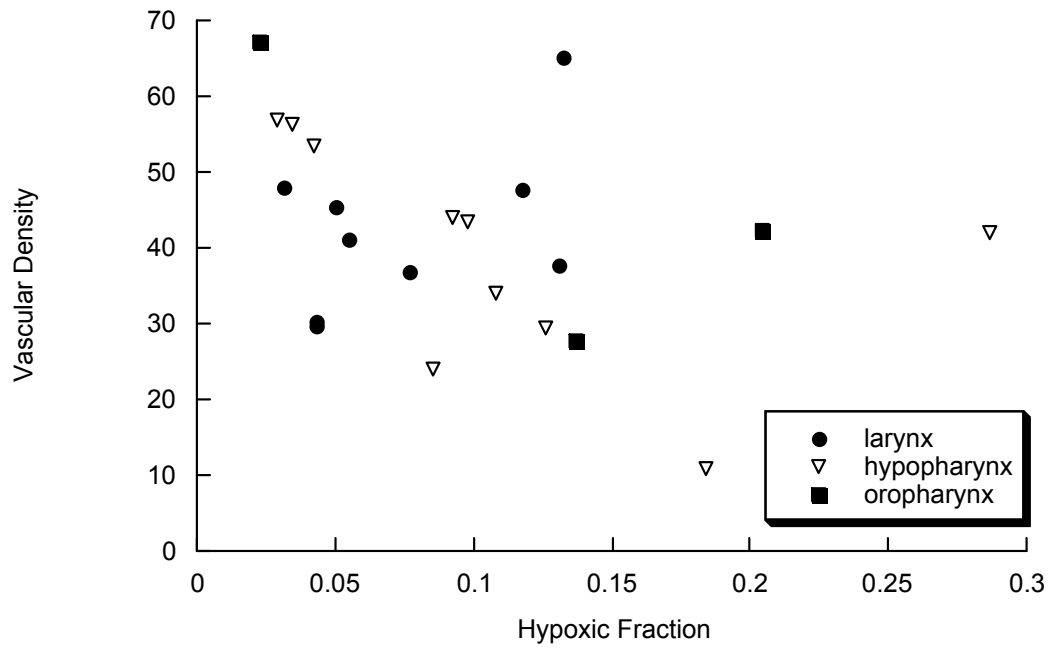


Figure 5. Vascular density (mm⁻²) versus hypoxic fraction in 22 tumours of three head and neck sites.

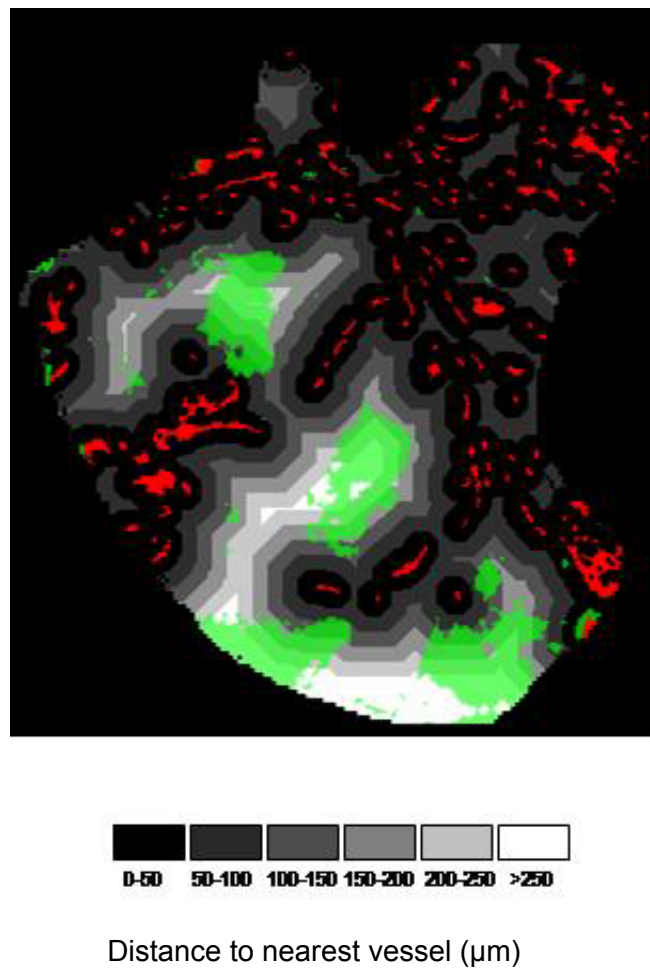


Figure 6. Binary image of vessels (red) and hypoxia (green) in tumour sccNij50 with the zones at increasing distances from the vessels superimposed.

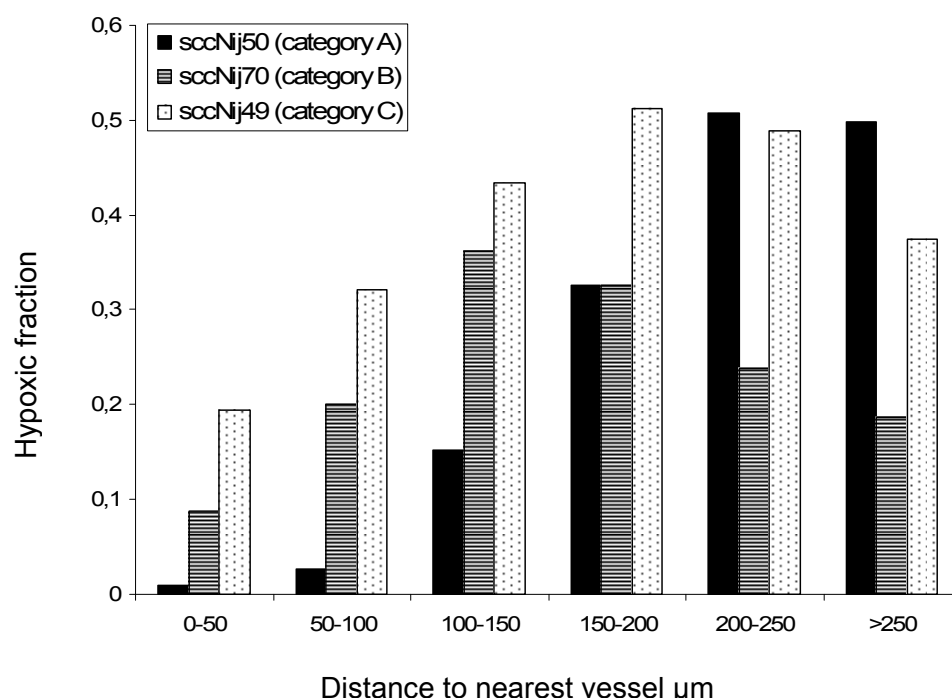


Figure 7. Relative hypoxic fractions in 50 µm zones at increasing distance from vessels. Example of three tumours (sccNij50, sccNij70, sccNij49).

Two investigators found an association between vascular density and local tumour control after radiation treatment.^{7,29} Unfortunately, the relationship was opposite in the two studies, one study⁷ demonstrating increased risk of local recurrence with low vascular density but the other²⁹ with high vascular density. The current study is being continued and patient numbers and follow-up will be increased to allow meaningful correlations between the micro-environmental parameters and treatment outcome.

Absolute values of vascular density are difficult to compare between studies, mainly because of methodological differences, in particular the type of endothelial marker used and the counting technique. Our values are in the lower range compared with other studies. This can be explained by the fact that in most studies vessels were counted in selected, highly vascularized areas (“hotspots”), whereas in the present analysis figures are based on the counting of an entire biopsy section. Indeed, the highest values obtained from the arbitrary subareas correspond better with values reported in literature. We found only a weak and non-significant correlation between the overall vascular density and hypoxic fraction. This indicates that a global assessment of vascularity is probably not a good parameter for tumour oxygenation, due to the heterogeneity in vasculature and oxygenation in tumours. Lyng et al.³⁰ also demonstrated that there are large

regional differences in vascularity and oxygenation in carcinomas of the uterine cervix. At the microregional level they did however observe a correlation between low pO_2 readings by the polarographic method (Eppendorf Histogram) and vascularity.

Hypoxia

Various methods have been described to measure tumour tissue oxygenation including polarographic oxygen electrodes, magnetic resonance spectroscopy, haemoglobin saturation assays, radionuclide assays, and, as used in the present study, by immunohistochemical markers. Methods for assessing the radiobiological hypoxic fraction include the classical paired survival curve assay and, more recently, the comet assay.³¹ Most clinical data have been obtained with the oxygen micro-electrodes. The low water solubility of the earlier immunohistochemical hypoxia markers prohibited their introduction in the clinic. Pimonidazole hydrochloride however has a high water solubility and can be easily administered intravenously in a small volume of aqueous solution. It distributes rapidly into the tissues where concentrations threefold of that in plasma are reached. These properties and the absence of any significant adverse effects with the amount required make this agent attractive for clinical use.

Raleigh et al.¹⁷ compared pimonidazole binding with micro-electrode measurements and with measurements of the radiobiologically hypoxic fraction in the C3H mouse mammary carcinoma. The oxygenation of these tumours was manipulated by the breathing of air, hyperoxic gases, injection of hydralazine and tumour clamping. They showed that pimonidazole binding was well correlated with both micro-electrode measurements and the radiobiological hypoxic fraction. A good correlation was found between pimonidazole binding and percentage of micro-electrode measurements ≤ 10 mm Hg. This is consistent with the intracellular binding properties of pimonidazole, rising steeply at $pO_2 < 10$ mm Hg. However, it was also clear from their data that the micro-electrodes systematically overestimate the extent of hypoxia at the cellular level. Under well-oxygenated circumstances where pimonidazole binding was almost negligible, the micro-electrodes still recorded a significant number of readings ≤ 10 mm Hg (36%). One of the explanations given was the presence of necrosis which produces low readings with the micro-electrodes while there is no pimonidazole binding in these areas.

Also when our results of hypoxic fraction assessed by pimonidazole binding (median 0.09) are compared with studies of micro-electrode measurements in head and neck cancer patients, the latter report substantially higher values.^{4,8,9} In

these studies the median of the fraction of pO_2 readings < 5 mm Hg varied from 0.29 to 0.41. The fraction of pO_2 values < 10 mm Hg was generally not reported. These measurements were mostly taken from metastatic neck nodes in contrast to our biopsy material which originated from the primary tumours in all cases. Central necrosis is often observed in cross-sectional CT-imaging of nodal metastasis, and this may be one explanation for the discrepancy between our results and those of the polarographic studies.

Initial studies on the clinical use of pimonidazole as a hypoxia marker came from the group from the University of North Carolina.¹³⁻¹⁵ Raleigh et al.¹⁴ reported on 18 patients with carcinomas of the uterine cervix and head and neck. The area fraction labelled with pimonidazole varied from almost zero to approximately 0.25 with a median of 0.02. Varia et al.¹⁵ reported on 10 patients with carcinoma of the uterine cervix. Values for pimonidazole binding were below 0.1 in 9 of the 10 patients. It is difficult to compare the results from these two studies with the current study because of the differences in tumour sites and the relatively small sample sizes. Also, different methodologies were used for assessment of the hypoxic fraction.

Another bioreductive compound of the nitroimidazole group is “EF5”, a pentafluorinated derivate of etanidazole. This recently developed immuno-histochemically detectable hypoxic marker has been tested in animal tumours and xenografted human tumours.³² Very recently, Evans et al.³³ reported the first clinical application of this marker.

Patterns of hypoxia

As demonstrated various patterns of hypoxia can be recognized (Figure 2). Differences between these patterns can be quantified by calculating the hypoxic fractions of arbitrary subareas (Figure 4) and, maybe more interesting, by quantifying hypoxia as a function of distance from the vessels (Figures 6 and 7). The categorization of the tumours was based on the visual aspect of the hypoxia staining combined with the quantitative analysis of the hypoxia distribution over the vascular zones. The tumours shown in figures 1 and 2b are typical examples of the classical “cord-like” tumour model described by Thomlinson and Gray.³⁴ Diffusion limited hypoxia was the predominant feature of all the tumours we analysed. However, the spatial relationship to the vessels was not always the same.

In the tumour of category A hypoxia was virtually absent within 100 μ m of vascular structures. Hypoxia was predominantly present at large (150 μ m to 250 μ m) distances from the vessels. In this tumour all necrotic areas could be excluded

from the analysis, i.e. figures 2A and 6 depict only viable tumour tissue. Thus, significant amounts of viable tumour tissue, both hypoxic and non-hypoxic (e.g. six o'clock position in Figure 6) were observed at large ($> 250\ \mu\text{m}$) distances from blood vessels. It can, however, not be excluded that these areas might have had oxygen and nutritional supply from vessels above or below the section examined. The analysis system used provides only a two-dimensional image of the tumour which obviously is a limitation. On the other hand, there is no good reason to assume that the vascular architecture will be any different in the third dimension. Since this category A tumour demonstrates large intervascular distances, it is most likely that vascular structures are sparse, also above and below the plane of the section analysed.

The category B tumour showed already some hypoxia in the first $50\ \mu\text{m}$ zone (hypoxic fraction 0.09) and a gradual increase of the hypoxic fraction in the second and the third zones. However, at distances $> 150\ \mu\text{m}$ hypoxia seemed to decrease again. The explanation for this unexpected phenomenon is a "contamination" by small areas of necrosis at these greater distances (see arrows in Figure 2B). This was confirmed in the haematoxylin-eosin staining. These necrotic areas were too small however to be excluded from the analysis and because they were not labelled by pimonidazole, in the computer calculations they were falsely considered as "viable non-hypoxic tumour tissue". Thus, in this particular tumour, the hypoxic fractions at distances $> 150\ \mu\text{m}$ were underestimated.

Nevertheless, it is an interesting observation that, while in one category of tumours (A) there are significant amounts of viable tissue at distances $> 250\ \mu\text{m}$, in other tumours there is already necrosis at $150\text{--}200\ \mu\text{m}$ (category B). These differences suggest that the balance between oxygen delivery and oxygen consumption may vary among tumours of the same histology resulting in different distributions of chronic hypoxia and necrosis.

The tumour of category C demonstrated a considerable amount of hypoxia within $100\ \mu\text{m}$ from the vessels with a hypoxic fraction of 0.20 at $0\text{--}50\ \mu\text{m}$. This suggests impaired functioning of particular vessels, either permanently or temporarily ("acute hypoxia"). This may also be the case, but to a lesser extent, in the category B tumour. In xenografted tumours we demonstrated that after 10 min of exposure to pimonidazole there is a weak binding in the hypoxic cells which increases between 10 and 30 min of exposure (unpublished data). This indicates that, with this assay, acute hypoxia probably will only be recognized if cells are hypoxic for at least 10 min.

Together with single parameters such as vascular density and hypoxic fraction, the pattern of hypoxic staining may give additional prognostic information and may help to select appropriate treatment modalities. We have previously demonstrated that carbogen can very efficiently reduce diffusion limited hypoxia in human squamous cell carcinoma xenografts.¹² However, preliminary data from our laboratory suggest that it is difficult to eradicate all the hypoxia at greater distance from the vessels. This may also be the case in the category A tumours. At the same time there seems to be limited value in adding vasoactive agents such as nicotinamide to the treatment of such tumours since they exhibit no or only very little acute hypoxia. Our clinical attempt to categorize tumours based on hypoxic patterns must be validated with a larger number of patients. This is the subject of ongoing investigations.

Conclusion

We have presented a quantitative method for multiparameter analysis of vascularity and hypoxia in head and neck tumours which is clinically feasible. These measurements can be of prognostic relevance. Moreover, this method yields information on architectural patterns which may improve our understanding of the tumour micro-environment and may in the future be of assistance with the selection of treatment strategies.

Acknowledgements

The authors would like to thank JPW Peters for expert technical assistance. We would like to thank the Dutch cancer society for the financial support of this study.

References

1. Schwartz G. Über desensibilisierung gegen röntgen und radiumstrahlen. *Munchener medizinischen wochenschrift* 1909;24:1-2.
2. Cramer W. The therapeutic action of radium on spontaneous mammary carcinomata of the mouse. *Annual report of the imperial cancer research fund report* 1935;11:127-146.
3. Gray LH, Conger AD, Ebert M, *et al.* The concentration of oxygen dissolved in tissues at the time of irradiation as a factor in radiotherapy. *Br J Radiol* 1953;26:638-648.
4. Gatenby RA, Kessler HB, Rosenblum JS, *et al.* Oxygen distribution in squamous cell carcinoma metastases and its relationship to outcome of radiation therapy. *Int J Radiat Oncol Biol Phys* 1988;14:831-838.
5. Dray TG, Hardin NJ, Sofferman RA. Angiogenesis as a prognostic marker in early head and neck cancer. *Ann Otol Rhinol Laryngol* 1995;104:724-729.
6. Zatterstrom UK, Brun E, Willen R, *et al.* Tumor angiogenesis and prognosis in squamous cell carcinoma of the head and neck. *Head Neck* 1995;17:312-318.
7. Jenssen N, Boysen M, Kjaerheim A, *et al.* Low vascular density indicates poor response to radiotherapy in small glottic carcinomas. *Pathol Res Pract* 1996;192:1090-1094.
8. Nordsmark M, Overgaard M, Overgaard J. Pretreatment oxygenation predicts radiation response in advanced squamous cell carcinoma of the head and neck. *Radiother Oncol* 1996;41:31-39.
9. Brizel DM, Sibley GS, Prosnitz LR, *et al.* Tumor hypoxia adversely affects the prognosis of carcinoma of the head and neck. *Int J Radiat Oncol Biol Phys* 1997;38:285-289.
10. Rijken PF, Bernsen HJ, van der Kogel AJ. Application of an image analysis system to the quantitation of tumor perfusion and vascularity in human glioma xenografts. *Microvasc Res* 1995;50:141-153.
11. Bussink J, Kaanders JH, Rijken PF, *et al.* Multiparameter analysis of vasculature, perfusion and proliferation in human tumour xenografts. *Br J Cancer* 1998;77:57-64.
12. Bussink J, Kaanders JH, Rijken PF, *et al.* Vascular architecture and microenvironmental parameters in human squamous cell carcinoma xenografts: effects of carbogen and nicotinamide. *Radiother Oncol* 1999;50:173-184.
13. Kennedy AS, Raleigh JA, Perez GM, *et al.* Proliferation and hypoxia in human squamous cell carcinoma of the cervix: first report of combined immunohistochemical assays. *Int J Radiat Oncol Biol Phys* 1997;37:897-905.
14. Raleigh JA, Calkins-Adams DP, Rinker LH, *et al.* Hypoxia and vascular endothelial growth factor expression in human squamous cell carcinomas using pimonidazole as a hypoxia marker. *Cancer Res* 1998;58:3765-3768.
15. Varia MA, Calkins-Adams DP, Rinker LH, *et al.* Pimonidazole: a novel hypoxia marker for complementary study of tumor hypoxia and cell proliferation in cervical carcinoma. *Gynecol Oncol* 1998;71:270-277.
16. Kaanders JH, Pop LA, Marres HA, *et al.* Radiotherapy with carbogen breathing and nicotinamide in head and neck cancer: feasibility and toxicity. *Radiother Oncol* 1995;37:190-198.
17. Raleigh JA, Chou SC, Arteel GE, *et al.* Comparisons among pimonidazole binding, oxygen electrode measurements, and radiation response in C3H mouse tumors. *Radiat Res* 1999;151:580-589.
18. Azuma C, Raleigh JA, Thrall DE. Longevity of pimonidazole adducts in spontaneous canine tumors as an estimate of hypoxic cell lifetime. *Radiat Res* 1997;148:35-42.
19. Schlingemann RO, Dingjan GM, Emeis JJ, *et al.* Monoclonal antibody PAL-E specific for endothelium. *Lab Invest* 1985;52:71-76.
20. Gasparini G, Weidner N, Maluta S, *et al.* Intratumoral microvessel density and p53 protein: correlation with metastasis in head-and-neck squamous-cell carcinoma. *Int J Cancer* 1993;55:739-744.
21. Albo D, Granick MS, Jhala N, *et al.* The relationship of angiogenesis to biological activity in human squamous cell carcinomas of the head and neck. *Ann Plast Surg* 1994;32:588-594.
22. Shpitzer T, Chaimoff M, Gal R, *et al.* Tumor angiogenesis as a prognostic factor in early oral tongue cancer. *Arch Otolaryngol Head Neck Surg* 1996;122:865-868.
23. Murray JD, Carlson GW, McLaughlin K, *et al.* Tumor angiogenesis as a prognostic factor in laryngeal cancer. *Am J Surg* 1997;174:523-526.
24. Leedy DA, Trune DR, Kronz JD, *et al.* Tumor angiogenesis, the p53 antigen, and cervical metastasis in squamous carcinoma of the tongue. *Otolaryngol Head Neck Surg* 1994;111:417-422.

25. Janot F, Klijanienko J, Russo A, *et al.* Prognostic value of clinicopathological parameters in head and neck squamous cell carcinoma: a prospective analysis. *Br J Cancer* 1996;73:531-538.
26. Moriyama M, Kumagai S, Kawashiri S, *et al.* Immunohistochemical study of tumour angiogenesis in oral squamous cell carcinoma. *Oral Oncol* 1997;33:369-374.
27. Salven P, Heikkilä P, Anttonen A, *et al.* Vascular endothelial growth factor in squamous cell head and neck carcinoma: expression and prognostic significance. *Mod Pathol* 1997;10:1128-1133.
28. Burian M, Quint C, Neuchrist C. Angiogenic factors in laryngeal carcinomas: do they have prognostic relevance? *Acta Otolaryngol* 1999;119:289-292.
29. Aebersold DM, Beer KT, Laissue J, *et al.* Intratumoral microvessel density predicts local treatment failure of radically irradiated squamous cell cancer of the oropharynx. *Int J Radiat Oncol Biol Phys* 2000;48:17-25.
30. Lyng H, Sundfor K, Rofstad EK. Oxygen tension in human tumours measured with polarographic needle electrodes and its relationship to vascular density, necrosis and hypoxia. *Radiother Oncol* 1997;44:163-169.
31. Olive PL, Johnston PJ, Banath JP, *et al.* The comet assay: a new method to examine heterogeneity associated with solid tumors. *Nat Med* 1998;4:103-105.
32. Fenton BM, Paoni SF, Lee J, *et al.* Quantification of tumour vasculature and hypoxia by immunohistochemical staining and HbO₂ saturation measurements. *Br J Cancer* 1999;79:464-471.
33. Evans SM, Hahn S, Pook DR, *et al.* Detection of hypoxia in human squamous cell carcinoma by EF5 binding. *Cancer Res* 2000;60:2018-2024.
34. Thomlinson RH, Gray LH. The histological structure of some human lung cancers and the possible implications for radiotherapy. *Br J Cancer* 1955;9:539-549.

Chapter 3

Pimonidazole binding and tumour vascularity predict for treatment outcome in head and neck cancer

J.H.A.M. Kaanders

K.I.E.M. Wijffels

H.A.M. Marres

A.S.E. Ljungkvist

L.A.M. Pop

F.J.A. van den Hoogen

P.C.M. de Wilde

J. Bussink

J.A. Raleigh

A.J. van der Kogel

Abstract

Hypoxia is associated with tumour aggressiveness and is an important cause of resistance to radiation treatment. Assays of tumour hypoxia could provide selection tools for hypoxia modifying treatments. This study correlated the exogenous 2-nitroimidazole hypoxia marker 1-[(2-hydroxy-3-piperidinyl)propyl]-2-nitroimidazole hydrochloride (pimonidazole) with the endogenous hypoxia-related marker carbonic anhydrase IX (CA-IX) and with vascular parameters using immunohistochemical techniques and a computerized image analysis system.

Tumour biopsies were obtained from patients with head and neck carcinomas that were potential candidates for a phase II trial with accelerated radiotherapy combined with carbogen and nicotinamide (ARCON). If, after completion of the diagnostic workup, the eligibility criteria were met and informed consent was obtained, patients were treated with ARCON. Those patients that were not eligible or refused ARCON were treated with radiotherapy, surgery or a combined modality. Forty-three biopsies were analyzed and the results were related with treatment outcome. The distribution patterns of pimonidazole and CA-IX were similar although the CA-IX signal was generally observed already at shorter distances from blood vessels. There was a weak but significant correlation between the relative tumour areas positive for pimonidazole binding and areas with CA-IX expression. Locoregional tumour control was significantly lower for patients who had hypoxic tumours or tumours with low vascular density. The 2-year control rates were 48% versus 87% for tumours with high and low pimonidazole binding levels (stratified by median, $p = 0.01$) and 48% and 88% for tumours with low and high vascular density (stratified by median, $p = 0.01$). These associations disappeared in the subgroup of patients treated with ARCON. There was no relationship between the level of CA-IX expression and treatment outcome.

It is concluded that pimonidazole binding and vascular density can predict treatment outcome in head and neck cancer and may be useful as selection tools for hypoxia modifying treatments. Pimonidazole and CA-IX demonstrate concordant staining patterns but the latter is a less specific marker for hypoxia.

Introduction

In almost all solid tumours there is to some extent an imbalance between oxygen delivery and oxygen consumption resulting in hypoxia.¹ Hypoxia is a powerful trigger for changes in gene expression and associated changes in the microenvironment. The altered genetic expression profile and the changed microenvironment stimulate clonal selection within the tumour cell population for cells with increased adaptation to hypoxia and drive the tumour towards a more malignant phenotype with increased resistance to anticancer treatments.^{2,3} Methods that identify hypoxic tumours could therefore provide a powerful selection tool for oxygenation modifying treatments.

Clinical studies using oxygen microelectrodes in carcinomas of the head and neck and uterine cervix have demonstrated a correlation between measurements of low tumour pO_2 and poor outcome after radiation treatment.^{2,4-6} In soft tissue sarcomas and in carcinomas of the uterine cervix, hypoxia was also related with outcome after surgical treatment.^{2,7,8} A limitation of the oxygen microelectrodes is the invasive nature of the procedure and their use is restricted to accessible tumours.

Exogenous and endogenous hypoxia markers detectable by immunohistochemistry require no additional intervention beyond the initial pretreatment biopsy and may be very suitable for widespread clinical use. They also provide a more sensitive and high resolution assay of the distribution of hypoxia at the micro-regional level. Clinically relevant exogenous markers are the 2-nitroimidazoles, pimonidazole³ hydrochloride and [2-(2-nitro-1H-imidazole-1-yl)-N-(2,2,3,3,3-pentafluoropropyl)acetamide] (EF-5).^{9,10} Hypoxic fraction estimated by pimonidazole binding agreed well with the hypoxic fraction measured using the comet assay in a number of animal and human tumours indicating that pimonidazole labelling can give a reliable estimate of radiobiologically relevant hypoxia.¹¹ Pimonidazole has proven to be an effective and nontoxic hypoxia marker for human squamous cell carcinomas of the cervix and head and neck.^{9,12-14} A disadvantage of the nitroimidazole markers is that they require i.v. injection before biopsy taking.

In addition to the well-known angiogenic factor, vascular endothelial growth factor, more recently, new and possibly more specific endogenous hypoxia-associated molecular markers have been described. Most promising at present is CA-IX which is regulated via the von Hippel-Lindau and HIF-1 pathway. Carbonic anhydrases are transmembrane enzymes catalyzing the reversible hydration of carbon dioxide to carbonic acid and are involved in respiration and acid-base balance.¹⁵ Immunohistochemistry revealed high-to-moderate expression of CA-IX

in normal adult tissues but mainly in highly specialized cells.¹⁶ High levels of expression were found in a large sample of cancer cell lines and fresh and archived tumour tissues.¹⁶ CA-IX had the greatest magnitude of induction among 12 hypoxia-overexpressed genes including vascular endothelial growth factor and was induced in many tumour cell lines.¹⁷ CA-IX-positive cells from cervical carcinoma xenografts were found to be clonogenic, resistant to killing by ionizing radiation, and preferentially able to bind pimonidazole.¹⁸ Immunohistochemical patterns of CA-IX expression are typically described as “perinecrotic”, consistent with the distribution of diffusion-limited hypoxia. Retrospective clinical studies support the notion that CA-IX represents tumour aggressiveness. High CA-IX expression predicted poor survival in carcinoma of the head and neck, lung, uterine cervix and breast.¹⁹⁻²²

In this study we relate pimonidazole binding and CA-IX expression in biopsy material of human squamous cell carcinomas of the head and neck. We demonstrate that the distribution pattern of the two markers relative to the vasculature is similar with increasing signal at greater distance from the blood vessels. CA-IX expression was often observed at shorter distances from the vessels, suggesting that CA-IX upregulation occurs at pO_2 levels higher than those required for pimonidazole binding. Although the patterns were concordant, there was only a weak correlation between the overall pimonidazole and CA-IX positive tumour areas. In patients with head and neck cancer, pimonidazole binding and vascularity were predictors of outcome but CA-IX expression was not. The poor outcome of hypoxic tumours could be corrected with hypoxia-modifying treatment with disappearance of the discriminative power of pimonidazole binding and vascularity. Our findings strongly support the notion that nitroimidazole markers together with vascular parameters can provide powerful selection tools for hypoxia-modifying treatment on an individual patient basis. Since CA-IX is upregulated at intermediate levels of oxygenation, its specificity and sensitivity as a hypoxia marker needs additional investigation.

Materials and methods

Patients

At the Department of Radiation Oncology of the University Medical Center Nijmegen, a Phase II clinical trial of ARCON in advanced squamous cell carcinomas of the head and neck has recently been completed.²³ ARCON combines accelerated radiotherapy with carbogen breathing and nicotinamide to

reduce diffusion-limited and perfusion-limited hypoxia. Eligibility criteria for this study were: (a) stage III or IV squamous cell carcinoma of the oral cavity, oropharynx, hypopharynx or larynx and stage II hypopharynx carcinomas with a greatest dimension of the primary tumour >2 cm; (b) age over 18 years; (c) WHO performance status of 0-2; (d) no distant metastases; (e) no severe heart or lung disease; (f) no severe liver or kidney function impairments; (g) no severe stridor; (h) no concurrent treatment for other malignant disease outside the upper aerodigestive tract.

Patients that were potential candidates for this trial were asked to participate in the current hypoxia marker study. After giving consent, the patients received a 20 min i.v. infusion of 500 mg/m² Hypoxyprobe-1 (pimonidazole hydrochloride, NPI, Inc., Belmont, MA). Approximately 2 h later tumour biopsies were taken under general anesthesia. Biopsies were taken for routine diagnostic purposes and additional biopsies were taken for hypoxia marker analysis. The latter were snap frozen and stored in liquid nitrogen until immunohistochemical processing. The diagnostic workup further included physical examination, chest X-ray, computed tomography scan, and/or magnetic resonance imaging scan of the head and neck area. If, after completion of the diagnostic workup, the eligibility criteria were met and informed consent was obtained, patients were treated with ARCON. Patients that were not eligible or refused inclusion in the trial were treated with radiotherapy, surgery or a combined modality. The ARCON-trial and the hypoxia marker study were approved by the ethics committee of the University Medical Center Nijmegen.

Immunohistochemistry

From the biopsy material, frozen sections of 5 µm were cut and mounted on poly-L-lysine coated slides and stored at -80°C until staining. Before staining, sections were fixed for 10 min in acetone of 4°C and rehydrated in phosphate buffered saline. Between all consecutive steps of the staining procedure, sections were rinsed three times for 2 min in PBS.

The sections were incubated for 30 min at 37°C with mouse anti-CA-IX antibody (Egbert Oosterwijk, Department of Urology, UMC Nijmegen, The Netherlands) diluted 1:100 in PLD (DPC Breda Diagnostic Products, The Netherlands) and pimonidazole polyclonal rabbit antibody (J.A. Raleigh²⁴) diluted 1:200 in PLD. The second incubation was for 30 min at 37°C with goat-anti-mouse(Fab)Cy3 antibody (Jackson Immuno Research Laboratories, West Grove, PA) 1:300 in PLD and donkey-anti-rabbit-AlexaA488 antibody (Molecular Probes, Leiden, The Netherlands) 1:200 in PLD. This was then followed by 30 min incubation with

donkey-anti-goatF(ab')₂ tetra-methyl rhodamine isothiocyanate (Jackson Immuno Research Laboratories) 1:200 in PLD at 37°C to block the first mouse monoclonal. Next, to stain the vessels, the sections were incubated with the mouse antibody PAL-E (Department Pathology, University Medical Center Nijmegen) 1:6 in PLD for 30 min at 37°C, followed by 30 min incubation at 37°C with chicken-anti-mouse-AlexaA647 (Molecular Probes) 1:200 in PLD. The monoclonal antibody PAL-E is a marker for human endothelium, especially useful in frozen tissue sections.²⁵ After the staining procedure, the sections were mounted in fluorostab (ICN Pharmaceuticals, Zoetermeer, The Netherlands).

Image acquisition and analysis

The sections were scanned on a 8-bit digital image analysis system with a high-resolution intensified solid-state camera on a fluorescence microscope (Axioskop, Zeiss, Göttingen, Germany) and a computer controlled motorized stepping stage. The signals captured by the camera were converted to binary images using the digital image application TCL-image (TNO, Delft, The Netherlands) on a Macintosh computer as described previously.^{26,27} Thresholds for the fluorescent signals were interactively set above the background staining for each individual marker. For each marker a composite binary image was obtained from the complete biopsy. In conference with a pathologist and guided by a haematoxylin-eosin staining of a consecutive section, the tumour area was delineated. This area was used as a mask in further analysis excluding nontumour tissue, large necrotic areas and artefacts. One section per biopsy was analyzed.

The VD was calculated as the number of vascular structures per mm². The RVA was defined as the PAL-E positive area divided by the total tumour area. HFpimo and HFCA-IX were defined as the tumour area positive for pimonidazole and CA-IX respectively, relative to the total tumour area. To quantitate the distribution patterns of pimonidazole and CA-IX relative to the vasculature, zones were chosen at increasing distance from the nearest vessel (0-25 µm, 25-50 µm, 50-100 µm and >100 µm). The area positive for pimonidazole or CA-IX in a particular zone divided by the total pimonidazole or CA-IX positive tumour area gave the proportion of marker distributed over that particular zone, HFpimo-distribution and HFCA-IX-distribution, respectively. The details of this analysis were described previously.²⁷

Statistics

Statistical analyses were done on a Macintosh computer using the Statistica software package. Correlations between ordinal variables were assessed using linear regression analysis. For differences in ordinal variables in relation to categorical tumour characteristics (site, T-stage, N-stage, histopathological grade) the Kruskal Wallis test was used. Cumulative control and survival rates were calculated from the date of pathologic diagnosis using the Kaplan-Meier method and the log-rank test was used to test for differences. Patients who never reached complete remission after treatment (as assessed by clinical examination) were considered as having locoregional failure from time zero. Cox regression analysis was used to analyze the associations between patient and tumour variables and locoregional tumour control and disease-free survival. $P < 0.05$ was considered significant.

Table 1. Clinical characteristics of 43 squamous cell carcinomas analyzed (UICC 1997).

	Treatment		
	ARCON	Non-ARCON ^a	Palliative
Site			
larynx	8	4	2
hypopharynx	7	5	--
oropharynx	7	6	--
oral cavity	1	2	1
T-stage			
T1	2	1	--
T2	3	7	--
T3	13	6	1
T4	5	3	2
N-stage			
N0	4	6	--
N1	7	3	--
N2	11	7	3
N3	1	1	--
Total	23 tumours 23 patients	17 tumours 16 patients	3 tumours 3 patients

^aReasons for non-ARCON:

Oral cavity/oropharynx tumours smaller than anticipated and still resectable: surgery with postoperative radiotherapy (N = 5); One larynx and one hypopharynx tumour larger than anticipated with extensive cartilage destruction: surgery with postoperative radiotherapy (N = 2); Larynx carcinomas smaller than anticipated and not eligible for ARCON: radiotherapy only (N = 2); Included in trial with neo-adjuvant chemotherapy and radiotherapy (N = 2); and refused participation in ARCON trial, radiotherapy only (N = 6, includes one patient with two primary tumours).

Results

Patients and treatment

Between May 1998 and February 2001, Hypoxyprobe-1 was administered to 55 patients before biopsy taking. Seven were women and 48 were men and age ranged from 37 to 85 years with a median of 59 years. Two patients had two synchronous primary head and neck tumours that were both biopsied. None of the patients had adverse reactions to Hypoxyprobe-1. Fourteen biopsies were excluded from additional analysis, 6 because they contained no or only very little invasive carcinoma, 6 because of poor quality attributable to mechanical damage during the biopsy procedure, and 2 because the histological diagnosis was not squamous cell carcinoma. Thus, 43 squamous cell carcinomas were analyzed. The clinical characteristics of these tumours are listed in Table 1. After completion of the diagnostic workup, 23 patients were eligible and gave consent for inclusion in the ARCON-trial. Sixteen patients were not included for various reasons and received other treatment as indicated in Table 1. One patient in this group had two primary tumours and was excluded from the analysis for locoregional control and disease-free survival. Also the 3 patients that were treated palliatively were excluded from outcome analysis. Overall, the ARCON patients had more advanced disease. Figure 1 summarizes the patient selection for the outcome analysis.

Patients in the ARCON trial received 64-68 Gy to the primary tumour and involved neck nodes and 44 Gy to electively treated areas. The dose per fraction was 2 Gy and two fractions per day were given during the last 1.5 weeks of the treatment with an overall treatment time of 36-38 days. During the irradiations, patients breathed carbogen, and they received nicotinamide, 60 mg/kg p.o., 1 h before the start of irradiations. This protocol has been described previously, and we refer to this publication for details of the treatment and compliance.²³ Patients who underwent surgery with postoperative radiotherapy received 50 Gy in fractions of 2 Gy to the surgical bed and 64 Gy to areas at high risk for recurrence using a conventional schedule of once daily fractionation. The other patients were treated with primary radiotherapy, 3 with a conventional schedule (66–70 Gy) and 6 with an accelerated schedule to 68 Gy as described above. Of the latter, 2 patients received neo-adjuvant chemotherapy with 5-fluorouracil and cisplatin. The median duration of follow-up was 18 months.

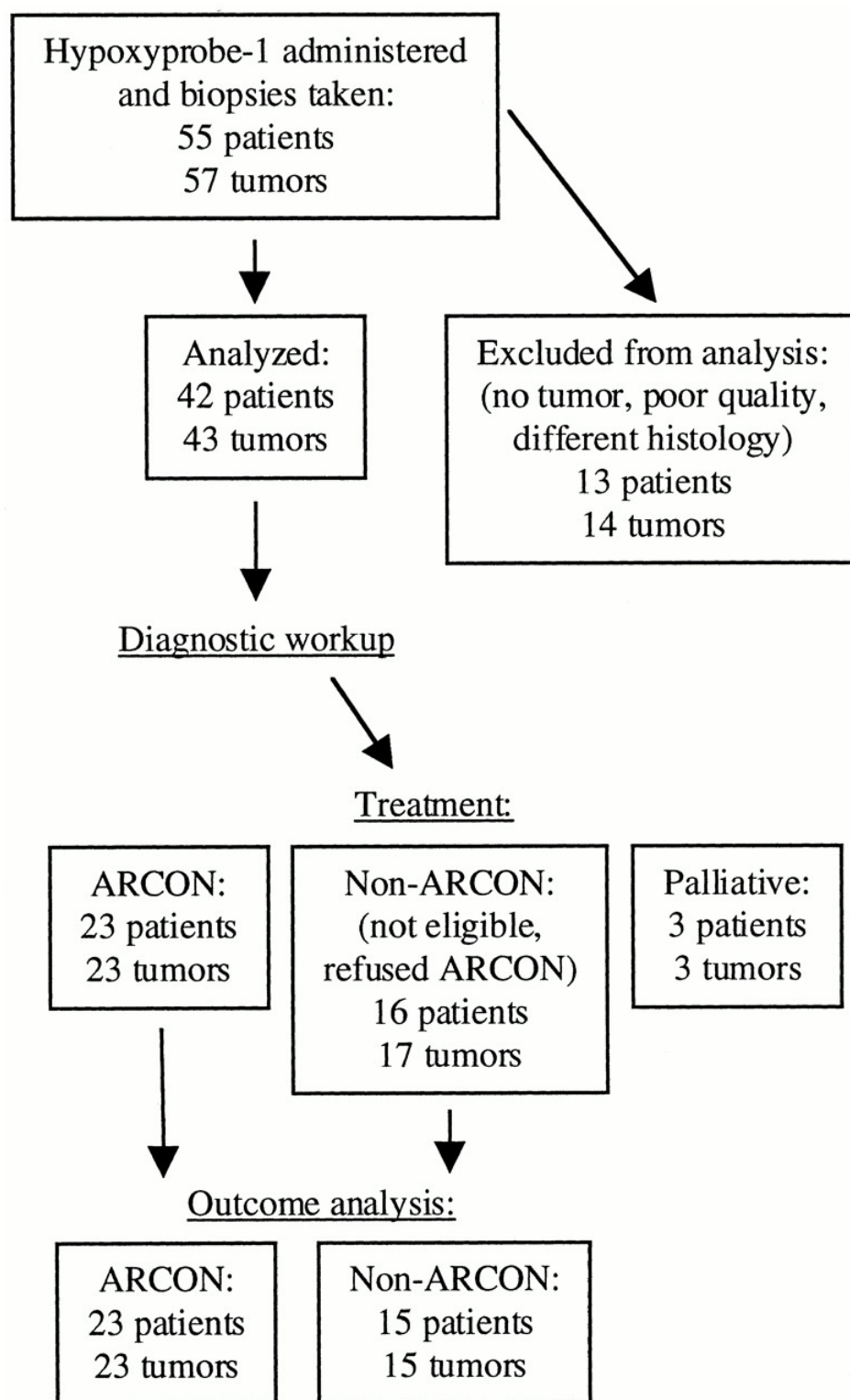


Figure 1. Diagram summarizing patient selection for treatment outcome analysis.

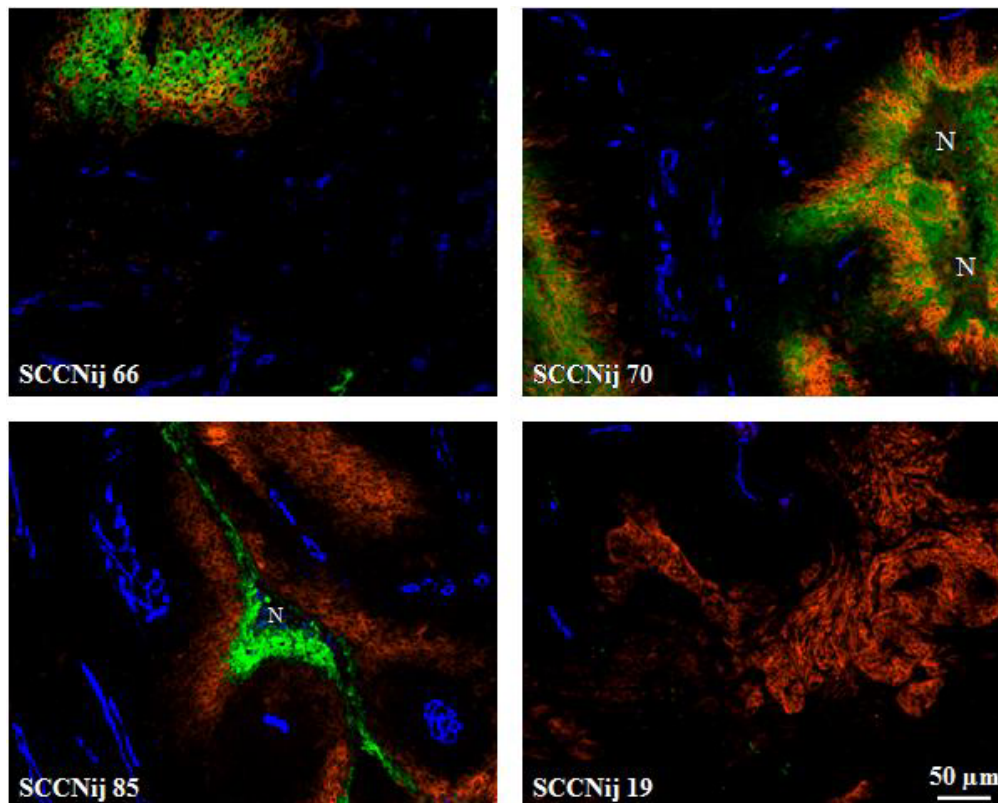


Figure 2. Fluorescent microscopic images of four head and neck carcinomas stained by triple immunofluorescence as described in the text. Blue: vessels; green: pimonidazole; red: CA-IX. Overlap of pimonidazole and CA-IX signal results in bright orange. SCCNij19 is a negative control, i.e. biopsy material from a patient that was not infused with pimonidazole; apart from a few very small artefacts this tumour shows no green fluorescence. N indicates necrosis with nonspecific staining.

Pimonidazole binding and CA-IX expression

The triple staining for vessels, pimonidazole and CA-IX gave bright fluorescent signals with very little background except in areas of necrosis and occasionally in the stromal components of the tumour (Figure 2). CA-IX staining was typically confined to the cell membrane although a weaker cytoplasmic stain was occasionally observed as well. Both pimonidazole and CA-IX positivity generally increased with distance from the vessels with considerable overlap of the two signals. CA-IX immunoreactivity was usually observed already at shorter distances from blood vessels compared to pimonidazole (Figure 3). There were also areas of mismatch where CA-IX was found but no pimonidazole and vice versa (Figure 4). All but 1 of the 43 biopsies showed good quality of the triple staining. One biopsy demonstrated significant artefacts in the CA-IX staining and was excluded from the comparison between CA-IX and pimonidazole. Mean and median values and range for HFpimo, HFCA-IX, VD and RVA in the biopsy material are given in Table 2.

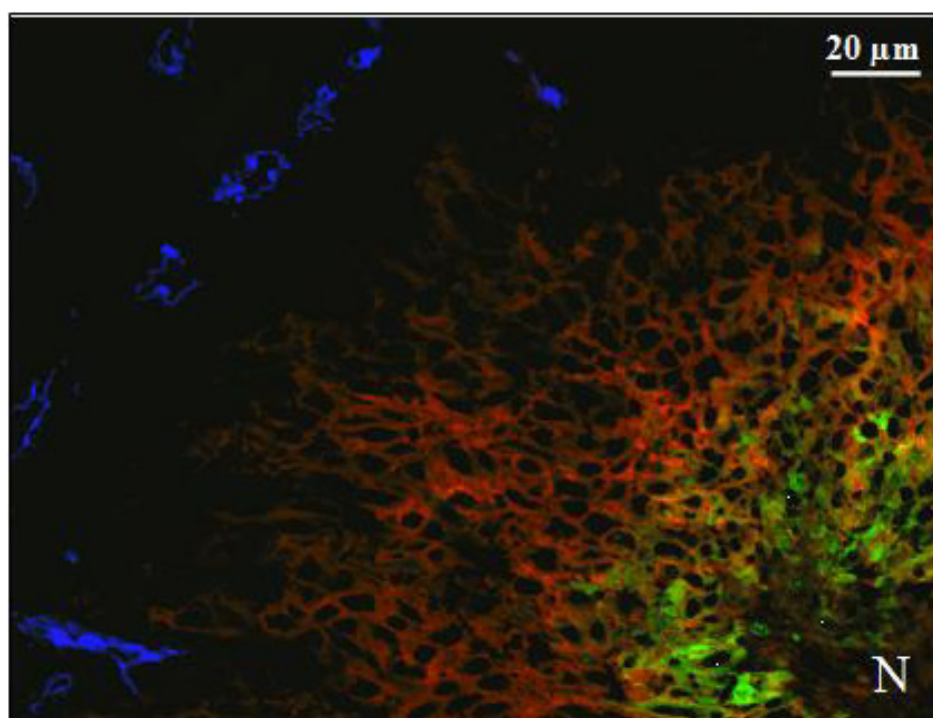


Figure 3. Fluorescent microscopic image of an oropharynx carcinoma. Blue: vessels; green: pimonidazole; red: CA-IX; N indicates necrosis.

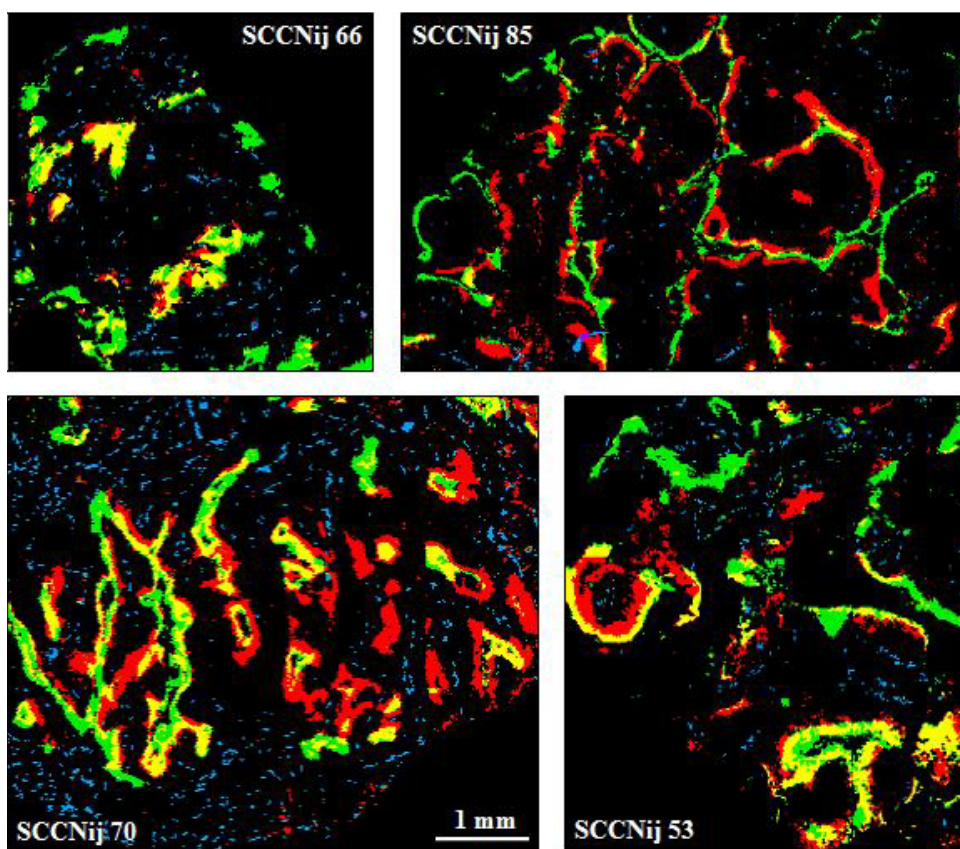


Figure 4. Composite binary images of four head and neck carcinomas: blue: vessels; green: pimonidazole; red: CA-IX; yellow: areas of pimonidazole and CA-IX overlap.

Table 2. Values for HFpimo, HFCA-IX, VD and RVA in biopsies of 43 squamous cell carcinomas of the head and neck.

	HFpimo (%)	HFCA-IX (%)	VD (mm ⁻²)	RVA (%)
Mean	6.0	6.4	20.9	1.8
Median	5.6	3.5	16.5	1.5
Range	0.3 – 17.2	0.6 – 29.4	6.2 – 58.2	0.5 – 4.2
SD	4.6	6.8	11.7	1.0

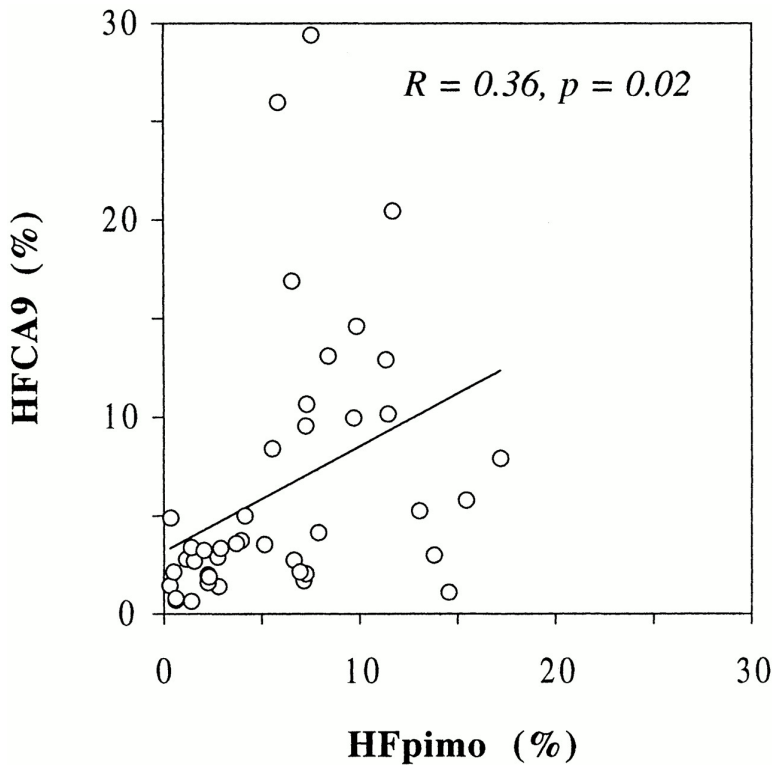


Figure 5. Comparison between the fraction of the tumour area that binds CA-IX antibody (HFCA-IX) with the fraction of the tumour area that binds pimonidazole antibody (HFpimo) in 42 squamous cell carcinomas of the head and neck. The linear best fit is shown.

HFpimo, HFCA-IX, VD and RVA were independent of site, T-stage, N-stage and histopathological grading. No correlations were found between HFpimo or HFCA-IX and the vascular parameters. Linear regression analysis showed a significant but weak correlation between HFpimo and HFCA-IX (Figure 5). The distribution pattern of the two markers relative to the vasculature was similar however, with increasing signal intensity at greater distance from vessels (Figure 6). CA-IX positivity was greater in the zones 25-50 μ m and 51-100 μ m from vessels relative to pimonidazole positivity which was more pronounced at distances >100 μ m. The first zone (0-25 μ m) directly adjacent to vessels included mainly stromal cells and extracellular matrix in the majority of the tumour samples. Only very small tumour areas were generally found in this zone. This zone was therefore excluded from the analysis because it represents mainly nontumour tissue.

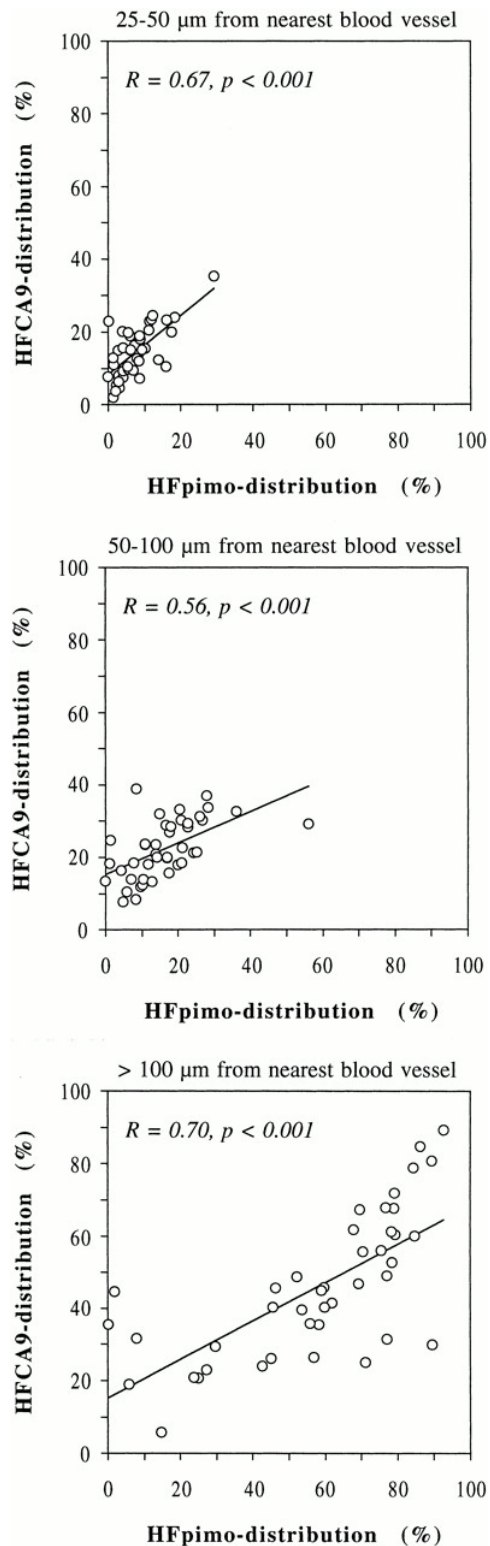


Figure 6. Comparison between the area that binds CA-IX antibody (HFCA-IX-distribution) with the area that binds pimonidazole antibody (HFpimo-distribution) in distinct zones divided by the total positive tumour area for the respective markers in 42 squamous cell carcinomas of the head and neck. The linear best fit is shown.

Correlations of patient and tumour characteristics with treatment outcome

Univariate Cox regression analysis demonstrated no associations between tumour site, T-stage, N-stage, or histopathological grade and locoregional control or disease-free survival (Table 3). HFpimo, HFCA-IX, VD and RVA were tested both as continuous variables and as dichotomous variables (stratification by median values; Table 3). When entered in the model as continuous variables, only VD showed a significant association with locoregional control. As dichotomous variables both HFpimo and VD demonstrated significant associations with locoregional control. Patients with high HFpimo or low VD did worse. Figure 7 shows Kaplan-Meier estimates for locoregional control and disease-free survival stratified by the median of HFpimo. Locoregional tumour control at 2 years was 48% for patients with hypoxic tumours versus 87% for patients with less hypoxic tumours ($p = 0.01$). Disease-free survival was 38% and 70% respectively ($p = 0.04$). When analyzed by treatment, ARCON versus non-ARCON, the difference in outcome between low and high HFpimo was mainly found in the non-ARCON group. The same phenomenon was observed for VD with 48% locoregional control for tumours with low vascularity and 88% for tumours with high vascularity ($p = 0.01$, Figure 8).

Table 3. Correlations of tumour characteristics with treatment outcome (univariate Cox regression analysis). HFpimo, HFCA-IX, VD and RVA analyzed as continuous and as dichotomous variables (stratification by median values).

Variables	Association with outcome	
	Locoregional control	Disease-free survival
Site	n.s. ^a	n.s.
T-stage	n.s.	n.s.
N-stage	n.s.	n.s.
Grade	n.s.	n.s.
HFpimo		
continuous	$p = 0.09$	n.s.
dichotomous	$p = 0.02$	$p = 0.09$
HFCA-IX		
continuous	n.s.	n.s.
dichotomous	n.s.	n.s.
VD		
continuous	$p = 0.02$	n.s.
dichotomous	$p = 0.02$	n.s.
RVA		
continuous	n.s.	n.s.
dichotomous	n.s.	n.s.

^an.s., not significant.

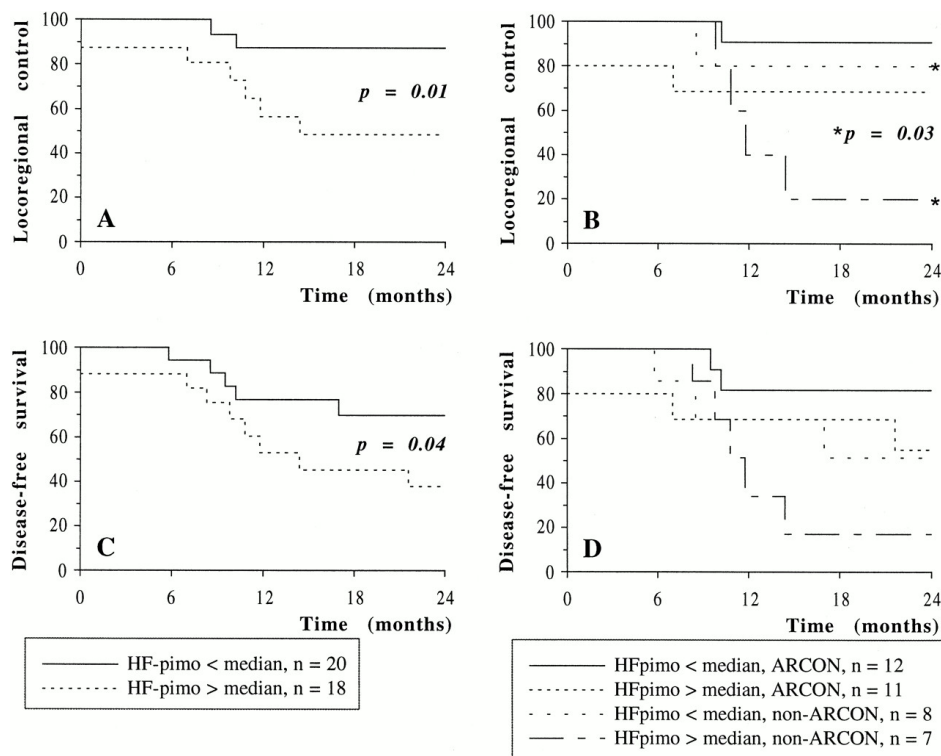


Figure 7. Kaplan-Meier estimates of locoregional control (A, B) and disease-free survival (C, D). Stratification is by the median of HFpimo. Comparison by log-rank test. Panels B and D show results by treatment group (ARCON versus non-ARCON).

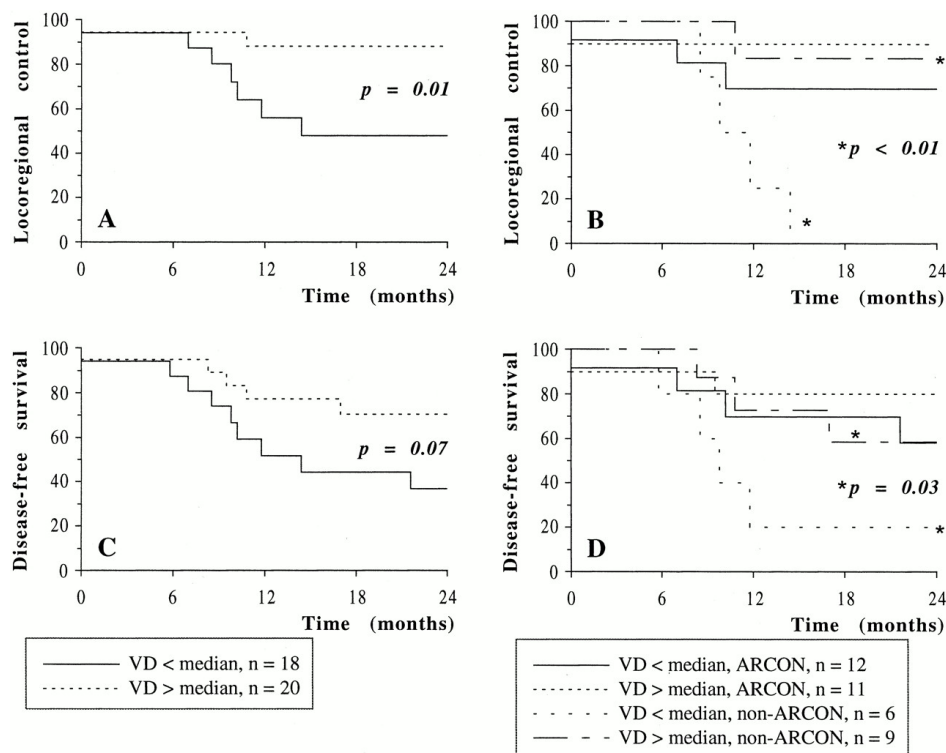


Figure 8. Kaplan-Meier estimates of locoregional control (A, B) and disease-free survival (C, D). Stratification is by the median of VD. Comparison by log-rank test. Panels B and D show results by treatment group (ARCON versus non-ARCON).

Discussion

CA-IX expression and hypoxia

Induction of the CA-IX protein by hypoxia has been observed in a number of cell lines including cell lines derived from squamous cell carcinomas of the head and neck.^{16,28,29} The time course of gene expression in response to hypoxia in a panel of human tumour lines was measured by real-time polymerase chain reaction.¹⁷ CA-IX had the greatest magnitude of induction among 12 hypoxia-overexpressed genes and was induced in the greatest number of tumour cell lines. Western blot analysis, using an antibody to CA-IX, showed that under hypoxia protein levels steeply increased from 4 to 24 h, which was similar to the transcript level time course. Experiments with graded hypoxia in one cell line demonstrated CA-IX induction from pO_2 levels of approximately 20 mmHg and downward.²⁸ In the present study, there was concordance between CA-IX expression and pimonidazole binding with increasing positivity at greater distance from the blood vessels. CA-IX expression was often observed at shorter distances from the vessels suggesting that CA-IX upregulation occurs at pO_2 levels higher than required for pimonidazole binding. In earlier work we demonstrated that, at a certain distance from the blood vessels, there is a rapid increase from background to maximum level of the fluorescent pimonidazole signal.²⁷ This is consistent with data from other studies, showing a steep rise in binding of the 2-nitroimidazole, misonidazole, at pO_2 values below 10 mmHg in multicellular spheroids³⁰, and comparable K_m and binding patterns of pimonidazole.³¹ Olive et al.¹⁸ demonstrated that in spheroids from human cervical cancer cells (SiHa) only 0.5% of the cells were sufficiently hypoxic to bind pimonidazole, yet 12% of the cells bound CA-IX antibodies. In tumour biopsies of patients with cervical cancer, the percentage of the tumour area with CA-IX immunostaining was twofold the area that was stained for pimonidazole.¹⁸ This indicates that CA-IX expression identifies low tissue oxygenation levels as well as intermediate levels. With double hypoxia marker experiments in xenografted head and neck tumours, although with higher pimonidazole doses, we demonstrated that the presence of pimonidazole for a period of 30 min is sufficient to stain all hypoxic areas.³² Tumour regions that were only temporarily hypoxic may stain for pimonidazole but not for CA-IX because upregulation of CA-IX requires at least several hours. This can explain, at least partly, the pimonidazole positive but CA-IX negative areas. Other reasons for mismatch can be additional positive or negative non-hypoxic stimuli influencing CA-IX expression or defective expression of CA-IX in some tumours. CA-IX is involved in intra- and extracellular pH homeostasis of tumour

cells. CA-IX is localized normally on differentiated cells specialized in acid/base regulation (collecting ducts of the kidney, gastrointestinal gland cells) suggesting a role for CA-IX in maintaining extracellular acidity in tumours.¹⁶ Thus, changes in the acid/base balance may provide additional stimuli for CA-IX expression. In bladder and skin carcinomas Wykoff et al. observed pimonidazole staining extending beyond CA-IX immunoreactivity, the latter being more tightly limited to perinecrotic regions.²⁸ This is in contrast to the results of the current study and those of Olive et al.¹⁸ Whether this truly represents differences between tumours of different origin and histology or if this should be explained by differences in immunohistochemical techniques is yet unclear. In the skin and bladder carcinomas no overall correlation between the percentage of tumour stained for pimonidazole and CA-IX was found.

It can be concluded that, although CA-IX is indicative for hypoxia, it is less specific compared to pimonidazole which can explain the weak correlation between relative pimonidazole and CA-IX positive areas in this study (Figure 5). The transmembrane carbonic anhydrases are regulated by HIF-1 which is considered to be a master regulator integrating physiological responses to hypoxia. HIF-1 itself is also gaining interest as an intrinsic hypoxia marker. Immunohistochemical detection of HIF-1 α demonstrated patterns similar to those of its target gene products with typical perinecrotic staining.^{33,34} However, more diffuse expression patterns with staining in proximity of blood vessels are also reported.^{33,34} In cervical cancer xenografts maximal HIF-1 α expression generally occurred at shorter distances from blood vessels than the maxima of EF-5 binding.³³ This suggest that HIF-1 upregulation occurs at higher pO₂ levels than required for nitroimidazole binding, similar to what we observed for CA-IX. HIF-1 α expression was inversely correlated with local failure-free survival, disease-free survival and overall survival in squamous cell carcinomas of the oropharynx treated with radiotherapy.³⁴

Prognostic value of tumour vascularity and hypoxia related markers

In this study there was a significant association between VD and locoregional tumour control. With our automated image processing system we analyzed complete tissue sections and the average number of vascular structures was calculated per mm² tumour area. This is different from hot-spot counting where vessel counting is restricted to selected areas of high vascularity yielding what is generally referred to as “microvascular density” (MVD). Three studies in head and neck carcinomas found an association between MVD and local tumour control

after radiation treatment.³⁵⁻³⁷ One study demonstrated an increased risk of local recurrence with low MVD in larynx carcinomas but another showed the opposite in oropharynx tumours. The largest study on head and neck tumours thus far published found a “U-shaped” relationship between MVD and survival after combined radiotherapy and chemotherapy.³⁷ An intermediate MVD defined a better survival, while both low MVD and high MVD were linked to poor outcome. This observation was explained by a poor treatment response due to insufficient oxygen and drug availability in the poorly vascularized cases and an increased metastatic potential in the highly vascularized tumours. The association between low VD and poor oxygenation and consequently unfavorable outcome after radiotherapy is compatible with the results of the current study. The suggestion is strengthened by the fact that the outcome of poorly vascularized tumours improved with ARCON. A weakness in this hypothesis is, however, the absence of a correlation between VD and HFPimo in the current material.

Retrospective clinical studies support the notion that CA-IX represents tumour aggressiveness. High CA-IX expression predicted poor survival in carcinoma of the head and neck, lung, uterine cervix and breast.¹⁹⁻²² One older study, however, showed the reverse in early cervical cancers.³⁸ The association of CA-IX expression with local tumour response is still equivocal. One retrospective study in patients with head and neck carcinomas treated with concurrent chemoradiotherapy did show a correlation with local control rate whereas a study in patients with cervical carcinomas treated with radiotherapy did not.^{19,22} In this study, we found no correlation with locoregional control nor with disease-free survival. Although not consistently so, the available data are supportive of a role for CA-IX as a predictor of tumour aggressiveness reflected in patient survival. Whether CA-IX can serve as a reliable marker of tumour hypoxia and predictor of local outcome remains unclear to date.

To our knowledge, this is the first report presenting data on the predictive value of pimonidazole. Direct measurements of hypoxia with oxygen microelectrodes have been associated with treatment outcome in squamous cell carcinomas of the head and neck and uterine cervix.^{2,4-6} Likewise, the pimonidazole binding assay being also a direct indicator of tumour hypoxia demonstrated a significant association with locoregional control and disease-free survival in the current study. Patients with hypoxic tumours showed a worse initial response to the treatment and more locoregional recurrences within the first 15 months of follow-up (Figure 7A). After this initial period there was no further divergence of the course of the locoregional control or disease-free survival curves (Figures 7A,C). This suggests that the worse outcome of hypoxic tumours is mainly determined by early locoregional

failures and not so much by later events such as distant metastases. Follow-up is still short however, and distant metastases may occur later than 2 years. The observation that the association with locoregional control exists mainly in the non-ARCON treatment group but hardly in the ARCON treatment group (Figure 7B) is a strong indication that pimonidazole binding indeed reflects hypoxic radiation resistance. This also indicates that the nitroimidazole binding assay together with vascular parameters may provide a selection tool for hypoxia modifying treatments on an individual patient basis.

An important limitation of this study is the relatively small sample size and the heterogeneity of the patient selection with regard to tumour site and stage. This could partly explain why no correlations were found between these classical clinical parameters and outcome. However, also in a larger series of 215 ARCON-treated patients, T-stage was no longer a prognostic indicator which may well be the result of the very high local control rates with this treatment.²³ Furthermore, treatment assignment was not randomized and various treatment modalities were used in the non-ARCON group and follow-up is still short. This precludes firm conclusions to be based on this material and verification of the results is needed in a larger patient cohort. A recently started randomized trial comparing ARCON with accelerated radiotherapy in laryngeal cancer with a projected accrual of 344 patients will provide sufficient material to validate the conclusions of this study.

References

1. Hockel M, Vaupel P. Tumor hypoxia: definitions and current clinical, biologic, and molecular aspects. *J Natl Cancer Inst* 2001;93:266-276.
2. Hockel M, Schlenger K, Aral B, *et al.* Association between tumor hypoxia and malignant progression in advanced cancer of the uterine cervix. *Cancer Res* 1996;56:4509-4515.
3. Rofstad EK. Microenvironment-induced cancer metastasis. *Int J Radiat Biol* 2000;76:589-605.
4. Brizel DM, Sibley GS, Prosnitz LR, *et al.* Tumor hypoxia adversely affects the prognosis of carcinoma of the head and neck. *Int J Radiat Oncol Biol Phys* 1997;38:285-289.
5. Nordsmark M, Overgaard J. A confirmatory prognostic study on oxygenation status and loco-regional control in advanced head and neck squamous cell carcinoma treated by radiation therapy. *Radiother Oncol* 2000;57:39-43.
6. Fyles A, Milosevic M, Hedley D, *et al.* Tumor hypoxia has independent predictor impact only in patients with node-negative cervix cancer. *J Clin Oncol* 2002;20:680-687.
7. Brizel DM, Scully SP, Harrelson JM, *et al.* Tumor oxygenation predicts for the likelihood of distant metastases in human soft tissue sarcoma. *Cancer Res* 1996;56:941-943.
8. Nordsmark M, Hoyer M, Keller J, *et al.* The relationship between tumor oxygenation and cell proliferation in human soft tissue sarcomas. *Int J Radiat Oncol Biol Phys* 1996;35:701-708.
9. Raleigh JA, Calkins-Adams DP, Rinker LH, *et al.* Hypoxia and vascular endothelial growth factor expression in human squamous cell carcinomas using pimonidazole as a hypoxia marker. *Cancer Res* 1998;58:3765-3768.
10. Evans SM, Hahn S, Pook DR, *et al.* Detection of hypoxia in human squamous cell carcinoma by EF5 binding. *Cancer Res* 2000;60:2018-2024.
11. Olive PL, Durand RE, Raleigh JA, *et al.* Comparison between the comet assay and pimonidazole binding for measuring tumour hypoxia. *Br J Cancer* 2000;83:1525-1531.
12. Kennedy AS, Raleigh JA, Perez GM, *et al.* Proliferation and hypoxia in human squamous cell carcinoma of the cervix: first report of combined immunohistochemical assays. *Int J Radiat Oncol Biol Phys* 1997;37:897-905.
13. Varia MA, Calkins-Adams DP, Rinker LH, *et al.* Pimonidazole: a novel hypoxia marker for complementary study of tumor hypoxia and cell proliferation in cervical carcinoma. *Gynecol Oncol* 1998;71:270-277.
14. Wijffels KI, Kaanders JH, Rijken PF, *et al.* Vascular architecture and hypoxic profiles in human head and neck squamous cell carcinomas. *Br J Cancer* 2000;83:674-683.
15. Sly WS, Hu PY. Human carbonic anhydrases and carbonic anhydrase deficiencies. *Annu Rev Biochem* 1995;64:375-401.
16. Ivanov S, Liao SY, Ivanova A, *et al.* Expression of hypoxia-inducible cell-surface transmembrane carbonic anhydrases in human cancer. *Am J Pathol* 2001;158:905-919.
17. Lal A, Peters H, St Croix B, *et al.* Transcriptional response to hypoxia in human tumors. *J Natl Cancer Inst* 2001;93:1337-1343.
18. Olive PL, Aquino-Parsons C, MacPhail SH, *et al.* Carbonic anhydrase 9 as an endogenous marker for hypoxic cells in cervical cancer. *Cancer Res* 2001;61:8924-8929.
19. Koukourakis MI, Giatromanolaki A, Sivridis E, *et al.* Hypoxia-regulated carbonic anhydrase-9 (CA-IX) relates to poor vascularization and resistance of squamous cell head and neck cancer to chemoradiotherapy. *Clin Cancer Res* 2001;7:3399-3403.
20. Chia SK, Wykoff CC, Watson PH, *et al.* Prognostic significance of a novel hypoxia-regulated marker, carbonic anhydrase IX, in invasive breast carcinoma. *J Clin Oncol* 2001;19:3660-3668.
21. Giatromanolaki A, Koukourakis MI, Sivridis E, *et al.* Expression of hypoxia-inducible carbonic anhydrase-9 relates to angiogenic pathways and independently to poor outcome in non-small cell lung cancer. *Cancer Res* 2001;61:7992-7998.
22. Lancaster JA, Harris AL, Davidson SE, *et al.* Carbonic anhydrase (CA IX) expression, a potential new intrinsic marker of hypoxia: correlations with tumor oxygen measurements and prognosis in locally advanced carcinoma of the cervix. *Cancer Res* 2001;61:6394-6399.
23. Kaanders JH, Pop LA, Marres HA, *et al.* ARCON: experience in 215 patients with advanced head-and-neck cancer. *Int J Radiat Oncol Biol Phys* 2002;52:769-778.
24. Azuma C, Raleigh JA, Thrall DE. Longevity of pimonidazole adducts in spontaneous canine tumors as an estimate of hypoxic cell lifetime. *Radiat Res* 1997;148:35-42.
25. Schlingemann RO, Dingjan GM, Emeis JJ, *et al.* Monoclonal antibody PAL-E specific for endothelium. *Lab Invest* 1985;52:71-76.

26. Rijken PF, Bernsen HJ, van der Kogel AJ. Application of an image analysis system to the quantitation of tumor perfusion and vascularity in human glioma xenografts. *Microvasc Res* 1995;50:141-153.
27. Rijken PF, Bernsen HJ, Peters JP, *et al.* Spatial relationship between hypoxia and the (perfused) vascular network in a human glioma xenograft: a quantitative multi-parameter analysis. *Int J Radiat Oncol Biol Phys* 2000;48:571-582.
28. Wykoff CC, Beasley NJ, Watson PH, *et al.* Hypoxia-inducible expression of tumor-associated carbonic anhydrases. *Cancer Res* 2000;60:7075-7083.
29. Beasley NJ, Wykoff CC, Watson PH, *et al.* Carbonic anhydrase IX, an endogenous hypoxia marker, expression in head and neck squamous cell carcinoma and its relationship to hypoxia, necrosis, and microvessel density. *Cancer Res* 2001;61:5262-5267.
30. Gross MW, Karbach U, Groebe K, *et al.* Calibration of misonidazole labeling by simultaneous measurement of oxygen tension and labeling density in multicellular spheroids. *Int J Cancer* 1995;61:567-573.
31. Arteel GE, Thurman RG, Yates JM, *et al.* Evidence that hypoxia markers detect oxygen gradients in liver: pimonidazole and retrograde perfusion of rat liver. *Br J Cancer* 1995;72:889-895.
32. Ljungkvist AS, Bussink J, Rijken PF, *et al.* Changes in tumor hypoxia measured with a double hypoxic marker technique. *Int J Radiat Oncol Biol Phys* 2000;48:1529-1538.
33. Vukovic V, Haugland HK, Nicklee T, *et al.* Hypoxia-inducible factor-1alpha is an intrinsic marker for hypoxia in cervical cancer xenografts. *Cancer Res* 2001;61:7394-7398.
34. Aebbersold DM, Burri P, Beer KT, *et al.* Expression of hypoxia-inducible factor-1alpha: a novel predictive and prognostic parameter in the radiotherapy of oropharyngeal cancer. *Cancer Res* 2001;61:2911-2916.
35. Jenssen N, Boysen M, Kjaerheim A, *et al.* Low vascular density indicates poor response to radiotherapy in small glottic carcinomas. *Pathol Res Pract* 1996;192:1090-1094.
36. Aebbersold DM, Beer KT, Laissue J, *et al.* Intratumoral microvessel density predicts local treatment failure of radically irradiated squamous cell cancer of the oropharynx. *Int J Radiat Oncol Biol Phys* 2000;48:17-25.
37. Koukourakis MI, Giatromanolaki A, Sivridis E, *et al.* Cancer vascularization: implications in radiotherapy? *Int J Radiat Oncol Biol Phys* 2000;48:545-553.
38. Brewer CA, Liao SY, Wilczynski SP, *et al.* A study of biomarkers in cervical carcinoma and clinical correlation of the novel biomarker MN. *Gynecol Oncol* 1996;63:337-344.

Chapter 4

The prognostic value of endogenous hypoxia-related markers for head and neck squamous cell carcinomas treated with ARCON

R.A. Jonathan#
K.I.E.M. Wijffels#
W. Peeters
P.C.M. de Wilde
H.A.M. Marres
M.A.W. Merks
E. Oosterwijk
A.J. van der Kogel
J.H.A.M. Kaanders

Abstract

Background and Purpose

Hypoxic radioresistance is an important cause for treatment failure in a number of tumour types including head and neck cancers. Recent studies suggest that outcome can be improved by oxygenation modifying treatments such as ARCON. A robust endogenous marker of hypoxia might be a valuable aid to select patients for such treatments. The aim of this investigation was to study associations between the putative endogenous hypoxia markers CA-IX, Glut-1 and Glut-3 and clinical tumour and patient characteristics and to evaluate the prognostic value of these markers.

Material and Methods

Tumour biopsies from 58 patients treated with ARCON in a phase II trial were included. Tumour sections were immunohistochemically stained for CA-IX, Glut-1 and Glut-3. Sections were scored for relative tumour area stained by the markers (CA-IX and Glut-3) and for intensity of staining (Glut-1 and Glut-3). Further, sections were stained for CD34, an endothelial marker to assess microvascular density.

Results

Staining of CA-IX and Glut-3 was observed at some distance from vessels and adjacent to necrosis. Glut-1 staining was generally very diffuse. The distribution of clinical characteristics was equal between tumours with high and low marker expression. Significant differences were found for locoregional control ($p=0.04$) and for freedom of distant metastases ($p=0.02$) in favour of patients with high CA-IX positivity ($>25\%$ of tumour area). High Glut-3 expression was associated with a better locoregional control ($p=0.04$). Higher Glut-1 intensity was associated with an increased rate of distant metastases ($p=0.0005$) and a worse overall survival ($p=0.001$).

Conclusions

The inconsistent associations with outcome of CA-IX and the glucose transporters indicate that different factors play a role in upregulation of these markers. Compared to studies with conventional treatment, the correlation between CA-IX expression and Glut-3 expression and outcome was reversed after treatment with ARCON. This does not support the potential of any of these proteins as very specific and robust hypoxia markers.

Introduction

Oxygenation status is an important factor in the radiation response of solid tumours. Hypoxia is associated with malignant tumour progression and is a cause of resistance to ionizing radiation. Tools increasingly used to study hypoxia are the exogenous nitro-imidazole markers, which are detectable by immunohistochemistry. Pimonidazole and etanidazole (EF-5) have been proven to be sensitive markers in experimental studies and are being evaluated in the clinical setting for assessment of tumour hypoxia.¹⁻⁶ A disadvantage of these markers is that they have to be injected intravenously prior to biopsy taking. An intrinsic marker of hypoxia, which does not require additional interventions beyond the initial pretreatment biopsy, is therefore attractive. In addition, studies can then be done retrospectively on archival biopsies. Several endogenous markers have been suggested as hypoxia or hypoxia-related markers, like HIF-1, CA-IX, Glut-1 and -3 (glucose transporter), VEGF and osteopontin.⁷⁻¹⁸ Carbonic anhydrase IX (CA-IX) is under transcriptional control by the hypoxia-inducible-factor 1 (HIF-1).^{12,17} It is a transmembrane glycoprotein often expressed in perinecrotic areas and a weak relationship with pimonidazole binding has been reported.^{3,17,19} Carbonic anhydrases are involved in energy metabolism and acid-base balance and catalyze the reversible hydration of CO_2 to HCO_3^- .²⁰ CA-IX has been described as being upregulated in head and neck squamous cell carcinomas.¹⁹ Expression of CA-IX has been shown to be associated with a more aggressive tumour behavior and a worse prognosis in some tumour types.^{9,13,19} Other studies, however, show no or reverse associations.^{3,10,21-23} Variable results are reported regarding the association with tumour vascularity.^{3,9,19}

The switch from oxidative phosphorylation to anaerobic glycolysis in hypoxic tumour cells is accompanied by an increase in glucose requirements and transport. Glucose transporters (Gluts) are upregulated in cells of many different tumours and mediate passive glucose uptake. They are induced by hypoxia and decreased oxidative phosphorylation, via HIF-1.¹⁸ Glut-1 is almost always expressed in head and neck squamous cell tumours while Glut-3 shows greater inter-tumour variability.²⁴ Few studies have explored the association between hypoxia and expression of glucose transporters in human tumours with equivocal results.^{8,14}

There is interest in measurements of vascularity as a reflection of oxygenation status but few clinical studies have addressed this issue and the results are inconclusive.^{3,9,25} Another indistinct point is the association between vascular density or other vascular parameters and prognosis. In the past decade, many

studies have been performed without really clarifying this relationship. Some investigators found a higher vascular density to be associated with an increased rate of distant metastases and a shorter overall survival,^{26,27} whereas others did not find any correlation.^{28,29}

In this study, we investigated the putative endogenous hypoxia markers CA-IX, Glut-3 and Glut-1 in a series of head and neck squamous cell carcinomas treated with primary radiotherapy. Correlations between the expression of the different markers and between marker expression and clinical tumour and patient characteristics were studied. In addition, we investigated the prognostic value of CA-IX, Glut-3 and -1 and microvascular density (MVD) in relation to locoregional control, freedom of distant metastases and overall survival after radiotherapy with hypoxic modification. We hypothesized that expression of these markers in tumour cells would predict an increased risk of distant metastases and a worse overall survival, because hypoxia is known to be associated with increased metastatic potential and a poor overall survival.³⁰⁻³² We anticipated that a potential association with locoregional control might be negated by the hypoxia modifying components of the treatment.

Materials and methods

Patients and treatment

At the Department of Radiation Oncology of the Radboud University Nijmegen Medical Centre, a phase II clinical trial of ARCON (accelerated radiotherapy with carbogen and nicotinamide) in advanced squamous cell carcinomas of the head and neck has recently been completed.³³ ARCON combines accelerated radiotherapy with carbogen breathing and nicotinamide to reduce diffusion-limited and perfusion-limited hypoxia, respectively. Eligibility criteria for this study were: (a) stage III or IV squamous cell carcinoma of the oral cavity, oropharynx, hypopharynx or larynx and stage II hypopharynx carcinomas with a greatest dimension of the primary tumour > 2 cm³⁴; (b) age over 18 years; (c) WHO performance status of 0-2; (d) no distant metastases; (e) no severe heart or lung disease; (f) no liver or kidney function impairments; (g) no severe stridor; (h) no concurrent treatment for other malignant disease outside the upper aero-digestive tract.

Biopsy material was obtained from patients that satisfied the eligibility criteria between January 1993 and September 2000. Further criteria were availability of biopsies and sufficient material in the biopsy. Biopsies were taken for routine

diagnostic purposes and were retrieved from the Department of Pathology in our hospital. All patients underwent a diagnostic workup, which included physical examination, blood cell count, blood chemistry, chest X-ray, CT-scan and/or MRI-scan of the head and neck area and examination under anaesthesia.

All patients were treated with ARCON as described previously.³³ They received 64-68 Gy to the primary tumour and involved neck nodes and 44 Gy to electively treated areas. The dose per fraction was 2 Gy and two fractions per day were given during the last 1.5 weeks of the treatment with an overall treatment time of 36-38 days. During the irradiations patients breathed carbogen and they received nicotinamide, 60-80 mg/kg orally, 1-1.5 h prior to the start of irradiations.

Immunohistochemistry

Staining for CA-IX and CD34

For vessel staining, 5 µm sections were incubated for 60 min with mouse monoclonal antihuman CD34, followed by 30 min with horse-antimouse antibody, and next with avidin-biotin complex for 30 min. Biotinyl-tyramide (Department of Pathology, Radboud University Nijmegen Medical Centre, The Netherlands) was applied for 5 min for subsequent amplification. After incubation with streptavidin β-galactosidase for 30 min, colour development was established with β-galactosidase (Department of Pathology, Radboud University Nijmegen Medical Centre, The Netherlands). For epitope retrieval of CA-IX, sections were boiled for 13 min in 10 mM citratebuffer of pH 6.0. Then sections were incubated with mouse anti-CA-IX antibody (Egbert Oosterwijk, Department of Urology, Radboud University Nijmegen Medical Centre) for 60 min, horse-antimouse antibody for 30 min, and ABC reagent for 30 min. Peroxidase activity was detected with di-amino benzidine (DAB). Finally, sections were counterstained with haematoxylin and mounted with Permount.

Staining for Glut-3 and CD34

The slides were incubated at 4°C overnight with mouse monoclonal antihuman CD34 and goat antihuman Glut-3. After rinsing with PBS, endogenous peroxidase was blocked with 3% H₂O₂ in methanol. Then, sections were incubated for 1 h with a mixture of secondary antibodies: alkaline-phosphatase conjugated donkey-anti-mouse and biotin conjugated donkey-anti-goatF(ab')₂. Sections were then incubated with fast red substrate solution for 25 min to develop an intense red vascular stain. After this, sections were incubated for 30 min with ABC-reagent. Peroxidase activity was detected with DAB. Finally, sections were counterstained with haematoxylin for 30 sec and mounted with Fluorostab.

For negative controls, instead of the primary antibodies, slides were incubated with MLD.

Staining for Glut-1 and CD34

The staining protocol for Glut-1 was similar to that of Glut-3. Instead of goat-antihuman Glut-3, rabbit-antihuman Glut-1 was used and biotin conjugated donkey-anti-rabbit was used as the secondary antibody.

Scoring

Scoring of CA-IX

We used a semi-quantitative method for scoring CA-IX positive areas as described and validated for pimonidazole staining by Raleigh et al.³⁵, with some modifications. The complete tumour area was scored with a light microscope using an objective of 25x and ocular of 12.5x magnification and the same light intensity for all tumours. The classes 0-5%, 5-15%, 15-30%, 30-50% and >50% CA-IX positive area per field of the tumour area were assigned semi-quantitative scores of 0, 1, 2, 3 and 4, respectively. Areas of stroma, necrosis, acellularity or keratinisation were not included as tumour area. A median value for each tumour was computed correcting for range width, using the formula:

$$Med = X_{ll} + \frac{\frac{n}{2} - F_{c-1}}{f_c} * (X_{ul} - X_{ll})$$

(X_{ll} , lower limit of class containing median of field scores; X_{ul} , upper limit of class containing median; f_c , frequency of class containing median; F_{c-1} , cumulative frequency of class under class containing median and n , total number of observations). When more than one biopsy per tumour was available both biopsies were pooled for analyses. All scoring was done without knowing patient outcome.

Scoring of Glut-3 and Glut-1

The same scoring system for staining area was used for Glut-3. There was a large variability in the intensity of the Glut-3 staining. We therefore also scored the staining intensity as described by Airley et al.⁷ Sections were viewed at a magnification of 50x and given a score for staining intensity (0, no staining; 1, weak staining; 2, medium staining; 3, heavy staining).

It was not possible to quantify the Glut-1 positive area because staining of the tumour was diffuse in most biopsies so Glut-1 was scored for intensity only.

Microvascular density

Microvascular density (MVD) was assessed as described often in literature. At low magnification three fields of vision of high vascularization per tumour were chosen. Microvessel counting was performed with an objective of 25x and ocular of 12.5x magnification. MVD was the mean value of the three appraised fields of vision.

Statistics

All statistical analyses were done on a personal computer using the SPSS 12.0.1[®] statistical package.

Correlations between numerical variables were obtained using Spearman's rank correlation. Survival analysis was performed by the Kaplan-Meier product limit method, and survival rates were compared using the logrank statistic. Cox regression analysis was used for confounder analysis. All time-dependent outcomes were calculated from time of pathological diagnosis, and patient data were censored when a disease event had not occurred at the last follow-up. For the endpoint "locoregional control" an event was recurrence at the primary tumour site or in the regional lymph nodes. Patients without locoregional recurrence were censored at the date of last follow-up. For the endpoint "freedom of distant metastases" an event was occurrence of hematogenous metastases. Patients without distant metastases were censored at the date of last follow-up. For overall survival, all deaths were analyzed as event and patients still alive were censored at the date of last follow-up. P-values below 0.05 were considered significant.

Results

Patients and clinical tumour characteristics

Biopsy material was obtained from 71 patients. Thirteen biopsies were excluded, 12 because the sample contained only little or no invasive carcinoma and one patient was diagnosed with two primary tumours. So, 58 patients with squamous cell carcinomas were included. Of those, 43 were men and 15 were women. Median age at the time of diagnosis was 58 years (range 41-87). Mean pre-treatment hemoglobin concentration was 14.2 g/dl (range 9.2-16.8). Two patients had a hemoglobin concentration under 11.3 g/dl (7.0 mmol/l). Primary tumours were localized in the larynx (42), oral cavity (5), hypopharynx (8) and oropharynx (3). Differentiation grade was distributed as follows: 2 tumours grade 1, 38 grade 2, 17 grade 3 and 1 grade 4. All patients were treated with ARCON. One patient

had to discontinue nicotinamide because of side effects and another patient refused carbogen and nicotinamide after a week and continued treatment with radiotherapy alone. Median follow-up time for patients alive at the time of analysis was 5.1 years. Patient and tumour characteristics and associations with marker expression are summarized in table 1.

Table 1. Patient and tumour characteristics of 58 head and neck cancer patients (UICC 1992)³⁴

	All	CA-IX area		Glut-3 area		Glut-1 intensity score		MVD	
		<med	>med	<med	>med	0-1	2-3	<med	>med
Age									
mean	60.0	59.5	60.4	59.6	60.4	60.2	59.0	57.0	62.4
range	41-87	41-87	46-82	41-82	46-87	41-87	47-76	41-82	47-87
Gender									
male	43	20	23	21	22	36	7	22	21
female	15	9	6	8	7	13	2	7	8
Tumour site									
larynx	42	22	20	18	24	34	8	21	21
hypopharynx	8	5	3	4	4	8	0	5	3
oropharynx	3	0	3	2	1	2	1	1	2
oral cavity	5	2	3	5	0	5	0	2	3
T-stage									
T1	4	2	2	1	3	2	2	2	2
T2	16	12	4	9	7	15	1	10	6
T3	27	12	15	11	16	22	5	12	15
T4	11	3	8	8	3	10	1	5	6
N-stage									
N0	25	11	14	10	15	22	3	14	11
N1	16	6	10	10	6	13	3	6	10
N2	17	12	5	9	8	14	3	9	8
Hemoglobin									
mean	14.2	14.0	14.0	14.2	14.0	14.2	13.7	14.4	14.0
range	9.2-16.8	9.8-16.8	9.2-16.3	12.3-16.3	9.2-16.8	9.2-16.8	9.8-15.5	12.3-16.3	9.2-16.8
Diff. Grade									
1	2	0	2	1	1	1	1	1	1
2	38	18	20	19	19	34	4	18	20
3	17	10	7	9	8	13	4	10	7
4	1	1	0	0	1	1	0	0	1

The distribution of clinical characteristics was equal between tumours with high and low marker expression. None of the clinical characteristics demonstrated a correlation with locoregional control or survival.

Staining of CA-IX and glucose-transporters

The median of CA-IX staining amongst all tumours was 6.0% of the tumour area. Many tumours demonstrated little or no CA-IX expression (Figure 1A). Staining was mostly limited to tumour cell membranes, but a weak cytoplasmatic staining was also observed. Positive staining, when present, was observed at some distance from vessels and around necrosis (Figures 2A and D).

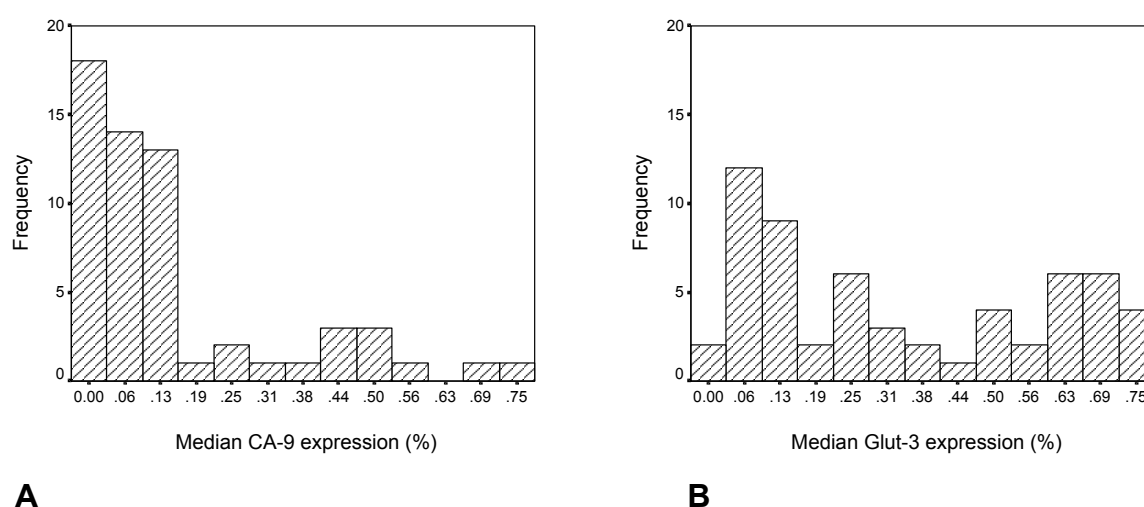


Figure 1. Distribution of median CA-IX expression (A) and Glut-3 expression (B).

Overall, Glut-3 expression was more pronounced than CA-IX, with a median staining area of all tumours of 25.1% of the total tumour area and larger heterogeneity between tumours (Figure 1B). Glut-3 expression was often observed at a distance from vessels (Figures 2B and E), but more diffuse staining patterns with Glut-3 in areas close to vessels were also observed. Glut-3 expression occurred in the cytoplasm of tumour cells and stromal areas. Between the Glut-3 positive area and the overall intensity of Glut-3 there was a significant correlation with $r_s = 0.71$ ($p < 0.01$).

For Glut-1, a very diffuse staining of the entire tumour area was generally observed (Figure 2C). Therefore, scoring of relative tumour area stained by Glut-1 was not possible and only intensity of staining was scored. The overall intensity of Glut-1 was weak in most cases (score 1), but the majority of the tumours (75%) also contained focal areas with higher staining intensity (Figure 2F).

Correlations between CA-IX, Glut-3 and microvascular density

Staining of CD34 was very intense and vessels were easy to identify (Figure 2). The median microvascular density (MVD) of all tumours was 38 per microscopic field (range 7-132). A very weak but significant negative correlation was found between MVD and CA-IX expression: $r_s = -0.27$ ($p = 0.04$). No correlation was found between MVD and Glut-expression.

Also, no correlations were found between CA-IX expression and Glut-expression, neither for relative marker positive tumour area nor for intensity of staining.

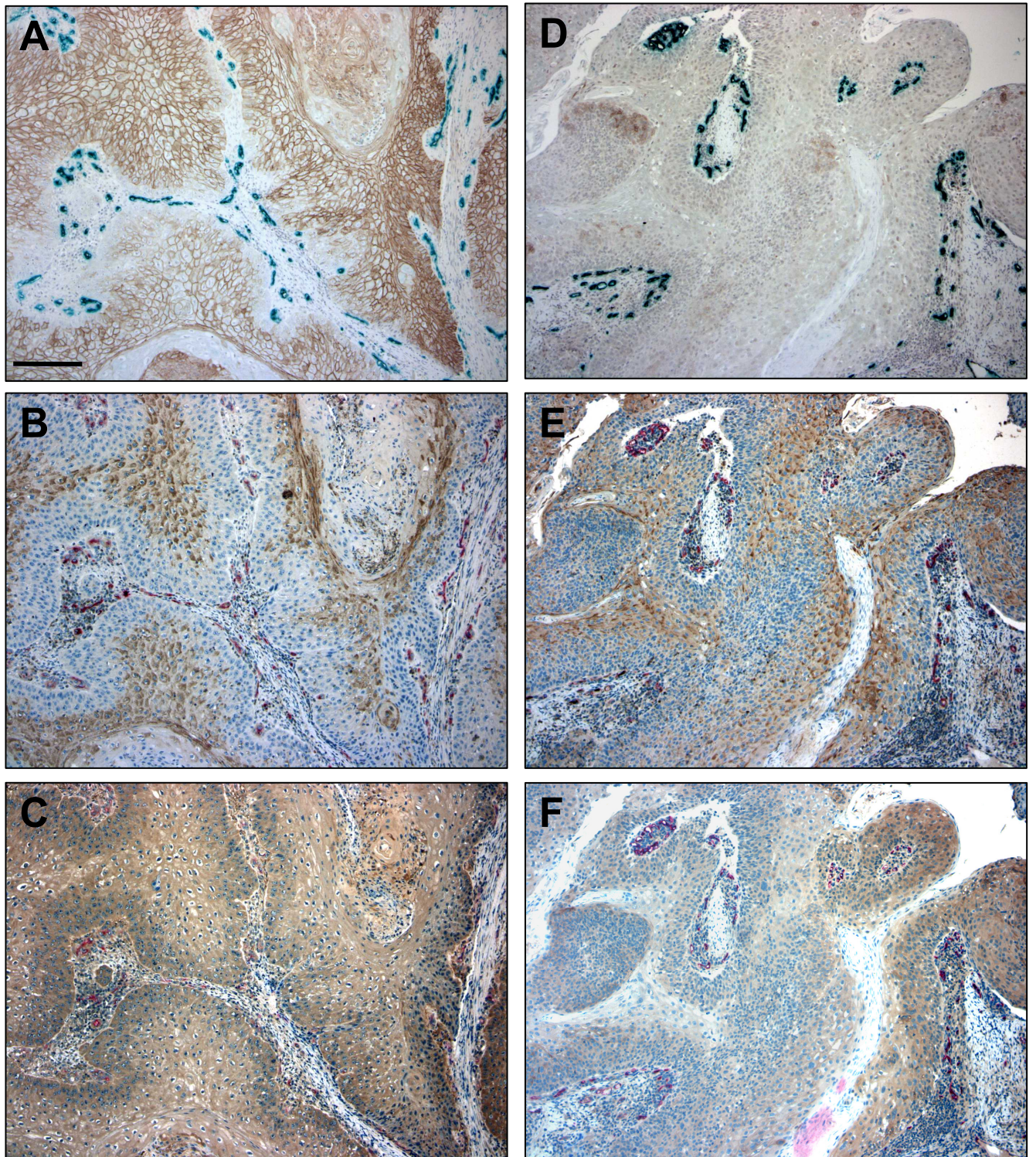


Figure 2. Different staining patterns and scores of CA-IX, Glut-3 and Glut-1 in consecutive sections of two different tumours (A-C and D-F). There is co-localization but also significant mismatch of the three markers. A) CA-IX, score 4; B) Glut-3, score 3; C) Glut-1, intensity score 3; D) CA-IX, score 0; E) Glut-3, score 4; F) Glut-1, intensity score 1, focal areas with intensity score 3. Bar represents 0.1 mm.

Table 2. Logrank analysis of outcome dichotomized by hypoxia-related marker expression and MVD. NS: not significant, significant at $p \leq 0.05$. [¶]In favour of patients with high CA-IX or Glut-3 expression. ^{\$}In favour of patients with low Glut-1 expression

Parameter	Overall survival	Locoregional control	Freedom from distant metastases
CA-IX area median	NS	NS	NS
CA-IX area 80 th percentile	NS	0.04 [¶]	0.02
Glut-3 area median	NS	NS	NS
Glut-3 intensity 0,1 vs 2,3	NS	0.04 [¶]	NS
Glut-1 intensity 0,1 vs 2,3	0.001 ^{\$}	NS	0.0005 ^{\$}
MVD median	NS	NS	NS

Correlations with outcome

Results of Kaplan-Meier estimates and logrank analyses are summarized in table 2.

CA-IX

When dichotomized by the median of relative tumour area staining positive for CA-IX, no correlations were found between CA-IX expression and outcome. Because of the skewed distribution and many low percentages of CA-IX positive areas (Figure 1A), an additional analysis was done after stratification by the 80th percentile resulting in a group with no to medium CA-IX expression (CA-IX staining area $\leq 25\%$, $n = 46$) and a group with high CA-IX expression (CA-IX staining area $> 25\%$, $n = 12$). This analysis demonstrated a significant association with outcome with better locoregional control ($p = 0.04$) and freedom of distant metastases ($p = 0.02$) for patients with high CA-IX expression (Figures 3A and B). Of the patients with tumours showing high CA-IX expression levels, none developed local or distant recurrences. CA-IX expression and the conventional prognostic factors T-stage, N-stage, site of tumour, differentiation, age and gender were included in a univariate Cox regression analysis. None of these factors except CA-IX expression had an effect on prognosis for any of the outcome parameters. Multivariate Cox regression analyses were then carried out to examine the prognostic significance of CA-IX, Glut-1 and -3 expression after allowing for age, gender, pre-treatment hemoglobin concentration, T- and N-stage, differentiation grade and tumour site. The adjusted relative risk of high CA-IX expression increased compared to the univariate analysis indicating that none of these factors acted as a confounder.

Glut-3

After stratification of the tumours by the median of Glut-3 relative staining area, no differences were found between the two groups for any of the endpoints. When stratifying for overall intensity of Glut-3 between no or weak staining (score 0 or 1) and medium to heavy staining (score 2 or 3), a significant difference was found for locoregional control ($p = 0.04$), no or weak staining having a worse prognosis than medium or heavy staining (Fig 3C).

Glut-1

For Glut-1, only intensity of staining was scored. Patients with a higher intensity score (score 2 and 3) had a higher distant metastases rate ($p = 0.0005$) and a worse overall survival ($p = 0.001$) compared with patients with low scores of overall intensity (score 0 and 1) (Figure 3D).

MVD

For MVD, no significant correlations with any of the endpoints were found.

Discussion

In this study we investigated the value of the putative endogenous hypoxia markers CA-IX, Glut-3 and Glut-1. Associations between the expression of the different markers and between marker expression and clinical tumour and patient characteristics were investigated. Further, the prognostic value of these hypoxia markers and MVD was studied in a series of patients with head and neck squamous cell carcinomas treated with ARCON.

Clinical parameters

In head and neck cancer important prognostic indicators for locoregional control and freedom from distant metastases are T-stage and N-stage. In this study we could not demonstrate any prognostic significance of these clinical parameters. This is consistent with a previous analysis of a larger series of head and neck cancer patients treated with ARCON and suggests that the more advanced tumours benefit most from oxygenation modifying treatment.³ With the disappearance of these major clinical parameters, biologic factors may become the more important predictors for treatment outcome. Also, in the current study, there was no association between tumour site and outcome but this can be explained by the fact that most of the patients had larynx tumours and only a minority (28%) had tumours at other head and neck sites.

No correlations were found between patient characteristics and clinical tumour parameters and expression of any of the hypoxia-related markers or MVD. This suggests that the expression of these molecular markers is relatively independent of host factors and tumour stage. Two other studies did find correlations between CA-IX expression and age and tumour stage in cervix carcinoma but the results were contradictory.^{13,22} The literature is more consistent with respect to the relationship with histological grade: in poorly differentiated tumours decreased CA-IX expression but increased expression of Glut-1 and Glut-3 has been described.^{20,22,36,37} This opposite relationship with differentiation grade could not be confirmed in the current material but it indicates that expression of CA-IX and the glucose transporters, although both HIF-1 and thus hypoxia-dependent, do not necessarily behave in a coherent fashion.

CA-IX

CA-IX is under transcriptional control by HIF-1 α and has been shown to be increasingly upregulated after exposure to decreasing oxygen tensions.^{12,17,38} This dependency and the observation that CA-IX is expressed in a variety of tumour types has led to the suggestion that it might be a useful endogenous marker of tumour hypoxia and a potential indicator of tumour aggressiveness and poor outcome. This hypothesis is supported by the study in head and neck cancers by Koukourakis et al. which demonstrated that patients with CA-IX-expressing tumours had significantly poorer local relapse-free survival and overall survival.²⁰ Assuming that ARCON counteracts hypoxic radiation resistance resulting in improvement of locoregional tumour control primarily in the patients with the more hypoxic tumours, we hypothesized that the predictive potential of CA-IX expression for locoregional control would decrease or disappear in the current material. A correlation with occurrence of distant metastases might still be found however, because the treatment is not expected to affect metastatic potential. Unexpectedly, patients with tumours showing a higher CA-IX staining area had a better locoregional control and freedom from distant metastases after treatment with ARCON. No confounders were found for this association. Although the group showing a high CA-IX staining was fairly small ($n = 12$), the difference between survival parameters for the two groups was considerable and consistent for the two endpoints. A previous study from our institute, also on a series of patients with head and neck tumours receiving different treatments, showed no correlation between CA-IX expression and outcome.¹⁹ However, a subgroup ($n = 24$) that was treated with ARCON showed a non-significant trend for better outcome with

high CA-IX expression as well. Whether this unexpected result can be attributed to the hypoxia-modifying components of the treatment is a question that cannot be resolved with the current material. An ongoing randomized trial with ARCON in larynx carcinoma may address this issue. There is one other study that has correlated CA-IX and Glut-1 expression with outcome after treatment with ARCON. This study by Hoskin et al. in 64 patients with bladder cancer showed that the two markers were highly correlated with each other and were independent predictors for overall and cause-specific survival but not for local control or distant metastases rate.¹¹

Studies exploring the prognostic relevance of CA-IX in other tumour types produced ambiguous results, some confirming the anticipated association with adverse outcome but others showing no or even the reverse association.^{9,10,13,22-24}

Several studies showed to some degree a co-localization of pimonidazole binding and CA-IX expression but the correlation is often weak.^{11,15,17,19,39} These clinical investigations indicate that the role of CA-IX as an intrinsic marker of hypoxia and a prognosticator of outcome remains equivocal. Combination with assays that assess other aspects of the tumour microenvironment as for example vascularity, proliferation and apoptosis, may provide a panel of markers and a more powerful approach towards development of predictive tools.^{20,40,41}

Glut-3

Compared to CA-IX, Glut-3 expression generally involved larger tumour areas. Like CA-IX, Glut-3 was often observed around necrotic areas but more diffuse staining near vessels was also observed. Further, the intensity of Glut-3 staining showed a larger variability. For this reason, both the relative positive area and the intensity of staining were scored. No correlations were found between Glut-3 and CA-IX positivity.

The relative Glut-3 staining area was not associated with outcome. Low overall intensity score of Glut-3 was correlated with worse locoregional control but there were no significant correlations with occurrence of distant metastases or overall survival. Only a few studies have related Glut-3 expression to outcome. A high Glut-3 expression was associated with a worse survival in laryngeal carcinoma and non-small cell lung carcinoma.^{36,37} Our observation is not in concordance with these reports, but is consistent with the reverse relationship also found for CA-IX in this material.

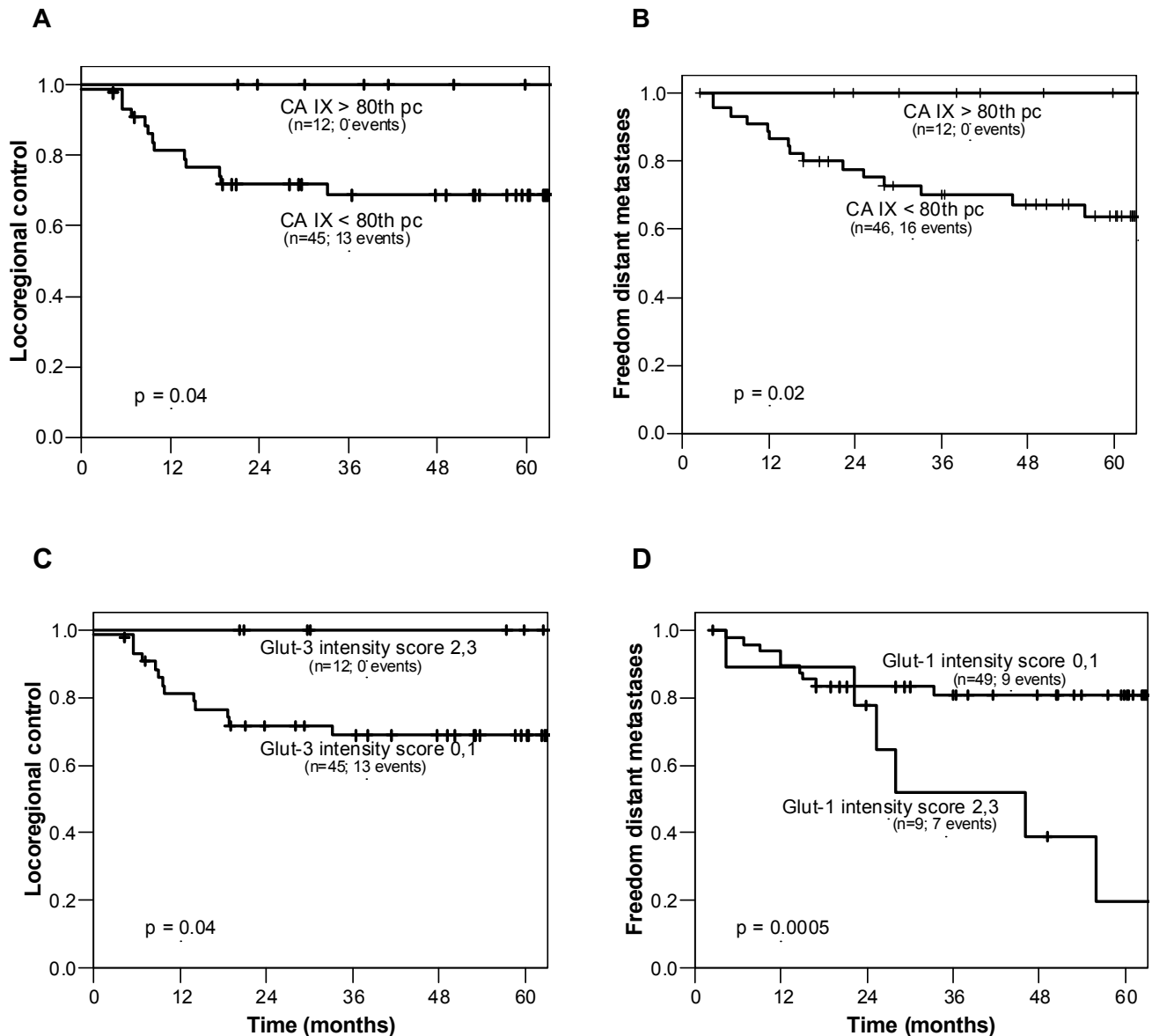


Figure 3. Locoregional control (A) and freedom from distant metastases (B) after stratification by the 80th percentile of CA-IX staining surface. Locoregional control stratified for overall intensity of Glut-3 staining (C) and freedom from distant metastases stratified for overall intensity of Glut-1 staining (D). Small vertical lines on plots indicate censored cases.

Glut-1

The expression of Glut-1 was weak and very diffuse in most biopsies. The Glut-1 isoform is expressed at some level in many cell types.⁴² Previous studies demonstrated that Glut-1 mRNA or the Glut-1 protein was elevated in almost all head and neck tumours,^{25,36,43,44} expression occurring early in the development of these tumours.²⁵ However, only one of these studies reported this diffuse expression of Glut-1.²⁵ For cervix carcinomas, diffuse staining was described as well.⁷ Whether these different observations must be explained by different staining

techniques, different antibodies or by organ-specific differences in expression is unclear. It does however indicate that results must be interpreted cautiously, especially when studies are compared that use different antibodies.

Patients with a higher overall intensity of Glut-1 staining had an increased rate of distant metastases and a worse overall survival compared with patients with low intensity scores but there was no difference in locoregional control. In particular the correlation with metastatic rate was highly significant. In contrast to our results for CA-IX and Glut-3 expression, this was in concordance with our hypothesis that, if the enhanced expression of glucose transporters represents hypoxia, no difference was expected for locoregional control, since ARCON counteracts hypoxic radioresistance responsible for the worse locoregional outcome. Glut-1 has been studied more extensively than Glut-3. Its prognostic value has been investigated for squamous cell carcinoma of the oral cavity, larynx, hypopharynx and oesophagus, and in breast, gastric, colorectal, bladder, cervix and non-small cell lung carcinomas, and was shown to be indicative of poor prognosis in most studies.^{7,36,37,43-49}

There was no correlation between CA-IX and Glut-1 expression. Both markers have been related to hypoxia, but there are some differences. The Glut-1 response to hypoxia exhibits an early and late phase. During the early phase of the response (0-2 h) Glut-1 proteins already present on the cell membrane are probably activated and their affinity increased, and Glut-1 proteins present in the cell are translocated to the cell membrane, resulting in a strongly enhanced glucose transport rate. The late phase (8-24 h) is characterized by a further enhancement of glucose transport associated with increments in cellular Glut-1 and Glut-1 mRNA content.⁴⁹ So Glut-1 might reflect both chronic and (sub-)acute hypoxia, since Glut-1 is constitutively present in the cell and can be activated almost immediately, in contrast to CA-IX that needs a longer time course to be upregulated. Secondly, Glut-1 expression is also a consequence of glucose starvation and reflects high, though inefficient, glucose metabolism, in contrast to CA-IX.⁵⁰ Thirdly, ARCON therapy might be a factor accounting for the inconsistent effects of the Glut's and CA-IX on survival endpoints, since both markers are associated with a worse outcome in studies employing conventional therapies. With ARCON, CA-IX and Glut-3 seem to be associated with a better outcome. Carbogen and nicotinamide can counteract hypoxia, but their effects on glucose availability are largely unknown. This might also explain why CA-IX and the Glut's predict differently for outcome after ARCON treatment.

MVD

No association between MVD and the various endpoints was found. Patients were also stratified by tertiles to investigate the 'U-shaped' association between death rate and MVD, as described by Koukourakis et al.⁵¹ These authors observed that tumours with very low MVD and very high MVD had poor outcome whereas tumours in the intermediate group did better. This association was not confirmed in the current material. There was a very weak but significant negative correlation between MVD and CA-IX area staining. This might indicate consistence with the significance of CA-IX as a marker of (chronic) hypoxia. No association was found between MVD and the other markers studied.

Conclusion

This study indicates that dissimilarities exist between the glucose transporters and CA-IX regarding their significance as clinically relevant hypoxia-related markers. There was no correlation between CA-IX staining area and Glut-3 or Glut-1 area or intensity and neither of the markers demonstrated any correlations with clinical patient and tumour characteristics. Further, their associations with outcome parameters were inconsistent indicating that other factors are also responsible for upregulating the different markers. This does not support the potential of any of these proteins as very specific and robust hypoxia markers. A limitation of this study is the relatively small sample size and the heterogeneity of the material. This precludes firm conclusions and verification of the results is needed in a larger patient cohort. An ongoing randomized trial comparing ARCON with accelerated radiotherapy in laryngeal cancer will provide sufficient material to validate the conclusions of the current study.

References

1. Evans SM, Hahn S, Pook DR, *et al.* Detection of hypoxia in human squamous cell carcinoma by EF5 binding. *Cancer Res* 2000;60:2018-2024.
2. Hoskin PJ, Sibtain A, Daley FM, *et al.* The immunohistochemical assessment of hypoxia, vascularity and proliferation in bladder carcinoma. *Radiother Oncol* 2004;72:159-168.
3. Kaanders JH, Pop LA, Marres HA, *et al.* ARCON: experience in 215 patients with advanced head-and-neck cancer. *Int J Radiat Oncol Biol Phys* 2002;52:769-778.
4. Olive PL, Durand RE, Raleigh JA, *et al.* Comparison between the comet assay and pimonidazole binding for measuring tumour hypoxia. *Br J Cancer* 2000;83:1525-1531.
5. Salmon HW, Siemann DW. Utility of ¹⁹F MRS detection of the hypoxic cell marker EF5 to assess cellular hypoxia in solid tumors. *Radiother Oncol* 2004;73:359-366.
6. Yaromina A, Holscher T, Eicheler W, *et al.* Does heterogeneity of pimonidazole labelling correspond to the heterogeneity of radiation-response of FaDu human squamous cell carcinoma? *Radiother Oncol* 2005;76:206-212.
7. Airley R, Loncaster J, Davidson S, *et al.* Glucose transporter glut-1 expression correlates with tumor hypoxia and predicts metastasis-free survival in advanced carcinoma of the cervix. *Clin Cancer Res* 2001;7:928-934.
8. Airley RE, Loncaster J, Raleigh JA, *et al.* GLUT-1 and CAIX as intrinsic markers of hypoxia in carcinoma of the cervix: relationship to pimonidazole binding. *Int J Cancer* 2003;104:85-91.
9. Giatromanolaki A, Koukourakis MI, Sivridis E, *et al.* Expression of hypoxia-inducible carbonic anhydrase-9 relates to angiogenic pathways and independently to poor outcome in non-small cell lung cancer. *Cancer Res* 2001;61:7992-7998.
10. Hedley D, Pintilie M, Woo J, *et al.* Carbonic anhydrase IX expression, hypoxia, and prognosis in patients with uterine cervical carcinomas. *Clin Cancer Res* 2003;9:5666-5674.
11. Hoskin PJ, Sibtain A, Daley FM, *et al.* GLUT1 and CAIX as intrinsic markers of hypoxia in bladder cancer: relationship with vascularity and proliferation as predictors of outcome of ARCON. *Br J Cancer* 2003;89:1290-1297.
12. Lal A, Peters H, St Croix B, *et al.* Transcriptional response to hypoxia in human tumors. *J Natl Cancer Inst* 2001;93:1337-1343.
13. Loncaster JA, Harris AL, Davidson SE, *et al.* Carbonic anhydrase (CA IX) expression, a potential new intrinsic marker of hypoxia: correlations with tumor oxygen measurements and prognosis in locally advanced carcinoma of the cervix. *Cancer Res* 2001;61:6394-6399.
14. Mayer A, Hockel M, Wree A, *et al.* Microregional expression of glucose transporter-1 and oxygenation status: lack of correlation in locally advanced cervical cancers. *Clin Cancer Res* 2005;11:2768-2773.
15. Olive PL, Aquino-Parsons C, MacPhail SH, *et al.* Carbonic anhydrase 9 as an endogenous marker for hypoxic cells in cervical cancer. *Cancer Res* 2001;61:8924-8929.
16. Said HM, Katzer A, Flentje M, *et al.* Response of the plasma hypoxia marker osteopontin to in vitro hypoxia in human tumor cells. *Radiother Oncol* 2005;76:200-205.
17. Wykoff CC, Beasley NJ, Watson PH, *et al.* Hypoxia-inducible expression of tumor-associated carbonic anhydrases. *Cancer Res* 2000;60:7075-7083.
18. Zhang JZ, Behrooz A, Ismail-Beigi F. Regulation of glucose transport by hypoxia. *Am J Kidney Dis* 1999;34:189-202.
19. Kaanders JH, Wijffels KI, Marres HA, *et al.* Pimonidazole binding and tumor vascularity predict for treatment outcome in head and neck cancer. *Cancer Res* 2002;62:7066-7074.
20. Koukourakis MI, Giatromanolaki A, Sivridis E, *et al.* Hypoxia-regulated carbonic anhydrase-9 (CA-IX) relates to poor vascularization and resistance of squamous cell head and neck cancer to chemoradiotherapy. *Clin Cancer Res* 2001;7:3399-3403.
21. Sly WS, Hu PY. Human carbonic anhydrases and carbonic anhydrase deficiencies. *Annu Rev Biochem* 1995;64:375-401.
22. Brewer CA, Liao SY, Wilczynski SP, *et al.* A study of biomarkers in cervical carcinoma and clinical correlation of the novel biomarker MN. *Gynecol Oncol* 1996;63:337-344.
23. Bui MH, Seligson D, Han KR, *et al.* Carbonic anhydrase IX is an independent predictor of survival in advanced renal clear cell carcinoma: implications for prognosis and therapy. *Clin Cancer Res* 2003;9:802-811.
24. Hussain SA, Palmer DH, Ganesan R, *et al.* Carbonic anhydrase IX, a marker of hypoxia: correlation with clinical outcome in transitional cell carcinoma of the bladder. *Oncol Rep* 2004;11:1005-1010.

25. Reisser C, Eichhorn K, Herold-Mende C, *et al.* Expression of facilitative glucose transport proteins during development of squamous cell carcinomas of the head and neck. *Int J Cancer* 1999;80:194-198.
26. Wijffels KI, Kaanders JH, Rijken PF, *et al.* Vascular architecture and hypoxic profiles in human head and neck squamous cell carcinomas. *Br J Cancer* 2000;83:674-683.
27. Artese L, Rubini C, Ferrero G, *et al.* Microvessel density (MVD) and vascular endothelial growth factor expression (VEGF) in human oral squamous cell carcinoma. *Anticancer Res* 2001;21:689-695.
28. Murray JD, Carlson GW, McLaughlin K, *et al.* Tumor angiogenesis as a prognostic factor in laryngeal cancer. *Am J Surg* 1997;174:523-526.
29. Janot F, Klijanienko J, Russo A, *et al.* Prognostic value of clinicopathological parameters in head and neck squamous cell carcinoma: a prospective analysis. *Br J Cancer* 1996;73:531-538.
30. Pignataro L, Carboni N, Midolo V, *et al.* Clinical relevance of microvessel density in laryngeal squamous cell carcinomas. *Int J Cancer* 2001;92:666-670.
31. Hockel M, Vaupel P. Tumor hypoxia: definitions and current clinical, biologic, and molecular aspects. *J Natl Cancer Inst* 2001;93:266-276.
32. Nordsmark M, Bentzen SM, Rudat V, *et al.* Prognostic value of tumor oxygenation in 397 head and neck tumors after primary radiation therapy. An international multi-center study. *Radiother Oncol* 2005;77:18-24.
33. Rofstad EK. Microenvironment-induced cancer metastasis. *Int J Radiat Biol* 2000;76:589-605.
34. International Union Against Cancer. TNM classification of malignant tumours. 4th ed. Geneva; 1992.
35. Raleigh JA, Chou SC, Bono EL, *et al.* Semiquantitative immunohistochemical analysis for hypoxia in human tumors. *Int J Radiat Oncol Biol Phys* 2001;49:569-574.
36. Baer S, Casaubon L, Schwartz MR, *et al.* Glut3 expression in biopsy specimens of laryngeal carcinoma is associated with poor survival. *Laryngoscope* 2002;112:393-396.
37. Younes M, Brown RW, Stephenson M, *et al.* Overexpression of Glut1 and Glut3 in stage I nonsmall cell lung carcinoma is associated with poor survival. *Cancer* 1997;80:1046-1051.
38. Sorensen BS, Hao J, Overgaard J, *et al.* Influence of oxygen concentration and pH on expression of hypoxia induced genes. *Radiother Oncol* 2005;76:187-193.
39. Troost EG, Bussink J, Kaanders JH, *et al.* Comparison of different methods of CAIX quantification in relation to hypoxia in three human head and neck tumor lines. *Radiother Oncol* 2005;76:194-199.
40. Buffa FM, Bentzen SM, Daley FM, *et al.* Molecular marker profiles predict locoregional control of head and neck squamous cell carcinoma in a randomized trial of continuous hyperfractionated accelerated radiotherapy. *Clin Cancer Res* 2004;10:3745-3754.
41. Hoogsteen IJ, Marres HA, Wijffels KI, *et al.* Colocalization of carbonic anhydrase 9 expression and cell proliferation in human head and neck squamous cell carcinoma. *Clin Cancer Res* 2005;11:97-106.
42. Flier JS, Mueckler M, McCall AL, *et al.* Distribution of glucose transporter messenger RNA transcripts in tissues of rat and man. *J Clin Invest* 1987;79:657-661.
43. Kunkel M, Reichert TE, Benz P, *et al.* Overexpression of Glut-1 and increased glucose metabolism in tumors are associated with a poor prognosis in patients with oral squamous cell carcinoma. *Cancer* 2003;97:1015-1024.
44. Mineta H, Miura K, Takebayashi S, *et al.* Prognostic value of glucose transporter 1 expression in patients with hypopharyngeal carcinoma. *Anticancer Res* 2002;22:3489-3494.
45. Haber RS, Rathana A, Weiser KR, *et al.* GLUT1 glucose transporter expression in colorectal carcinoma: a marker for poor prognosis. *Cancer* 1998;83:34-40.
46. Kang SS, Chun YK, Hur MH, *et al.* Clinical significance of glucose transporter 1 (GLUT1) expression in human breast carcinoma. *Jpn J Cancer Res* 2002;93:1123-1128.
47. Kato H, Takita J, Miyazaki T, *et al.* Glut-1 glucose transporter expression in esophageal squamous cell carcinoma is associated with tumor aggressiveness. *Anticancer Res* 2002;22:2635-2639.
48. Kawamura T, Kusakabe T, Sugino T, *et al.* Expression of glucose transporter-1 in human gastric carcinoma: association with tumor aggressiveness, metastasis, and patient survival. *Cancer* 2001;92:634-641.
49. Younes M, Juarez D, Lechago LV, *et al.* Glut 1 expression in transitional cell carcinoma of the urinary bladder is associated with poor patient survival. *Anticancer Res* 2001;21:575-578.

50. Wertheimer E, Sasson S, Cerasi E, *et al.* The ubiquitous glucose transporter GLUT-1 belongs to the glucose-regulated protein family of stress-inducible proteins. *Proc Natl Acad Sci U S A* 1991;88:2525-2529.
51. Koukourakis MI, Giatromanolaki A, Sivridis E, *et al.* Cancer vascularization: implications in radiotherapy? *Int J Radiat Oncol Biol Phys* 2000;48:545-553.

Chapter 5

Patterns of proliferation related to vasculature in human head and neck carcinomas before and after transplantation in nude mice

K.I.E.M. Wijffels

J.H.A.M. Kaanders

H.A.M. Marres

J.Bussink

H.P.W. Peters

P.F.J.W. Rijken

F.J.A. van den Hoogen

P.C.M. de Wilde

A.J. van der Kogel

Abstract

Purpose

The predictive potential of tumour cell kinetic parameters may be improved when they are studied in relation to other microenvironmental parameters. The purpose of this investigation was to quantitatively categorize human tumour samples according to proliferation patterns. Second, it was examined whether these characteristics are retained after xeno-transplantation.

Materials and methods

Fifty tumour samples from head and neck cancer patients were immunohistochemically stained for Ki-67 and vessels. Also, parts of the samples were transplanted into nude mice. Tumours were categorized according to previously described patterns of proliferation. Vascular and proliferation patterns were analyzed using an image processing system.

Results

The 50 tumours were categorized into four patterns of proliferation by visual assessment: marginal (6), intermediate (10), random (21) and mixed (12). One tumour could not be classified. These patterns were quantified by calculating the Ki-67 labelling index in distinct zones at increasing distance from vessels yielding good discrimination and significant differences between patterns.

The probability of growth after xenotransplantation was significantly higher for tumours with a labelling index and vascular density above the median value compared to tumours with both parameters below the median (82% vs. 35%). Fifty percent of the tumours retained their proliferation patterns after xeno-transplantation.

Conclusion

The categorization by proliferation pattern previously described by others was reproduced quantitatively and spatially related to the vascular network using a computerized image processing system. The combination of quantitative and architectural information of multiple microenvironmental parameters adds a new dimension to the study of treatment resistance mechanisms. Tumour models representative of the various patterns can be used to further investigate the relevance of these architectural patterns.

Introduction

In various studies, the value of proliferation markers as predictors for treatment outcome in patients with head and neck tumours has been examined.¹⁻⁴ The results are conflicting, with some studies showing positive association with outcome while others do not. This might be explained by differences in patient categories and treatment modalities, low patient numbers, and by differences in the methodologies used for the analyses. Most studies rely on endogenous markers for proliferation such as Ki-67, proliferating cell nuclear antigen (PCNA) and markers of the cyclin group, or on the incorporation of thymidine analogues such as iododeoxyuridine and bromodeoxyuridine (IdUrd, BrdUrd) in the DNA of S-phase cells.

A multicenter analysis including IdUrd- or BrdUrd- labelled biopsies from 467 patients receiving radiotherapy alone demonstrated that labelling index (LI) assessed by flow cytometry was a weak predictor of outcome.⁵ It was suggested by the authors and by other investigators^{5,6} that the predictive potential of cell kinetic parameters might be improved by relating these parameters with other biological parameters and with the microregional architecture of tumours. Bennett *et al.*⁷ and Wilson *et al.*⁶ described four different histologic patterns of proliferation and found that the pattern of proliferation was the more important predictor for outcome over LI.

In this study we have categorized tumour samples of patients with head and neck carcinomas according to the proliferation patterns described by Bennett *et al.*⁷ and Wilson *et al.*⁶ In an attempt to develop this approach further, we have quantified these patterns in relation to the vasculature using a computerized image analysis system. In addition, we have examined whether individual tumours retain these proliferation characteristics after transplantation into nude mice. This would then provide tumour models that can be instrumental to further investigate the relevance of these architectural patterns.

Materials and Methods

Collection and processing of tumour material

Between February 1995 and April 1997, surgical resection specimen of 28 patients with squamous cell carcinoma of the head and neck were collected. The fresh resected tumour specimen of each patient was brought to the pathology department. In agreement with the pathologist, a sample (0.25 - 0.5 cm³) of viable

tumour tissue was cut from the macroscopically identified tumour. One-half of this sample was put in L15 culture medium (Life Technology, Breda, The Netherlands) with penicillin and gentamycin, and transported to the animal laboratory where 1 mm³ pieces of viable tumour were transplanted subcutaneously in the flank of five nude mice (Balb/c nu/nu mouse). The other half of the sample was immediately frozen into isopentane cooled by liquid nitrogen and stored at -190 °C until frozen sections were cut and stained.

During a second period between May 1998 and December 1998, multiple biopsies were taken under general anesthesia from 21 patients, who were planned to be treated by radiotherapy. Apart from the biopsy for routine histopathologic examination we obtained two additional biopsies from each patient. One sample was immediately frozen in liquid nitrogen, the other was put in L15 medium and was transplanted in five nude mice afterwards as described above.

After growing in the nude mice, tumours were passaged when they reached a diameter of 1 cm. For the purpose of this investigation the ability of a tumour to grow as a xenograft was defined as growth of tumour in the mice in at least the first and the subsequent passage.

Approval from the local ethics committee was obtained for this study.

Immunohistochemical staining of the human resection and biopsy material

Before the staining procedure, frozen sections were fixed in acetone of 4° C for 10 min. Then the sections were rehydrated in phosphate buffered saline (PBS). Between all the consecutive steps of the staining procedure, the sections were rinsed three times for 2 min in PBS. All antibodies were diluted in PBS. The DNA in the tissue sections was denatured by incubation with hydrochloric acid 2 N for 10 min. To neutralize the pH, sections were rinsed in 0.1 M borax for 10 min. The sections were then incubated overnight at 4° C with undiluted Ki-67 antibody (mouse monoclonal, clone 7B11, Zymed, San Francisco, CA). This was followed by incubation for 1 h at room temperature (RT) with fluorescein isothiocyanate (FITC)-conjugated rabbit anti-mouse antibody (Jackson Immuno Research Laboratories, West Grove, PA, USA) 1:100. To enhance the signal, this step was followed by incubation for 1 h at RT with FITC-conjugated donkey anti-rabbit antibody (Jackson Immuno Research Laboratories) 1:100.

Next, the vessels were stained by an incubation at RT for 1 h with PAL-E (Department of Pathology, University Medical Center St. Radboud, The Netherlands) 1:5. The mouse monoclonal antibody PAL-E is a marker for human endothelium, especially useful in frozen tissue sections.⁸ The staining procedure

was followed by 1 h incubation at RT with tetramethyl rhodamine isothiocyanate (TRITC)-conjugated goat anti-mouse antibody (Jackson Immuno Research Laboratories) 1:100. To enhance the signal, this was followed by incubation for 1 h with TRITC-conjugated donkey anti-goat antibody (Jackson Immuno Research Laboratories) 1:100.

Finally, all nuclei were stained with fast blue (Sigma-Aldrich Chemie BV, Zwijndrecht, The Netherlands) 1:1000 in PBS for 15 min at RT. Slides were then rinsed and mounted in PBS for quantitative imaging of the proliferation, vasculature and all nuclei.

Immunohistochemical staining of the xenograft material

The first part of the staining procedure of the xenograft material was identical to that of the human material, including the incubation with the Ki-67 antibody. Next, the staining procedure was continued by incubation for 1 h at RT with biotin-conjugated donkey anti-mouse antibody (Jackson Immuno Research Laboratories) 1:100. This was followed by incubation for 1 h at RT with streptavidin Alexa Fluor 488 (Molecular Probes, Eugene, Oregon) 1:100 in PBS.

Next the sections were incubated overnight at 4° C with undiluted 9F1 (rat monoclonal antibody to mouse endothelium, Department of Pathology, University Medical Center St. Radboud, The Netherlands), followed by 1 h incubation at RT with TRITC-conjugated goat anti-rat antibody (Jackson Immuno Research Laboratories) 1:100, to visualize the vessels. The vessel signal was enhanced by incubation for 1 h with donkey anti-goat Alexa Fluor 546 conjugated antibody (Molecular Probes) 1:100. Finally, all nuclei were stained with fast blue (Sigma-Aldrich Chemie) 1:1000 in PBS for 15 min at RT. Slides were then rinsed and mounted in PBS for quantitative imaging of the proliferation, vasculature and all nuclei.

Scanning of tumour sections and image processing

For quantitative analysis, the slides were scanned by a computerized digital image processing system using a high-resolution intensified solid-state camera on a fluorescence microscope (Zeiss Axioskop) with a computer-controlled motorized stepping stage. The scanning method has been described in detail by Rijken *et al.*⁹ and has been previously used to visualize and quantify vessels, kinetic parameters¹⁰ and hypoxic markers¹¹.

Each tumour section was scanned three times at 200x magnification. After each scan, which consisted of 64 fields (8x8, field size 0.31 mm²), a composite binary

image was reconstructed from these fields. For the vessels (TRITC-signal, Alexa Fluor 546, 510-560 nm excitation) a 690 nm emission filter was used and for Ki-67 labelled nuclei (FITC-signal, Alexa Fluor 488, 450-490 nm excitation) a 520 nm emission filter was used. For the nuclei (fast blue, 365 nm excitation) a 420 nm emission filter was used. After the scanning procedure, the three composite binary images of the vascular structures, the proliferating nuclei, and all nuclei were superimposed. The tumour area was delineated using a hematoxylin-eosin staining of a consecutive tumour section. This area was used as a mask in further image analysis excluding nontumour tissue and large necrotic areas from the analysis. A pathologist supervised the delineation of the tumour area.

Analysis of proliferation and vascular parameters

The composite binary images were used for computerized calculations of various parameters. The vascular density (VD) was calculated as the number of vascular structures per mm². The relative vascular volume was defined as the PAL-E or 9F1 positive surface divided by the total tumour surface. The LI was defined as the ratio of the Ki-67-labelled area to the total nuclear area.

To quantitate the distribution of proliferation in relation to the vasculature, zones were chosen arbitrarily at increasing distance from the surface of the nearest vessel (0-15 µm, 15-30 µm, 30-70 µm and >70 µm). In each zone the LI was calculated as the Ki-67-stained surface in a zone divided by the total nuclear surface in that zone.

Patterns of proliferation

We categorized the tumours into four different groups according to the visual proliferation staining patterns that were previously described by Bennett *et al.*⁷ The marginal pattern shows proliferating cells only in the basal or suprabasal cell layers. The second, intermediate pattern shows proliferating cells in the basal and suprabasal layers, but also in more distant layers. The random pattern shows a diffuse distribution of proliferation without obvious organization. Finally, the mixed pattern shows a combination of the above mentioned patterns. Two observers categorized the tumours independently according to these criteria.

Statistics

Mean values of VD and LI of subgroups of tumours were compared by the Student's-t-test. Correlations between vascular and kinetic parameters were tested by linear least-squares regression analysis. Fisher's exact test was used to compare growing and non-growing xenografted tumours in relation to VD and LI.

The statistical analyses were done on a Macintosh computer using Statistica 4.0 software.

Results

Patients

Of the 28 patients undergoing surgery, 1 patient was diagnosed with two different primary tumours (laryngeal and oral cavity) which were both analyzed. Thus, 29 resection specimen were collected with tumours originating from larynx (13), hypopharynx (5), oral cavity (7), oropharynx (3) and nasal cavity (1). In six cases the specimens were derived from a local recurrence after previous radiotherapy. Of the 21 patients from whom only biopsies were obtained, 1 patient presented with two synchronous primaries (oropharynx and hypopharynx). Tumour sites from which biopsies were collected were: larynx (9), hypopharynx (10) and oropharynx (3). In one case the biopsy material was insufficient for xenografting. Thus, we obtained tumour samples of 51 head and neck squamous cell carcinomas, of which 50 were transplanted in nude mice, which were the subject of the study. One tumour was well differentiated, 3 tumours were well to moderately differentiated, 30 were moderately differentiated, and 16 were poorly differentiated.

Proliferation

A strong fluorescent green staining of Ki-67 positive nuclei was seen with little background staining (Figure 1). The Ki-67 LI varied from 0.01 to 0.32, with a median of 0.07 (Figure 2). There was no correlation between the LI and the differentiation grade or the primary tumour site. The tumours were classified into four categories according to their proliferation patterns as described by Bennett *et al.*⁷ Examples are shown in figure 3.

The proliferation pattern was classified as marginal in 6 tumours, intermediate in 10, random in 21 and mixed in 12. One tumour contained only few proliferating nuclei and could not be classified. The tumours in the intermediate category had a higher mean overall LI compared to the tumours in the other categories: 0.15 (SD 0.11) vs. 0.08 (SD 0.07) (*t*-test: *p* = 0.01). There was no correlation between the different proliferation patterns and the pathological grading of the tumours.

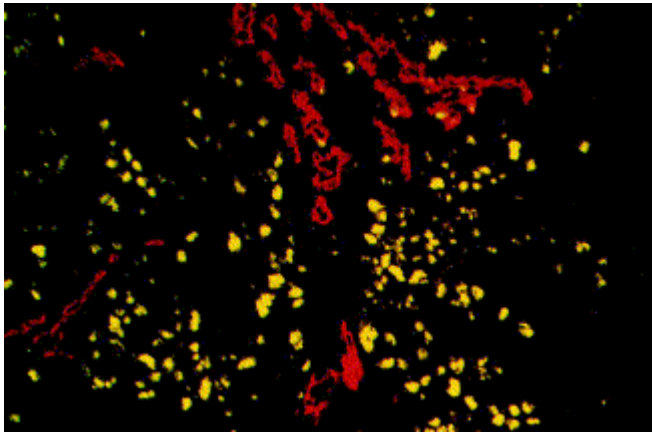


Figure 1. Fluorescence microscopic image of a xenografted tumour section (200x magnification) after staining for proliferation with Ki-67 (yellow) and vessels with 9F1 (red). The proliferation pattern is typical for the intermediate classification showing multiple layers of proliferating nuclei close to the vessels.

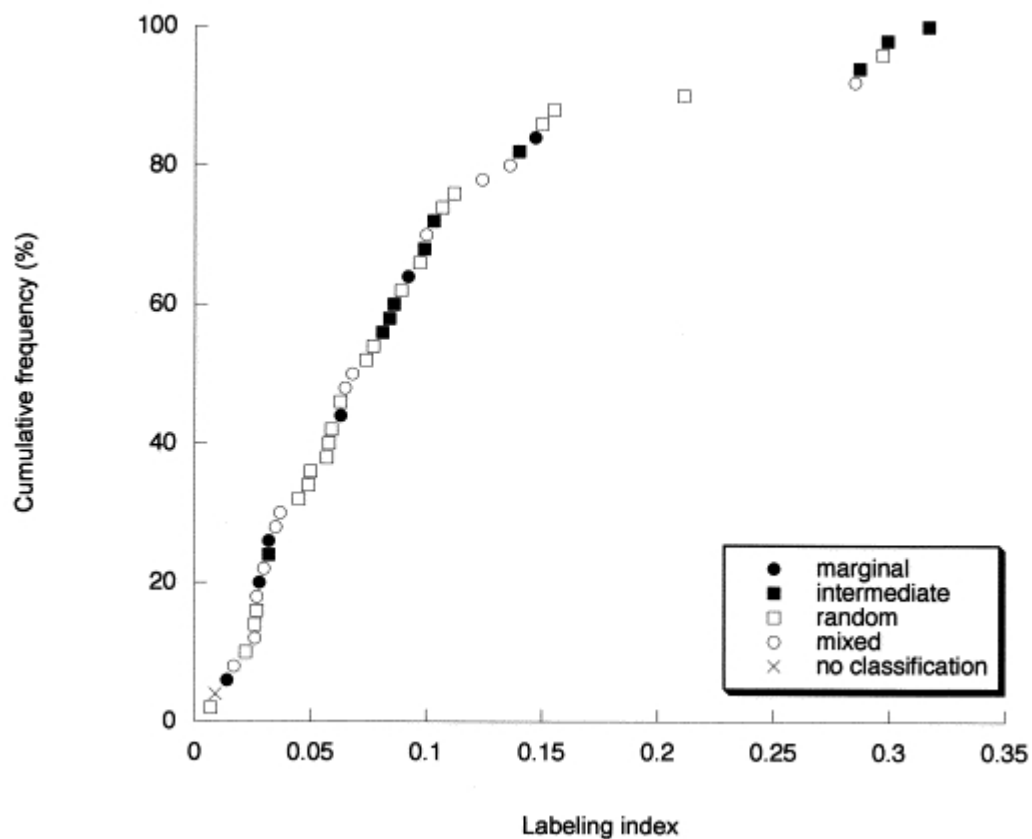


Figure 2. Cumulative plot of labelling indices of 50 tumours showing different proliferation patterns.

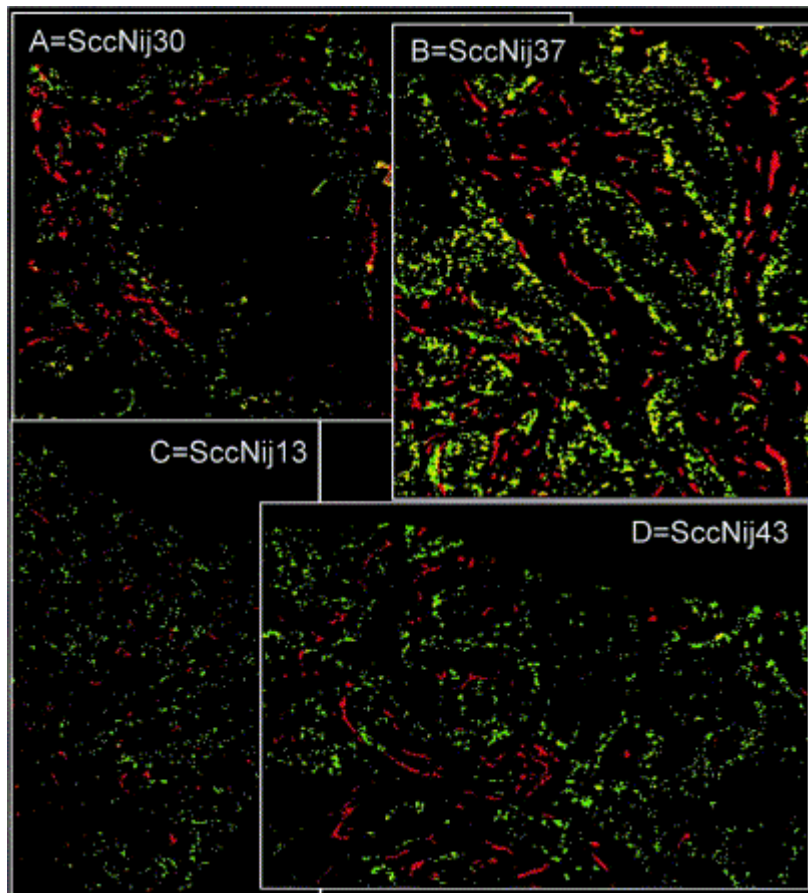


Figure 3. Composite binary images of four different patterns of proliferation in primary human tumours; marginal (ScCNij30), intermediate (ScCNij37), random (ScCNij13) and mixed (ScCNij43). Ki-67 stained green, vessels (Pal-E) stained red. Proliferating cells in close proximity to vessels produce a yellow color.

Figure 4 shows the distribution of the proliferative activity as a function of distance from the nearest vessel. The tumours are grouped according to their proliferation pattern and the figure shows median values of the Ki-67 labelling index in distinct vascular zones (0-15 μm , 15-30 μm , 30-70 μm and > 70 μm) for the four groups.

The tumours with marginal proliferation patterns demonstrated proliferative activity almost exclusively within a 1-2 cell layer thick zone directly adjacent to vessels. The intermediate type tumours had even more active proliferation in this first zone but there was also activity in the more distant zones. The tumours with random proliferation patterns showed a more homogeneous distribution of proliferating cells although there was still a gradient in relation to the vasculature. The mixed type showed histologic features of the three other types, but in quantitative aspect is most similar to the random type.

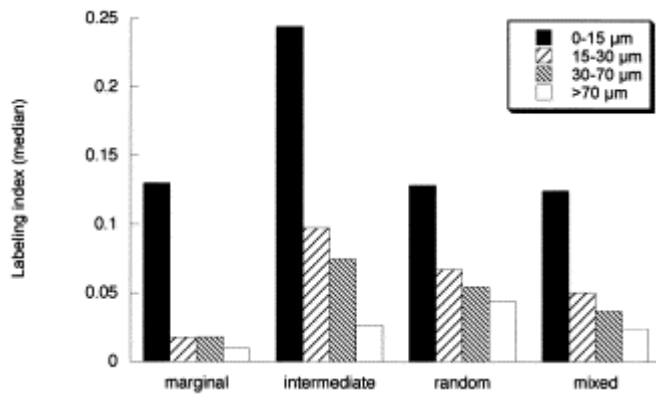


Figure 4. Median labelling indices at increasing distance from the vessels. Tumours are categorized into four groups according to proliferation patterns.

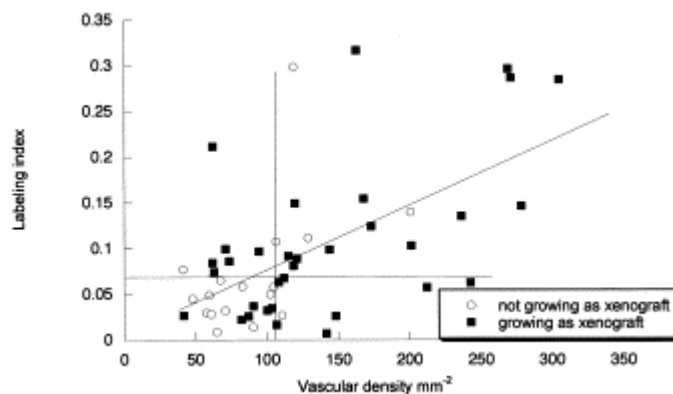


Figure 5. Labelling index vs. vascular density in 50 different human tumours. Circles represent tumours not growing in nude mice, squares represent tumours growing in nude mice. Median of LI and VD is indicated by horizontal and vertical lines. Regression line is shown ($r = 0.58$, $p < 0.0001$).

Vasculature

The vessels showed a bright red stain without any background staining (Figure 1). The VD varied from 41 mm⁻² to 305 mm⁻² with a median of 106 mm⁻² (Figure 5). The relative vascular volume varied from 0.6 to 8.4%, with a median of 2.2%. No correlation was found between the vascular parameters and differentiation grade or primary tumour site. There was a weak ($r = 0.58$) but highly significant ($p < 0.0001$) correlation between VD and LI (Figure 5). The tumours with marginal and intermediate proliferation patterns had a higher mean VD (144 mm⁻², SD 74) than the other categories (116 mm⁻², SD 63) but the difference was not statistically significant ($p = 0.17$).

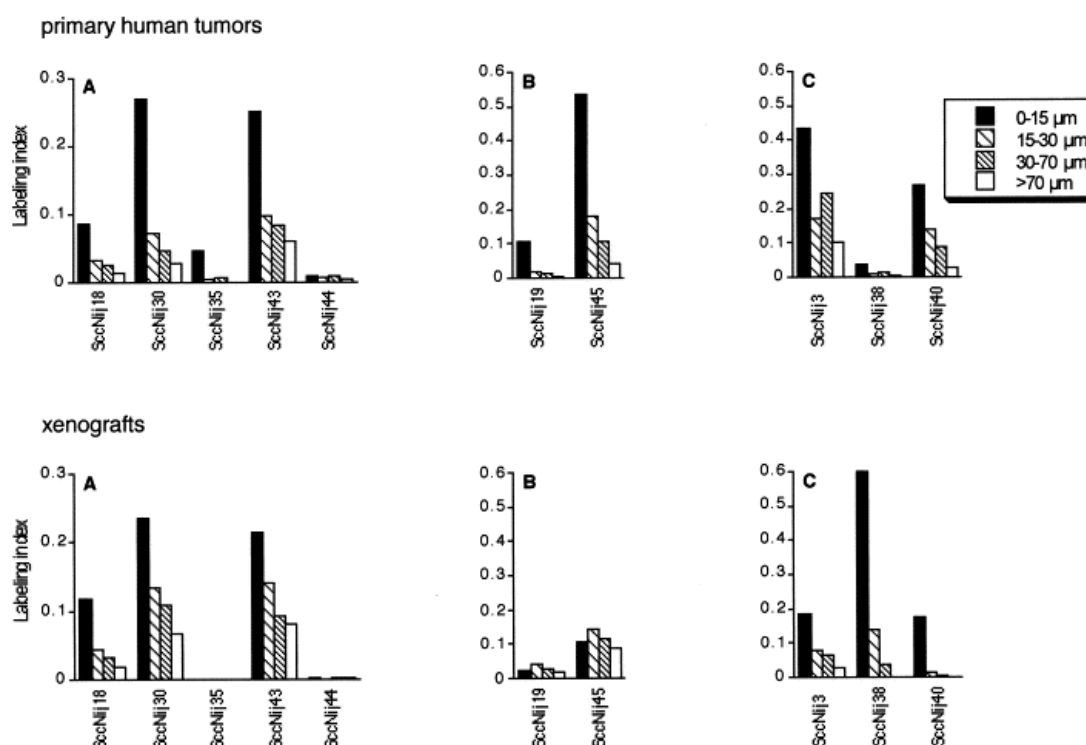


Figure 6. Labelling indices at increasing distance from vessels comparing human tumours and corresponding xenografts. Panel A shows 5 pairs demonstrating good resemblance both visually and quantitatively. Panel B shows 2 tumours with good resemblance visually but not quantitatively. Panel C shows 3 tumours with no resemblance visually nor quantitatively.

Xenografted tumours

Of the 50 transplanted tumours, 33 (66%) demonstrated growth as a xenograft in at least the first and subsequent passage. Figure 5 shows that tumours are more likely to grow as a xenograft when they have either a LI which is higher than the median (0.07) (Fisher exact: $p = 0.04$), or a VD higher than the median (106 mm^2) (Fisher exact: $p = 0.008$). When tumours with a LI greater than median and a VD greater than median are compared with tumours having both parameters below the median there is a highly significant difference (Fisher exact: $p = 0.001$) in the probability that tumours will grow in mice (82% vs. 35%).

Early passages of 10 xenografted tumours were stained for vessels and proliferation and were compared with the resected tumour tissue from which they originated. In seven tumours there was a good resemblance of the visually assessed proliferation staining pattern between the xenograft and the original human tumour. In five of these seven tumour sets the correspondence of the visually assessed proliferation patterns was supported by the quantitative analysis (Figure 6A). In two of the seven tumour sets the quantitative analysis did not

support the visual correlation (Figure 6B). Three of the xenografted tumours did not show any resemblance with the original human material, nor by visual comparison or by quantitative analysis (Figure 6C).

Discussion

The use of fluorescence immunohistochemistry together with computerized image analysis to quantify multiple parameters in one tumour section was earlier described by our group.⁹⁻¹¹ The quantification of proliferation markers by this method has been validated.¹⁰ There was a good correlation between the LI based on computerized surface analysis and the manual counting technique and flow cytometry. The advantage of this method over flow cytometry is that the tissue architecture is preserved. This enabled us to visualize and quantify architectural patterns of proliferation, in close relation to other structures such as vasculature. The VD observed in this material (median 106 mm⁻²) is considerably higher than reported in a previous paper involving a comparable group of patients (median 42 mm⁻²).¹¹ This can be explained by different magnification factors used, 200x and 100x respectively. We could confirm this by scanning a number of sections repeated at both magnification factors. At the larger magnification many small vessels were identified which remained undetected with the 100x scan. Also when VD was determined in hot spot areas, Aebersold *et al.*¹² found higher values of 54 – 282 vessels per optical field (median 104) in squamous cell carcinomas of the oropharynx. These differences show the dependence of vascular parameters on the methods used for vessel counting as we discussed in our previous paper.¹¹

There are many studies on the prognostic relevance of proliferation markers in human tumours, including carcinomas of the head and neck area.^{1-5,13-15} We used the endogenous marker Ki-67, a nuclear antigen that is expressed in all phases of the cell cycle except G0.¹⁶ Other commonly used proliferation markers include PCNA, the cyclins and the thymidine analogues BrdUrd and IdUrd. Because of the different expression profiles of these markers and differences in methods for analysis, direct comparison between studies is difficult. Nevertheless, when LI of these various markers is related with treatment outcome of head and neck cancers, conflicting results are reported.

There is increasing recognition that a combination of factors can be responsible for treatment failure. It is also becoming clear that radiation response cannot be

accurately predicted by the value of a single parameter such as LI or potential doubling time. It was suggested that the predictive potential might be increased when cell kinetic parameters are studied in relation to the microenvironment and combined with other biological parameters.^{5,17} Wilson *et al.*⁶ studied BrdUrd labelled tumour biopsies from 115 head and neck cancer patients by flow cytometry and immunohistochemistry. In a multivariate analysis the proliferation pattern appeared to be the predominant predictor for outcome after accelerated radiotherapy. In the present study we were able to reproduce the proliferation patterns described by Wilson *et al.*⁶ (Figure 3). In addition we could relate these patterns to the vascular architecture of tumours and quantify them by automated image analysis. When ranking the proliferation patterns by local control rates, Wilson *et al.*⁶ found the best local control for tumours with proliferation patterns of the marginal type while outcome was progressively worse for the intermediate, mixed and random patterns. The authors gave some suggestions to explain this, including possible differences in proliferative organization, growth fraction, cell cycle time and cell loss rate. An alternative explanation comes from our quantitative analysis of the patterns in relation to the vasculature. Figure 4 shows that, in the same order from the marginal to the random type, there is an increase in the relative number of proliferating tumour cells at distances greater than 70 μm from vessels. It is likely that at such distances from vessels oxygenation is poor and at least conditions of intermediate hypoxia can be expected. This suggests a viable, actively proliferating and relatively hypoxic cell population which may well be the resistant subpopulation of the tumour and which apparently is more prominent in some tumours than in others. This is only a hypothetical explanation but it clearly illustrates the importance of multiparameter analysis to better understand tumour biology and therapy resistance mechanisms. This may ultimately result in better selection for new treatments, based on architectural characteristics. We are currently expanding our technique of computerized multiparameter analysis by introducing both exogenous and endogenous markers of hypoxia and analyzing these in conjunction with vascularity and proliferation patterns.

Since the discovery of the nude mouse mutant by Flanagan¹⁸, various human tumour lines were xenografted in these athymic nude mice. These tumours are widely used as a model to study human tumour biology and to test cytotoxic drugs and radiation treatments. Nearly all tumour types have been xenografted with varying degrees of success. Take rates partly depend on the histological type and site of the primary tumour. Different success rates (26% - 77%) were reported for

squamous cell carcinomas of the head and neck.¹⁹⁻²¹ In the present study 66% of the transplanted tumours demonstrated growth in at least the first two passages. An important finding from this study was the dependence of take rate on LI and VD. Tumours with a high LI or a high VD, or both, had a significantly higher probability of growth compared to tumours with both low LI and VD, which has not been reported in the literature so far. It has been reported though that the macroscopic growth curve of first passage xenografts significantly predicts the chances of establishment of a xeno-transplantation line after serial subpassagings.²² Thus, clearly, selection of model systems occurs favoring well vascularized and actively proliferating tumours.

Another observation concerned the retention of proliferation characteristics after xeno-transplantation. Of the 10 xenografted tumours, 5 demonstrated good resemblance with the proliferation pattern of the original tumour both by visual and quantitative computerized assessment. We are currently examining whether other microenvironmental characteristics such as patterns of hypoxia are retained as well both in early and in later passages. It has been demonstrated that human malignant tumours can retain the cytological and histological appearance of the inoculated human material after long-term serial transplantation over many years.²³ Half of the transplanted tumours in our material did retain the characteristics of the primary tumours, expressing similar patterns of vascularity and proliferation. We will use these tumour lines to study the interrelationships of the microenvironmental parameters, including oxygenation, in greater detail. Furthermore, they can be used to test various treatment modifications comparing the responses of tumours with different microenvironmental characteristics.

In conclusion, the computerized simultaneous analysis of multiple micro-environmental parameters allows objective and quantitative categorization of tumours and can improve our understanding of treatment resistance mechanisms. Tumour lines derived from xenotransplantation can be used to further explore these mechanisms and test subsequent treatment modifications.

References

1. Sittel C, Ruiz S, Volling P, *et al.* Prognostic significance of Ki-67 (MIB1), PCNA and p53 in cancer of the oropharynx and oral cavity. *Oral Oncol* 1999;35:583-589.
2. Hoyer M, Jorgensen K, Bundgaard T, *et al.* Lack of predictive value of potential doubling time and iododeoxyuridine labelling index in radiotherapy of squamous cell carcinoma of the head and neck. *Radiother Oncol* 1998;46:147-155.
3. Kropveld A, Slootweg PJ, Blankenstein MA, *et al.* Ki-67 and p53 in T2 laryngeal cancer. *Laryngoscope* 1998;108:1548-1552.
4. Lera J, Lara PC, Perez S, *et al.* Tumor proliferation, p53 expression, and apoptosis in laryngeal carcinoma: relation to the results of radiotherapy. *Cancer* 1998;83:2493-2501.
5. Begg AC, Haustermans K, Hart AA, *et al.* The value of pretreatment cell kinetic parameters as predictors for radiotherapy outcome in head and neck cancer: a multicenter analysis. *Radiother Oncol* 1999;50:13-23.
6. Wilson GD, Dische S, Saunders MI. Studies with bromodeoxyuridine in head and neck cancer and accelerated radiotherapy. *Radiother Oncol* 1995;36:189-197.
7. Bennett MH, Wilson GD, Dische S, *et al.* Tumour proliferation assessed by combined histological and flow cytometric analysis: implications for therapy in squamous cell carcinoma in the head and neck. *Br J Cancer* 1992;65:870-878.
8. Schlingemann RO, Dingjan GM, Emeis JJ, *et al.* Monoclonal antibody PAL-E specific for endothelium. *Lab Invest* 1985;52:71-76.
9. Rijken PF, Bernsen HJ, van der Kogel AJ. Application of an image analysis system to the quantitation of tumor perfusion and vascularity in human glioma xenografts. *Microvasc Res* 1995;50:141-153.
10. Bussink J, Kaanders JH, Rijken PF, *et al.* Multiparameter analysis of vasculature, perfusion and proliferation in human tumour xenografts. *Br J Cancer* 1998;77:57-64.
11. Wijffels KI, Kaanders JH, Rijken PF, *et al.* Vascular architecture and hypoxic profiles in human head and neck squamous cell carcinomas. *Br J Cancer* 2000;83:674-683.
12. Aebbersold DM, Beer KT, Laissue J, *et al.* Intratumoral microvessel density predicts local treatment failure of radically irradiated squamous cell cancer of the oropharynx. *Int J Radiat Oncol Biol Phys* 2000;48:17-25.
13. Nylander K, Schildt EB, Eriksson M, *et al.* PCNA, Ki-67, p53, bcl-2 and prognosis in intraoral squamous cell carcinoma of the head and neck. *Anal Cell Pathol* 1997;14:101-110.
14. Bjork-Eriksson T, West CM, Cvetskovska E, *et al.* The lack of correlation between proliferation (Ki-67, PCNA, LI, Tpot), p53 expression and radiosensitivity for head and neck cancers. *Br J Cancer* 1999;80:1400-1404.
15. Sittel C, Eckel HE, Damm M, *et al.* Ki-67 (MIB1), p53, and Lewis-X (LeuM1) as prognostic factors of recurrence in T1 and T2 laryngeal carcinoma. *Laryngoscope* 2000;110:1012-1017.
16. Gerdes J, Lemke H, Baisch H, *et al.* Cell cycle analysis of a cell proliferation-associated human nuclear antigen defined by the monoclonal antibody Ki-67. *J Immunol* 1984;133:1710-1715.
17. Wilson GD SM, Daley FM. Predicting the outcome of fractionated radiotherapy (Abstr.). *Proceedings 47th Annual meeting of the Radiation Research society April 29 - May 3, Albuquerque, NM* 2000.
18. Flanagan SP. 'Nude', a new hairless gene with pleiotropic effects in the mouse. *Genet Res* 1966;8:295-309.
19. Lindenberger. Aspects of xenografted tumors of the ear, nose and throat: morphology, cell kinetics, growth behaviour and immunology. Stuttgart: Fischer Verlag; 1981.
20. Braakhuis BJ, Sneeuwloper G, Snow GB. The potential of the nude mouse xenograft model for the study of head and neck cancer. *Arch Otorhinolaryngol* 1984;239:69-79.
21. Elprana D, Kuijpers W, Van den Broek P, *et al.* Growth characteristics of head and neck squamous cell carcinoma in nude mice. *Eur J Cancer Clin Oncol* 1986;22:1211-1222.
22. Bassukas ID, Eberle V, Maurer-Schultze B. The growth curve of the first passage xenografts of human tumors in nude mice predicts their transplantation behaviour. *Oncol Rep* 1998;5:257-259.
23. Povlsen CO, Visfeldt J, Rygaard J, *et al.* Growth patterns and chromosome constitutions of human malignant tumours after long-term serial transplantation in nude mice. *Acta Pathol Microbiol Scand [A]* 1975;83:709-716.

Chapter 6

Tumour cell proliferation under hypoxic conditions in human head and neck squamous cell carcinomas

K.I.E.M. Wijffels

H.A.M. Marres

J.P.W. Peters

P.F.J.W. Rijken

A.J. van der Kogel

J.H.A.M. Kaanders

Abstract

Purpose

Two mechanisms of radiotherapy resistance of major importance in head and neck cancer are tumour cell repopulation and hypoxia. Hypoxic tumour cells that retain their clonogenic potential can survive radiation treatment and lead to local recurrences. The aim of this study was to quantify this cellular population in a cohort of human head and neck carcinomas and to investigate the prognostic significance.

Materials and Methods

The proliferation marker iododeoxyuridine (IdUrd) and the hypoxia marker pimonidazole were administered intravenously prior to biopsy taking in patients with stage II-IV squamous cell carcinoma of the head and neck. Triple immunohistochemical staining of blood vessels, IdUrd and pimonidazole was performed and co-localization of IdUrd and pimonidazole was quantitatively assessed by computerized image analysis. The results were related with treatment outcome.

Results

Thirty-nine biopsies were analyzed. Tumours exhibited different patterns of proliferation and hypoxia but generally the IdUrd signal was found in proximity to blood vessels whereas pimonidazole binding was predominantly at a distance from vessels. Overall, no correlations were found between proliferative activity and oxygenation status. The fraction of IdUrd-labelled cells positive for pimonidazole ranged from 0% to 16.7% with a mean of 2.4% indicating that proliferative activity was low in hypoxic areas and occurring mainly in the well-oxygenated tumour compartments. IdUrd positive cells in hypoxic areas made up only 0.09% of the total viable tumour cell mass. There were no associations between the magnitude of this cell population and local tumour control or survival.

Conclusions

Co-localization between proliferating cells and hypoxia in head and neck carcinomas was quantified using an immunohistochemical triple staining technique combined with a computerized simultaneous analysis of multiple parameters. The proportion of cells proliferating under hypoxic conditions was small and no correlation with treatment outcome could be found.

Introduction

Radiotherapy is one of the prime treatment modalities in the management of squamous cell carcinoma of the head and neck area. Early stages are often treated with radiotherapy alone whereas combinations with surgery or chemotherapy are generally used for the more advanced cases. Clinically relevant factors determining the response of squamous cell carcinomas to radiation treatment include tumour cell repopulation and hypoxia.¹⁻³

The concept of accelerated fractionation is based on the assumption that a reduction of the overall treatment time will restrict the opportunity for repopulation by clonogenic tumour cells. Clinical studies have proven the benefit of accelerated radiotherapy but at the cost of increased toxicity.^{4,5} Selection of patients that are most likely to benefit from accelerated fractionation based on reliable predictive assays is therefore desirable. However, the prognostic and predictive value of assays that measure the proliferative activity of the tumour prior to the start of the treatment remains controversial.⁶⁻¹² Different markers have been used for assessment of proliferation. These include endogenous markers such as Ki-67, proliferating nuclear antigen (PCNA) and members of the cyclin group, or the intravenous administration of the thymidine analogues bromodeoxyuridine (BrdUrd) and iododeoxyuridine (IdUrd).^{7,10} The latter have a short half-life and are rapidly incorporated in the DNA of S-phase cells. The parameter that is mostly used to quantify these markers is the proportion of tumour cells identified as positive for a certain marker, the labelling index (LI). Knowledge of the time elapsed between administration of the thymidine analogues and biopsy taking and analysis by flow cytometry can also provide information on S-phase time (T_s) and potential doubling time (T_{pot}). However, neither of these parameters have consistently shown strong associations with treatment outcome.^{7,8,12}

Methods that measure tumour oxygenation have shown to be more promising as prognostic indicators of treatment outcome. Studies using oxygen microelectrodes consistently show significant correlations between low tumour pO_2 and poor response to radiation treatment.^{13,14} A limitation is the invasive nature of the procedure and their use is restricted to accessible tumours. Endogenous hypoxia-related markers that are detectable by immunohistochemistry offer an attractive alternative because they require no additional intervention beyond the initial pre-treatment biopsy and may be very suitable for widespread clinical use. Examples are HIF-1 α , CA-IX and the glucose transporters –1 and –3. Expression of these markers has been associated with poor outcome although the data are not unequivocal.¹⁵⁻²² Also, there are reservations as to whether they are very robust

markers of hypoxia because only weak correlations are found with microelectrode readings and nitroimidazole-marker binding.²²⁻²⁴ Clinically relevant exogenous markers are the 2-nitroimidazoles pimonidazole hydrochloride and EF-5.^{22,25}

In a previous study we demonstrated a significant association between the pimonidazole binding assay and loco-regional control and disease-free survival in patients with head and neck carcinomas.²² A disadvantage of the nitroimidazole markers is that they require intravenous injection before biopsy taking.

Clinical studies that have used measurements of proliferation and hypoxia in a combined assay are sparse. Co-registration of hypoxia and proliferative activity may identify an important cellular subpopulation in the tumour that may be responsible for treatment resistance and tumour progression. In the current study we have used exogenous markers of hypoxia (pimonidazole) and proliferation (IdUrd) to investigate the magnitude of this subpopulation in a cohort of patients with squamous cell carcinomas of the head and neck.

Materials and methods

Patients

Patients with a primary stage III or IV squamous cell carcinoma of the oral cavity, oropharynx or larynx, or a stage II-IV carcinoma of the hypopharynx were entered in this study. These were patients that were also potential candidates for a phase II trial combining accelerated radiotherapy with carbogen breathing and nicotinamide (ARCON).²⁶ The hyperoxic gas carbogen (95-98% O₂ + 2-5% CO₂) and the vasoactive agent nicotinamide are added to counteract diffusion-limited and perfusion-limited hypoxia, respectively. Other inclusion criteria were: age over 18 years, WHO performance status of 0-2, no severe heart or lung disease, no severe liver or kidney dysfunction, no severe stridor, no distant metastases, no concurrent treatment for other malignant disease outside the upper aerodigestive tract, and written informed consent. Approval was obtained from the Institutional Review Board of the Radboud University Medical Centre Nijmegen. Approximately 2 h before biopsies were taken, the patients received a 20 min. i.v. infusion of 500 mg/m² of the hypoxia marker pimonidazole ((1-((2-hydroxy-3-piperidiny)propyl)-2-nitroimidazole hydrochloride, Hypoxyprobe-1; Natural Pharmacia International, Belmont, MA) dissolved in 100 ml NaCl 0.9%. Pimonidazole is a bio reductive chemical probe with an immunorecognizable side chain. Necrotic areas are not stained by pimonidazole because the probe binds only in viable cells as a result of hypoxia-dependent bio reduction by cellular

nitroreductases. The S-phase marker 2'-deoxy-5-iodouridine (Iododeoxyuridine/IdUrd; Centre Hospitalier Universitaire Vaudois, Lausanne, Switzerland) was injected i.v. in 5 min in a dose of 200mg, 20 min before biopsy. IdUrd is a thymidine analogue with a short half-life and is rapidly incorporated into the DNA of S-phase cells. Under general anaesthesia, biopsies were taken for routine diagnostic purposes and additional biopsies were collected for hypoxia and proliferation marker analysis. The latter were snap frozen and stored in liquid nitrogen until immunohistochemical processing. The diagnostic workup further included physical examination, chest X-ray, CT-scan and/or MRI-scan of the head and neck area. After completion of the diagnostic workup, the patients were treated with ARCON. Patients that were not eligible or refused ARCON were treated with radiotherapy alone, surgery or a combined modality.

Immunohistochemistry

From the biopsy material, sections of 5 µm were cut and mounted on poly-L-lysine coated slides and stored at -80°C. Prior to staining the sections were fixed in acetone of 4°C for 10 min and rehydrated in phosphate buffered saline (PBS) twice for 2 min. Between all consecutive steps of the staining procedure, sections were rinsed in PBS three times for 5 min. DNA was denaturated during 10 min with 2N HCL followed by 10 min in 0.1 M Borax to neutralize the pH. Then during 30 min a pooled incubation was done at 37 °C with mouse-anti-PAL-E (Department of Pathology, Radboud University Medical Centre Nijmegen, The Netherlands) 1:6 and with rabbit-anti-pimonidazole polyclonal rabbit antibody (J.A. Raleigh, Department of Radiation Oncology and Toxicology, University of North Carolina, Chapel Hill, North Carolina) 1: 400 in polyclonal liquid diluent (PLD, DPC Breda Diagnostic Products, Breda, The Netherlands). The monoclonal antibody PAL-E is a marker for human endothelium especially useful in frozen tissue sections.²⁷ This was followed by a second pooled incubation with goat-anti-mouse (Fab)Cy3 (Jackson ImmunoResearch Laboratories, West Grove, PA, USA) 1:100 and donkey-anti-rabbit-Alexa488 (Molecular Probes, Leiden, The Netherlands) 1:400 in PLD during 60 min at 37 °C. Next the sections were incubated with donkey-anti-goat (Fab)2 tetra-methyl rhodamine isothiocyanate (TRITC, Jackson ImmunoResearch Laboratories) 1:200 during 45 min at 37 °C. Then the sections were incubated overnight with mouse-anti-IdUrd (Caltag laboratories, Burlingame, CA, USA) 1:1000 in monoclonal liquid diluent (MLD, Euro-DPC, Breda, The Netherlands) at 4 °C. The next morning the sections were incubated during 30 min in donkey-anti-mouse Biotin (Jackson ImmunoResearch Laboratories) 1:400 in PLD at 37 °C, followed by an incubation with STREP-ALEXA350 (Molecular

Probes, Leiden, The Netherlands) 1:200 in PLD during 30 min at 37 °C. After the staining procedure, the sections were mounted in fluorostab (ICN Pharmaceuticals, Zoetermeer, The Netherlands).

After image acquisition of the IdUrd, pimonidazole and vessels signals (see below), all nuclei were stained with Fast Blue (Sigma-Aldrich Chemie BV, Zwijndrecht, The Netherlands) 1:1000 in PBS during 5 min at room temperature. Slides were then rinsed and mounted in PBS for quantitative imaging of all nuclei.

Image acquisition

The sections were scanned by a computerized image processing system using a high-resolution intensified solid-state camera on a fluorescence microscope (Axioskop, Zeiss, Göttingen, Germany).²⁸ Each tumour section was scanned four times at 200x magnification; starting with the IdUrd staining (blue) followed by the pimonidazole signal (green), next the vessels (red) and finally the fast blue signal for the nuclei (blue). For the IdUrd signal (Alexa350) and all nuclei (Fast Blue) (blue signals, 365 nm excitation) a 420 nm emission filter was used. For the hypoxia signal (Alexa488, green, 450-490 nm excitation) a 520 nm emission filter was used. For the vessels (TRITC, red signal, 510-560 nm excitation) a 590 nm emission filter was used.

Thresholds were interactively set above the background staining resulting in a composite binary image for each individual marker. After completion of the scanning procedure the four composite images showing IdUrd, pimonidazole, PAL-E and Fast-Blue were superimposed as previously described by Rijken et al.²⁸ The scanning procedure was followed by a delineation of the tumour area excluding necrosis, artefacts, and non-tumour tissue. This delineation was done with use of a haematoxylin-eosin staining of a consecutive tumour section and was supervised by a pathologist.

Image analysis

Computerized image analysis was performed for the entire delineated tumour section, but also for predefined areas within certain distances from the vessels. The hypoxic fraction (HF pimo) was defined as the pimonidazole positive surface divided by the total tumour surface. The vascular density (VD) was defined as the number of vascular structures per mm² of tumour surface. The labelling index (IdUrd LI) was determined as the area of IdUrd positively stained nuclei relative to the total area of nuclei (Fast Blue). In order to quantitate the distribution of hypoxia and proliferation in relation to the vasculature, zones were chosen arbitrarily at increasing distance from the surface of the nearest vessel (0-50 µm, 50-100 µm,

100-150 μm , 150-200 μm , 200-250 μm , >250 μm). Both IdUrd LI and HF pimo were also calculated within these vascular zones. The labelling index in hypoxia (IdUrd LIH) was defined as the surface positive for both IdUrd and pimonidazole divided by the total nuclear surface (Fast Blue). The fraction of IdUrd-labelled cells positive for pimonidazole (FI_{pimo}) was defined as the area that stained positive for both pimonidazole and IdUrd divided by the total IdUrd-positive area.

Statistics

The statistical analyses were done with the SPSS 12.0.1 software package. Correlations between the biological parameters (HF pimo, IdUrd LI, IdUrd LIH, FI_{pimo} , VD) were assessed using the two-tailed Spearman test. For differences in biological parameters in relation to categorical tumour characteristics (site, stage, histopathological grade) the Kruskal Wallis test was used. Associations between the proliferation parameters and treatment outcome were examined by Cox regression analysis.

Results

Patients and treatment

In the period from May 1998 to February 2001, 55 patients were injected with pimonidazole and IdUrd before biopsy taking. Sixteen biopsies were excluded from further analysis, 6 because they contained no or only very little invasive carcinoma, 7 because of poor quality due to mechanical damage during the biopsy procedure or poor staining quality and 3 because the histological diagnosis was not squamous cell carcinoma.

There were 32 men and 7 women with age ranging from 40 to 85 years and a median of 60 years. The tumour characteristics and treatment are summarized in Table 1. None of the patients reported any adverse reaction after either pimonidazole or IdUrd administration. The duration of follow-up for surviving patients ranged from 42 to 84 months with a median of 73 months.

Staining patterns

The triple staining for vessels, pimonidazole and IdUrd produced bright fluorescent signals with very little background except in areas of necrosis and occasionally in the stromal components of the tumour (Figure 1). The pimonidazole staining was cytoplasmatic whereas IdUrd was confined to the nuclei. Generally, the IdUrd signal was mostly found in proximity to the blood

vessels but with variations between tumours, some with IdUrd labelling also at somewhat larger distance from vessels and others showing a more random pattern of proliferation. Pimonidazole binding was predominantly at a distance from vessels but also the hypoxia patterns differed between tumours. Some tumours are characterized by hypoxic zones of only few cell layers wide while others exhibit larger areas of hypoxia, often but not always with necrosis. Figure 2 shows examples of different hypoxic and proliferation patterns. At visual assessment in most tumours no or only little overlap is observed between pimonidazole and IdUrd positivity. Only very few tumour biopsies clearly demonstrated significant amounts of IdUrd labelled nuclei in hypoxic areas. One such exceptional case is shown in Figure 3.

Table 1. Characteristics of 39 squamous cell carcinomas analyzed (UICC 1997).

	No. of patients
Site	
larynx	14
hypopharynx	11
oropharynx	12
oral cavity	2
T-stage	
T1	3
T2	8
T3	19
T4	9
N-stage	
N0	9
N1	9
N2	19
N3	2
Differentiation grade	
well	1
moderate	23
poor	15
Treatment	
none	1
ARCON	19
radiotherapy alone	9
surgery and radiotherapy	6
chemotherapy and radiotherapy	4
Total	39

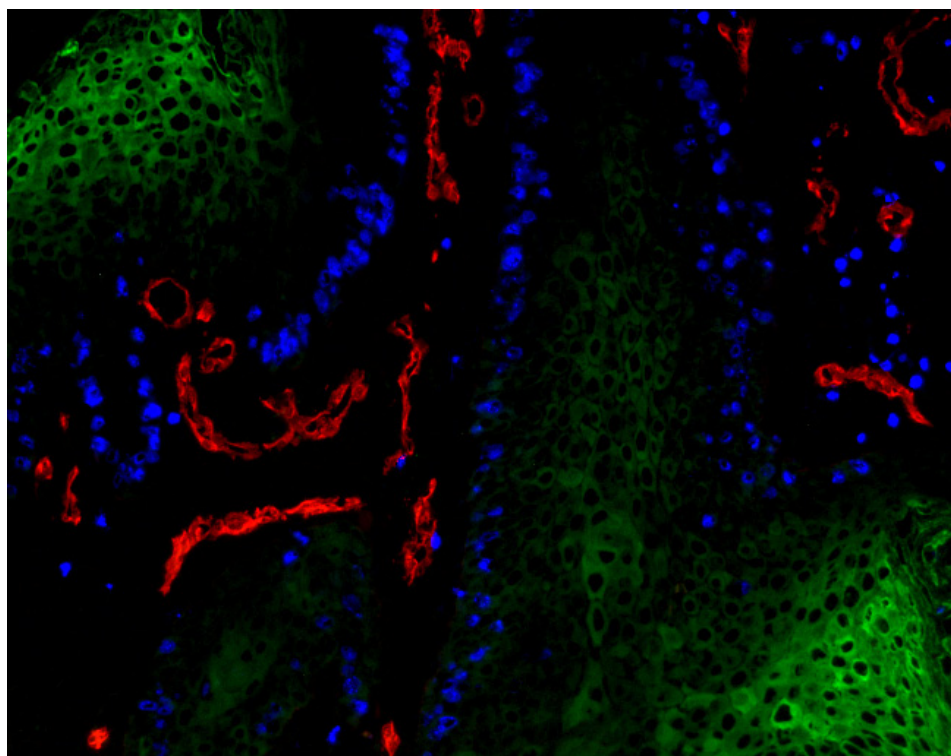


Figure 1. Fluorescent microscopic image of a hypopharynx carcinoma. Red: vessels; blue: IdUrd, nuclear stain; green: pimonidazole, cytoplasmic stain.

Quantitative analysis

Mean and median values and range for HF Pimo, IdUrd LI, IdUrd LIH, $Fid_{[Pimo]}$ and VD for the 39 tumour biopsies are given in Table 2. None of these parameters correlated with clinical tumour characteristics such as tumour site, T-stage, N-stage or histopathological grade. There was a significant ($p < 0.001$) albeit weak ($r = 0.57$) negative correlation between VD and HF pimo (Figure 4). No correlations were found between HF pimo or VD and the proliferation parameters. $Fid_{[pimo]}$ ranged from 0% to 16.7% with a mean of 2.4% indicating that proliferative activity was low in hypoxic areas and occurred mainly in the well-oxygenated tumour compartments. IdUrd positive cells in hypoxic areas made up 0.09% (mean) of the total viable tumour cell mass (IdUrd LIH).

Relative to the vasculature, IdUrd and pimonidazole binding demonstrated opposite distribution patterns (Figure 5). The pimonidazole signal increased with increasing distance from vessels and was most pronounced at distances $>150 \mu m$. IdUrd labelling decreased with distance from vessels although IdUrd labelled cells could still be found at distances $>200 \mu m$. However, also at these larger distances, IdUrd labelling was predominantly in well-oxygenated tumour areas.

The fraction of dual labelled cells (IdUrd and pimonidazole) was slightly higher at greater distance but IdUrd LIH was well below 0.3% in all zones.

No associations were found between the proliferation parameters (IdUrd LI, IdUrd LIH, FId_[pimo]) and the treatment outcome endpoints local control, metastasis-free survival, disease-free survival and overall survival.

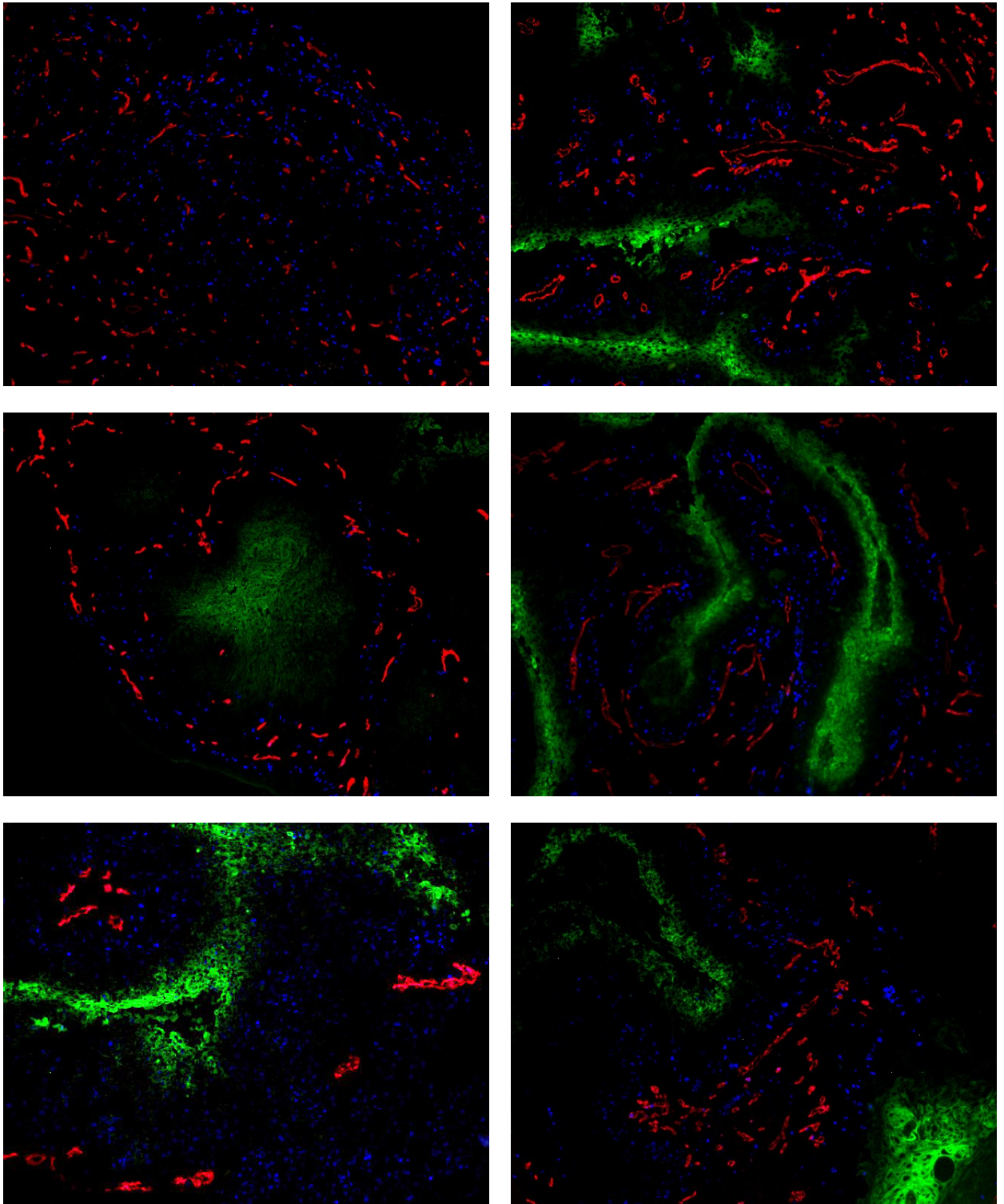


Figure 2. Fluorescent microscopic images of six different head and neck carcinomas. Red: vessels; blue: IdUrd; green: pimonidazole. Note differences in patterns of hypoxia and proliferation and relation to blood vessels.

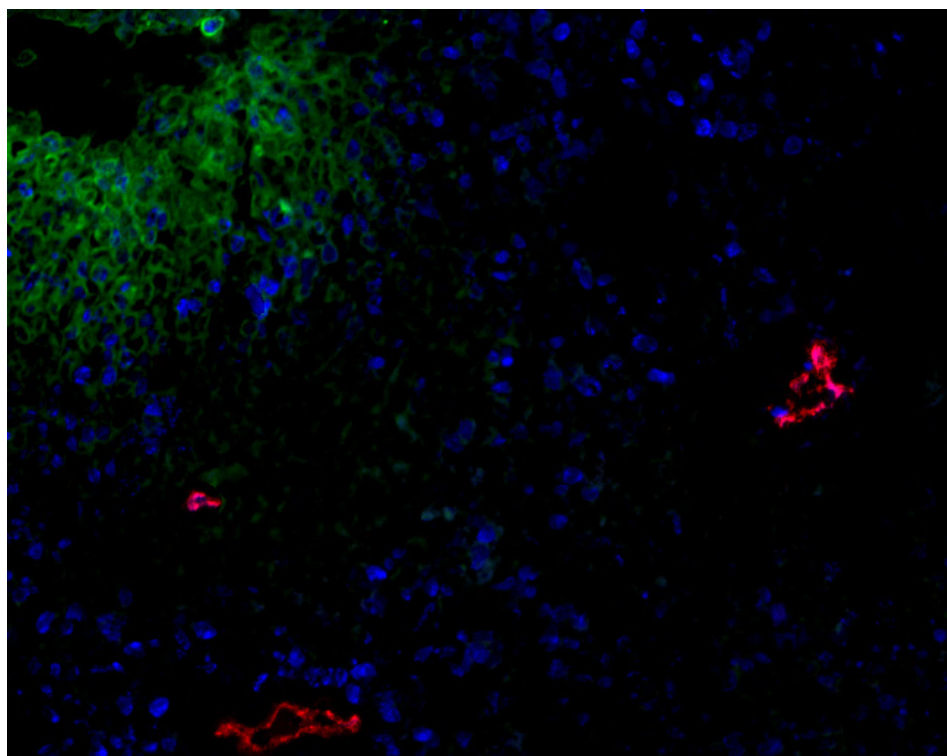


Figure 3. Fluorescent microscopic image of an oropharynx carcinoma. Red: vessels; blue: IdUrd; green: pimonidazole. IdUrd labelling in pimonidazole positive areas indicating active DNA-synthesis under hypoxic conditions.

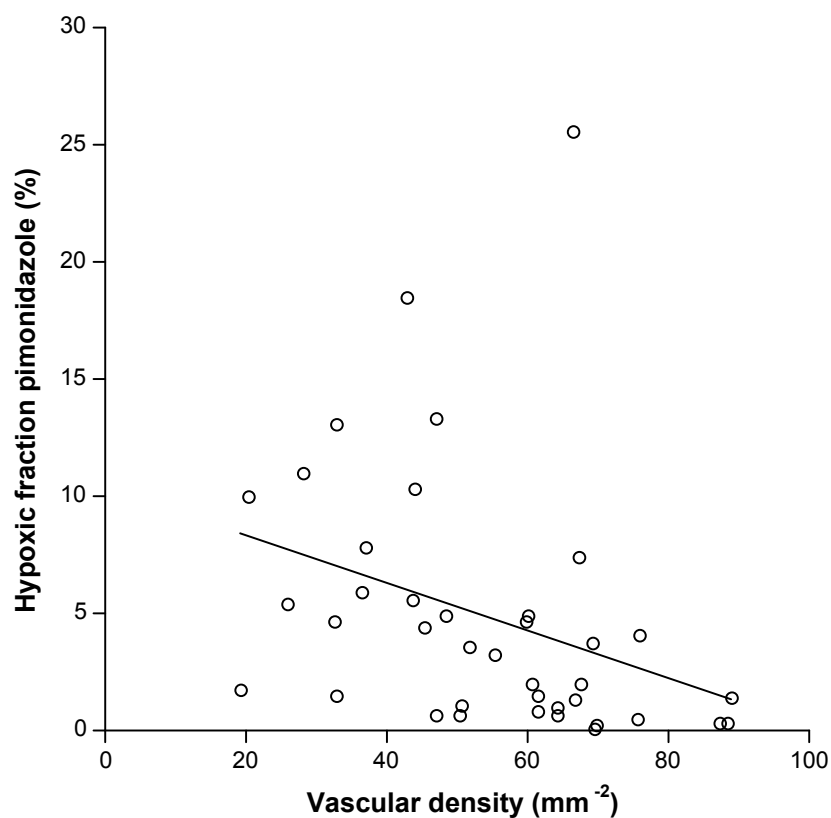


Figure 4. Comparison between the fraction of the tumour area that binds pimonidazole (HF pimo) and vascular density (VD). The linear best fit is shown.

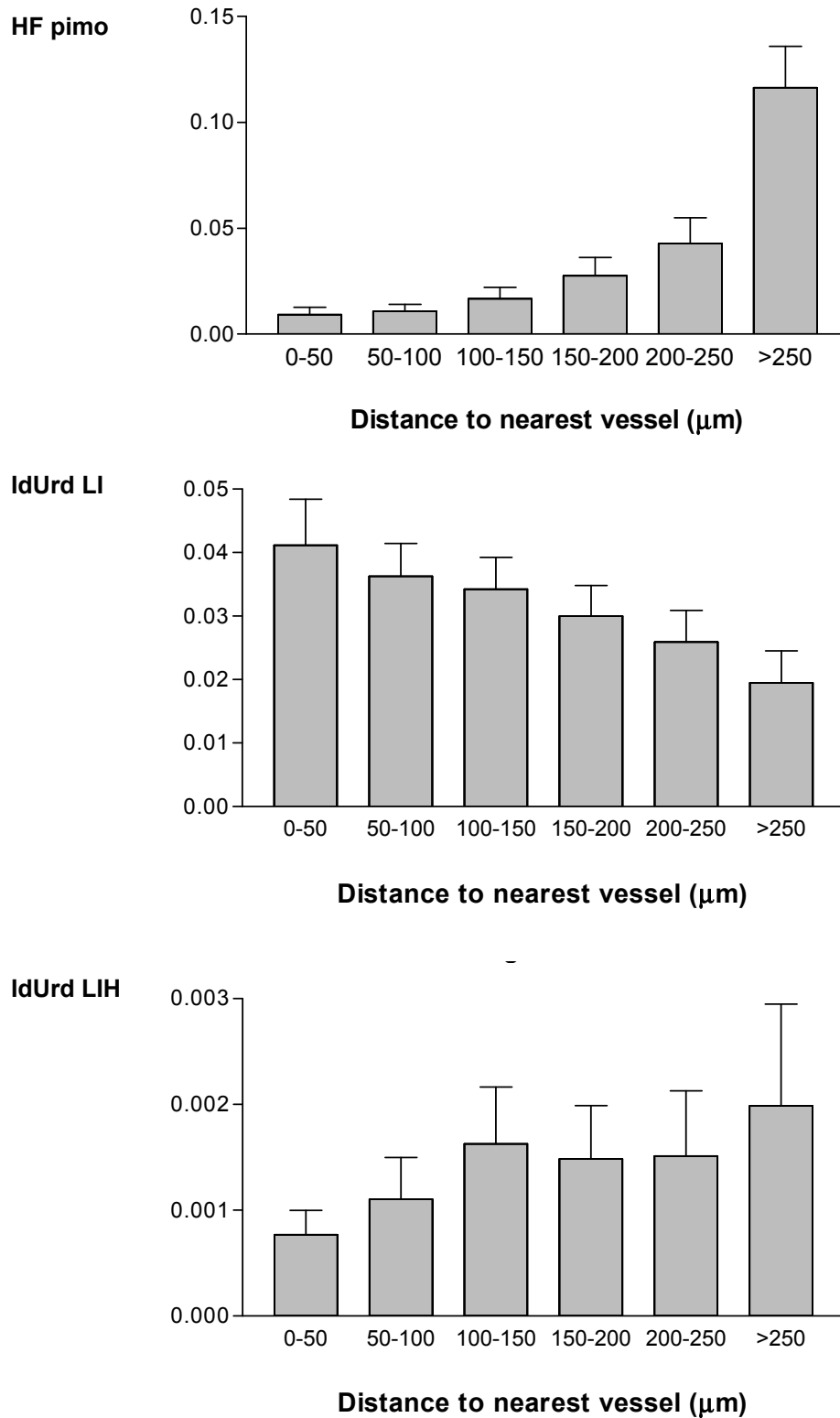


Figure 5. Relative hypoxic fraction (HF pimo), IdUrd labelling index (IdUrd LI) and area positive for both IdUrd and pimonidazole relative to total nuclear area (IdUrd LIH) as a function of distance to nearest vessels. Plots show average values of 39 tumours.

Discussion

Malignant tumours tend to outgrow their vascular supply which leads to deficiencies in nutrients and oxygen. This is further enhanced by the chaotic organization of the vascular bed and inefficient transport function. As a consequence of these gradients of oxygen and nutrient availability, functionally and kinetically distinct populations of cells exist within a tumour. Heterogeneities in oxygenation and proliferative activity within a tumour reflect the dynamic nature of evolving and regressing subpopulations of cells. It is likely that certain specific cellular subpopulations will have a greater impact on tumour aggressiveness and treatment response than others.²⁹

Under sustained hypoxic conditions, tumour cells undergo a variety of biological responses including activation of several signalling pathways for the regulation of proliferation, angiogenesis and apoptosis.^{30,31} These adaptation mechanisms allow clonogenic tumour cells to survive and even proliferate under hypoxic conditions. Because hypoxia protects against radiation damage, these cells may survive radiation treatment and eventually lead to local recurrences. This study aimed to identify and quantify this cell population by using a triple marker assay for vasculature, hypoxia and proliferation.

Patterns of hypoxia and proliferation

Different patterns of hypoxia and proliferation are observed between tumours. A detailed description of these patterns was the subject of previous studies.^{32,33} Characterization of these patterns was based on the spatial relationship with the vasculature. Some tumours exhibit large hypoxic areas with viable cells even at great distance from vessels (Figure 2C) whereas other tumours have hypoxic zones of only few cell layers wide with necrosis at slightly greater distance (Figures 2D,F). In addition, inter-tumour variations of distances from vessels to the “hypoxic front” were described.³² Similarly, different patterns of proliferation have been described varying from proliferation restricted to only few cell layers around vessels (Figures 2B,C) to random proliferative activity throughout the tumour (Figure 2E) and intermediate patterns (Figure 2F).^{33,34} These phenotypic patterns are the reflection of a dynamic system and depend on the metabolic and kinetic activity of the tumour cells.

Tumour cell proliferation under hypoxic conditions

Proliferative activity was mainly found in the well oxygenated compartments of the tumour and decreased in hypoxic areas more distant from the vasculature. This

does not necessarily mean that the overall proliferative activity is less in hypoxic tumours or vice versa. The current study showed a weak inverse correlation between hypoxic fraction (HF pimo) and VD indicating that there is a trend for poorly vascularized tumours to be more hypoxic. However, the overall proliferative activity was independent of tumour vascularity and overall oxygenation status. This is consistent with results from other studies that have used combined assays of proliferation and hypoxia.³⁵⁻⁴⁵

A limitation when comparing these studies is that a variety of endogenous and exogenous markers were used for assessment of hypoxia and proliferation. Also the methods of analysis differed and included quantitative and semi-quantitative immunohistochemistry, flow cytometry and microelectrode pO₂ measurements. Nevertheless, all studies except one small study in cervical carcinoma³⁶ concur that there is no correlation between overall labelling index of the proliferation markers and measurements of hypoxia. However, only few studies used methods that enabled quantification of the cell population that is proliferating under hypoxic conditions.

Two studies combined pO₂ measurements by Eppendorf microelectrodes with flow cytometric analysis of BrdUrd or IdUrd labelling.^{39,40} This combination of methods does not allow a spatial correlation at the micro regional level and thus only global associations can be investigated.

Two other studies analyzed immunolabelling with BrdUrd and nitroimidazole hypoxia markers by flow cytometry.^{41,42} Although with this approach information about the architectural context is lost, it did provide quantitative data on the amount of dual labelled cells. This was less than 2% of the total tumour cell population in the xenografted human cervix cancer line SiHa⁴² and 3.6% in the murine sarcoma SaF.⁴¹ There are three reports that used a combination of nitroimidazole markers (pimonidazole, EF-5 or CCI-103F) and endogenous proliferation markers (Ki-67, MIB-1, or PCNA), analyzed by semi-quantitative immunohistochemistry.^{35,36,43} A limitation of these studies was that the staining for the hypoxia markers and proliferation markers was done in separate albeit consecutive tissue sections. This allows a qualitative assessment of the histological patterns of hypoxia and proliferation and areas of co-localization of the markers but no quantitative analysis. Two of these investigations were on human tumours and reported that proliferation was only rarely seen in hypoxic tumour areas.^{35,36} The study by Zeman et al.⁴³ in canine tumours described overlap to varying extents. Quantitation of dual labelling in immunohistochemical assays requires staining of both markers in the same tissue section and computerized

image analysis. To our knowledge only the current study and the studies by Hoogsteen et al.⁴⁵ and by van Laarhoven et al.³⁸ which are also from our group, used this technology. Our results have shown that in human head and neck cancers, active DNA synthesis as measured by IdUrd labelling occurs only sporadically under hypoxic conditions. The proportion of cells labelled by both IdUrd and pimonidazole ($FId_{[pimo]}$) was 2.4% of all IdUrd positive cells and this was only 0.09% of the total tumour cell population. The same technique was applied to liver metastases of colorectal cancer and yielded a significantly higher $FId_{[pimo]}$ value of 7.9%.³⁸ Also, the histological patterns of hypoxia and proliferation differed from those generally found in head and neck cancers. This clearly illustrates the differences in micro regional organization and kinetics between tumours of different origin and histology.

Characteristics of markers

A diversity of immunohistochemical markers with different characteristics is being used for assessment of hypoxia and proliferation. Intracellular binding of pimonidazole requires pO_2 levels below 10 mmHg. The tumour-associated transmembrane enzyme carbonic anhydrase IX (CA-IX) is used as an endogenous hypoxia-related marker and is upregulated under pO_2 levels from 20 mmHg downward. Both hypoxia markers demonstrate concordant staining patterns but because expression of CA-IX occurs at higher pO_2 levels than pimonidazole binding, CA-IX is often seen at shorter distance from blood vessels. This explains why we found a much higher proportion of IdUrd labelled cells in CA-IX positive tumour areas (11%) in a previous study, also in head and neck cancers⁴⁵, as compared to the current study with pimonidazole (2.4%).

Also the proliferation markers identify different cell populations. IdUrd and BrdUrd are thymidine analogues and label only those cells that are actively synthesizing DNA. Flow cytometric analysis of murine tumours revealed the presence of viable cells in necrotic tumour areas with S-phase DNA content but which had not incorporated BrdUrd.⁴⁶ One of the reasons proposed for the existence of these cells has been that they were hypoxic and had arrested in S-phase. This suggests that thymidine analogues might underestimate the proportion of S-phase cells under hypoxic conditions. Experiments using two hypoxic markers (pimonidazole and CCI-103F) together with BrdUrd in a murine tumour model possibly indicate that this can be a temporary arrest.⁴⁷ These experiments showed that at 28 h after a single dose of irradiation the overall cell density in the tumour had decreased to 55% of the initial value and cells that were hypoxic (stained by first hypoxic marker) at the time of irradiation had been reoxygenated (not stained by second

hypoxic marker). A significant proportion of these previously hypoxic cells had resumed proliferation as identified by BrdUrd labelling.

The endogenous proliferation markers are expressed during different phases of the cell cycle. Ki-67 is expressed in all cycling cells whereas PCNA shows highest expression during S-phase. PCNA however has a long half-life and can also be found in other phases and even in a certain fraction of non-cycling cells.⁴⁸ Cyclins are regulatory subunits of kinases that regulate the cell cycle. The pattern of cyclin expression varies with a cell's progression through the cell cycle, and this specific cyclin expression pattern defines the relative position of the cell within the cell cycle.

It is thus clear that combinations of different hypoxic and proliferation markers will yield different results. The question that remains to be answered is which set of markers is best at identifying the subpopulation of cells that is clinically most relevant.

Clinical relevance

In the current study, the proportion of cells proliferating under hypoxic conditions was small, especially if this was related to the total viable tumour cell population (0.09%). This does not necessarily mean that it is also an insignificant population. If these cells are resistant to treatment and represent tumour aggressiveness they can be responsible for recurrence formation even if low in number. In the current material there was no association between the magnitude of this cell population and treatment outcome. However, a possible relation cannot be fully excluded because a limitation of this study is the relatively small sample size and the heterogeneity of the patient selection with regard to tumour site, stage and treatment. This precludes definite conclusions and verification of the results is needed in a larger patient cohort. Hoogsteen et al.⁴⁵ observed that a high fraction of IdUrd-labelled cells positive for CA-IX was significantly correlated with worse disease-free survival rates in head and neck cancer. This suggests that the population of cells under intermediate hypoxic conditions may be more relevant for tumour behavior and treatment outcome than cells that are already severely hypoxic.

Conclusion

Using an immunohistochemical triple staining technique combined with a computerized simultaneous analysis of multiple parameters we were able to

assess co-localization between proliferating cells and hypoxia in head and neck carcinomas. In the current analysis, the proportion of proliferating cells in hypoxia was small and showed no relation with treatment outcome. Which combination of immunohistochemical markers is most useful to identify a clinically relevant cell population is currently under investigation in a larger patient material.

Acknowledgements

This study was supported by Dutch Cancer Society Grant KUN 98-1814.

The authors wish to thank Peter C.M. de Wilde for supervising the pathological assessment of tumour sections.

References

1. Kaanders JH, Bussink J, van der Kogel AJ. Clinical studies of hypoxia modification in radiotherapy. *Semin Radiat Oncol* 2004;14:233-240.
2. Janssen HL, Haustermans KM, Balm AJ, *et al.* Hypoxia in head and neck cancer: how much, how important? *Head Neck* 2005;27:622-638.
3. Kim JJ, Tannock IF. Repopulation of cancer cells during therapy: an important cause of treatment failure. *Nat Rev Cancer* 2005;5:516-525.
4. Overgaard J, Hansen HS, Specht L, *et al.* Five compared with six fractions per week of conventional radiotherapy of squamous-cell carcinoma of head and neck: DAHANCA 6 and 7 randomised controlled trial. *Lancet* 2003;362:933-940.
5. Fu KK, Pajak TF, Trotti A, *et al.* A Radiation Therapy Oncology Group (RTOG) phase III randomized study to compare hyperfractionation and two variants of accelerated fractionation to standard fractionation radiotherapy for head and neck squamous cell carcinomas: first report of RTOG 9003. *Int J Radiat Oncol Biol Phys* 2000;48:7-16.
6. Kropveld A, Slootweg PJ, Blankenstein MA, *et al.* Ki-67 and p53 in T2 laryngeal cancer. *Laryngoscope* 1998;108:1548-1552.
7. Begg AC, Haustermans K, Hart AA, *et al.* The value of pretreatment cell kinetic parameters as predictors for radiotherapy outcome in head and neck cancer: a multicenter analysis. *Radiother Oncol* 1999;50:13-23.
8. Bjork-Eriksson T, West CM, Cvetskovska E, *et al.* The lack of correlation between proliferation (Ki-67, PCNA, LI, Tpot), p53 expression and radiosensitivity for head and neck cancers. *Br J Cancer* 1999;80:1400-1404.
9. Sittel C, Eckel HE, Damm M, *et al.* Ki-67 (MIB1), p53, and Lewis-X (LeuM1) as prognostic factors of recurrence in T1 and T2 laryngeal carcinoma. *Laryngoscope* 2000;110:1012-1017.
10. Liu M, Lawson G, Delos M, *et al.* Prognostic value of cell proliferation markers, tumour suppressor proteins and cell adhesion molecules in primary squamous cell carcinoma of the larynx and hypopharynx. *Eur Arch Otorhinolaryngol* 2003;260:28-34.
11. Wilson GD, Saunders MI, Dische S, *et al.* Pre-treatment proliferation and the outcome of conventional and accelerated radiotherapy. *Eur J Cancer* 2006;42:363-371.
12. Dobrowsky W, Dobrowsky E, Wilson GD. In vivo cell kinetic measurements in a randomized trial of continuous hyperfractionated accelerated radiotherapy with or without mitomycin C in head-and-neck cancer. *Int J Radiat Oncol Biol Phys* 2003;55:576-582.
13. Nordsmark M, Bentzen SM, Rudat V, *et al.* Prognostic value of tumor oxygenation in 397 head and neck tumors after primary radiation therapy. An international multi-center study. *Radiother Oncol* 2005;77:18-24.
14. Brizel DM, Sibley GS, Prosnitz LR, *et al.* Tumor hypoxia adversely affects the prognosis of carcinoma of the head and neck. *Int J Radiat Oncol Biol Phys* 1997;38:285-289.
15. Jonathan RA, Wijffels KI, Peeters W, *et al.* The prognostic value of endogenous hypoxia-related markers for head and neck squamous cell carcinomas treated with ARCON. *Radiother Oncol* 2006;79:288-297.
16. Aebbersold DM, Burri P, Beer KT, *et al.* Expression of hypoxia-inducible factor-1alpha: a novel predictive and prognostic parameter in the radiotherapy of oropharyngeal cancer. *Cancer Res* 2001;61:2911-2916.
17. Koukourakis MI, Giatromanolaki A, Sivridis E, *et al.* Hypoxia-regulated carbonic anhydrase-9 (CA-IX) relates to poor vascularization and resistance of squamous cell head and neck cancer to chemoradiotherapy. *Clin Cancer Res* 2001;7:3399-3403.
18. Beasley NJ, Wykoff CC, Watson PH, *et al.* Carbonic anhydrase IX, an endogenous hypoxia marker, expression in head and neck squamous cell carcinoma and its relationship to hypoxia, necrosis, and microvessel density. *Cancer Res* 2001;61:5262-5267.
19. Baer S, Casaubon L, Schwartz MR, *et al.* Glut3 expression in biopsy specimens of laryngeal carcinoma is associated with poor survival. *Laryngoscope* 2002;112:393-396.
20. Oliver RJ, Woodward RT, Sloan P, *et al.* Prognostic value of facilitative glucose transporter Glut-1 in oral squamous cell carcinomas treated by surgical resection; results of EORTC Translational Research Fund studies. *Eur J Cancer* 2004;40:503-507.
21. Kunkel M, Reichert TE, Benz P, *et al.* Overexpression of Glut-1 and increased glucose metabolism in tumors are associated with a poor prognosis in patients with oral squamous cell carcinoma. *Cancer* 2003;97:1015-1024.
22. Kaanders JH, Wijffels KI, Marres HA, *et al.* Pimonidazole binding and tumor vascularity predict for treatment outcome in head and neck cancer. *Cancer Res* 2002;62:7066-7074.

23. Janssen HL, Haustermans KM, Sprong D, *et al.* HIF-1A, pimonidazole, and iododeoxyuridine to estimate hypoxia and perfusion in human head-and-neck tumors. *Int J Radiat Oncol Biol Phys* 2002;54:1537-1549.
24. Wykoff CC, Beasley NJ, Watson PH, *et al.* Hypoxia-inducible expression of tumor-associated carbonic anhydrases. *Cancer Res* 2000;60:7075-7083.
25. Evans SM, Hahn S, Pook DR, *et al.* Detection of hypoxia in human squamous cell carcinoma by EF5 binding. *Cancer Res* 2000;60:2018-2024.
26. Kaanders JH, Pop LA, Marres HA, *et al.* ARCON: experience in 215 patients with advanced head-and-neck cancer. *Int J Radiat Oncol Biol Phys* 2002;52:769-778.
27. Schlingemann RO, Dingjan GM, Emeis JJ, *et al.* Monoclonal antibody PAL-E specific for endothelium. *Lab Invest* 1985;52:71-76.
28. Rijken PF, Bernsen HJ, van der Kogel AJ. Application of an image analysis system to the quantitation of tumor perfusion and vascularity in human glioma xenografts. *Microvasc Res* 1995;50:141-153.
29. Hoogsteen IJ, Marres HA, Bussink J, *et al.* The tumor microenvironment in head and neck squamous cell carcinomas: predictive value and clinical relevance of hypoxic markers. *Head Neck* 2006;in press.
30. Hockel M, Vaupel P. Tumor hypoxia: definitions and current clinical, biologic, and molecular aspects. *J Natl Cancer Inst* 2001;93:266-276.
31. Harris AL. Hypoxia--a key regulatory factor in tumour growth. *Nat Rev Cancer* 2002;2:38-47.
32. Wijffels KI, Kaanders JH, Rijken PF, *et al.* Vascular architecture and hypoxic profiles in human head and neck squamous cell carcinomas. *Br J Cancer* 2000;83:674-683.
33. Wijffels KI, Kaanders JH, Marres HA, *et al.* Patterns of proliferation related to vasculature in human head-and-neck carcinomas before and after transplantation in nude mice. *Int J Radiat Oncol Biol Phys* 2001;51:1346-1353.
34. Bennett MH, Wilson GD, Dische S, *et al.* Tumour proliferation assessed by combined histological and flow cytometric analysis: implications for therapy in squamous cell carcinoma in the head and neck. *Br J Cancer* 1992;65:870-878.
35. Evans SM, Hahn SM, Magarelli DP, *et al.* Hypoxic heterogeneity in human tumors: EF5 binding, vasculature, necrosis, and proliferation. *Am J Clin Oncol* 2001;24:467-472.
36. Kennedy AS, Raleigh JA, Perez GM, *et al.* Proliferation and hypoxia in human squamous cell carcinoma of the cervix: first report of combined immunohistochemical assays. *Int J Radiat Oncol Biol Phys* 1997;37:897-905.
37. Hoskin PJ, Sibtain A, Daley FM, *et al.* The immunohistochemical assessment of hypoxia, vascularity and proliferation in bladder carcinoma. *Radiother Oncol* 2004;72:159-168.
38. van Laarhoven HW, Kaanders JH, Lok J, *et al.* Hypoxia in relation to vasculature and proliferation in liver metastases in patients with colorectal cancer. *Int J Radiat Oncol Biol Phys* 2005.
39. Tsang RW, Fyles AW, Milosevic M, *et al.* Interrelationship of proliferation and hypoxia in carcinoma of the cervix. *Int J Radiat Oncol Biol Phys* 2000;46:95-99.
40. Nordsmark M, Hoyer M, Keller J, *et al.* The relationship between tumor oxygenation and cell proliferation in human soft tissue sarcomas. *Int J Radiat Oncol Biol Phys* 1996;35:701-708.
41. Webster L, Hodgkiss RJ, Wilson GD. Simultaneous triple staining for hypoxia, proliferation, and DNA content in murine tumours. *Cytometry* 1995;21:344-351.
42. Durand RE, Raleigh JA. Identification of nonproliferating but viable hypoxic tumor cells in vivo. *Cancer Res* 1998;58:3547-3550.
43. Zeman EM, Calkins DP, Cline JM, *et al.* The relationship between proliferative and oxygenation status in spontaneous canine tumors. *Int J Radiat Oncol Biol Phys* 1993;27:891-898.
44. Ljungkvist AS, Bussink J, Rijken PF, *et al.* Vascular architecture, hypoxia, and proliferation in first-generation xenografts of human head-and-neck squamous cell carcinomas. *Int J Radiat Oncol Biol Phys* 2002;54:215-228.
45. Hoogsteen IJ, Marres HA, Wijffels KI, *et al.* Colocalization of carbonic anhydrase 9 expression and cell proliferation in human head and neck squamous cell carcinoma. *Clin Cancer Res* 2005;11:97-106.
46. Rutgers DH, Niessen DP, van der Linden PM. Cell kinetics of hypoxic cells in a murine tumour in vivo: flow cytometric determination of the radiation-induced blockage of cell cycle progression. *Cell Tissue Kinet* 1987;20:37-42.
47. Ljungkvist AS, Bussink J, Kaanders JH, *et al.* Dynamics of hypoxia, proliferation and apoptosis after irradiation in a murine tumor model. *Radiat Res* 2006;165:326-336.

48. Wijsman JH, Van Dierendonck JH, Keijzer R, *et al.* Immunoreactivity of proliferating cell nuclear antigen compared with bromodeoxyuridine incorporation in normal and neoplastic rat tissue. *J Pathol* 1992;168:75-83.

Chapter 7

Absence of hypoxia in malignant salivary gland tumours: preliminary results

K.I.E.M. Wijffels
I.J. Hoogsteen
J. Lok
P.F.J.W. Rijken
H.A.M. Marres
P.C.M. de Wilde
A.J. van der Kogel
J.H.A.M. Kaanders

Abstract

Purpose

Hypoxia is detected in most solid tumours and is associated with malignant progression and adverse treatment outcome. However, the oxygenation status of malignant salivary gland tumours has not previously been studied. The aim of this study was to investigate the potential clinical relevance of hypoxia in this tumour type.

Methods and materials

Twelve patients planned for surgical resection of a salivary gland tumour were preoperatively injected with the hypoxia marker pimonidazole and the proliferation marker iododeoxyuridine (IdUrd). Tissue samples of the dissected tumour were immunohistochemically stained for blood vessels, pimonidazole, carbonic anhydrase-IX (CA-IX), the glucose transporters-1 and -3 (Glut-1, Glut-3), hypoxia-inducible factor-1 α (HIF-1 α), IdUrd and for the epidermal growth factor receptor (EGFR). The tissue sections were quantitatively assessed by computerized image analysis.

Results

Tissue material from 8 patients was of sufficient quality for quantitative analysis. All tumours were negative for pimonidazole binding as well as for CA-IX, Glut-1, Glut-3 and HIF-1 α . Vascular density was high with a median value of 285 mm⁻² (range 209 – 546 mm⁻²). IdUrd labelling index varied from <0.1% to 12.2% with a median of 2.2%. EGFR expression levels were mostly moderate to high. In half of the cases nuclear expression of EGFR was observed.

Conclusion

The absence of detectable pimonidazole binding as well as the lack of expression of hypoxia-associated proteins in all tumours indicates that malignant salivary gland tumours are generally well oxygenated. It is unlikely that hypoxia is a relevant factor for their clinical behavior and treatment responsiveness.

Introduction

Hypoxia has been recognized as an important factor determining the aggressiveness of tumours and their responsiveness to treatment. Tumour hypoxia plays a role in promoting genetic instability, tumour cell invasiveness, metastasis and overall adverse clinical outcome.^{1,2} It may serve as a physiological selection pressure in tumours by promoting apoptosis in some cells but survival of those cells that have lost their apoptotic potential.³ The causes of hypoxia are multifactorial and include factors such as abnormal tumour vasculature, impaired blood perfusion, rate of oxygen consumption and anemia. Several techniques have become available for measurement of tumour oxygenation including invasive techniques like polarographic needle electrodes and minimal invasive methods such as exogenous hypoxia markers, endogenous molecular markers and functional imaging with positron emission tomography (PET) and dynamic contrast-enhanced magnetic resonance imaging.⁴ Clinically relevant hypoxia is detected in approximately 50% of all solid tumours irrespective of their size and histological features.⁵ It has been shown to decrease the therapeutic efficacy of radiation treatment, surgery and some forms of chemotherapy.

One tumour type where hypoxia is strongly related to treatment responsiveness and outcome is squamous cell carcinoma of the head and neck. A number of clinical studies using various methods for assessment of hypoxia have demonstrated that hypoxia is a strong predictor for locoregional tumour control and survival.^{4,6} Treatment strategies that counteract hypoxic resistance have been most successful in head and neck squamous cell carcinomas.⁷ A less common category of head and neck cancers are the salivary gland tumours. These tumours are generally considered less sensitive to radiotherapy and chemotherapy. To what extent hypoxia plays a role in these tumours is unknown and has not previously been investigated in clinical studies.

The aim of this study was to assess the oxygenation status of salivary gland tumours using the exogenous nitroimidazole marker pimonidazole and a panel of vascular and endogenous hypoxia-related immunohistochemical markers including carbonic anhydrase IX (CA-IX), the glucose transporters-1 and -3 (Glut-1 and Glut-3) and hypoxia-inducible factor-1 α (HIF-1 α). An additional aim was to study the proliferative activity and epidermal growth factor receptor (EGFR) expression patterns in relation to the oxygenation status in these tumours.

Materials and methods

Patients

In the period from 1999 to 2004 tumour tissue was collected from 12 patients who underwent resection of a salivary gland carcinoma after administration of immunohistochemical markers for hypoxia and proliferation. The diagnostic workup included physical examination, biopsies, chest X-ray, CT-scan and/or MRI-scan of the head and neck area.

Approximately 2 h before tumour resection the patients received a 20 min intravenous infusion of 500 mg/m² of the hypoxia marker pimonidazole ((1-((2-hydroxy-3-piperidiny)propyl)-2-nitroimidazole hydrochloride, Hypoxyprobe-1; Natural Pharmacia International, Belmont, MA) dissolved in 100 ml NaCl 0.9%. Pimonidazole is a bioreductive chemical probe with an immunorecognizable side chain. Necrotic areas are not stained by pimonidazole because the probe binds only in viable cells as a result of hypoxia-dependent bioreduction by cellular nitroreductases. The S-phase marker 2'-deoxy-5-iodouridine (IdUrd; Centre Hospitalier Universitaire Vaudois, Lausanne, Switzerland) was injected intravenously in 5 min in a dose of 200 mg, 20 min before tumour resection. IdUrd is a thymidine analogue with a short half-life and is rapidly incorporated into the DNA of S-phase cells. The tumours were removed under general anesthesia and the specimen were transported to the pathology department where representative samples were taken. These tissue samples were snap frozen and stored in liquid nitrogen until immunohistochemical processing.

Approval for this study was obtained from the Institutional Review Board of the Radboud University Medical Centre Nijmegen and all patients gave written informed consent.

Immunohistochemistry

Six staining procedures were performed with different marker combinations: 1) staining for hypoxia using antibodies against CA-IX and pimonidazole and for blood vessels using PAL-E, a monoclonal antibody for human endothelium especially useful in frozen tissue sections⁸; 2) staining for hypoxia by pimonidazole, proliferation by IdUrd and vasculature by PAL-E; 3) Glut-1 and vasculature (PAL-E); 4) Glut-3 and vasculature (PAL-E); 5) HIF-1 α and vasculature (PAL-E); 6) staining combination for EGFR, pimonidazole and PAL-E. In all staining procedures negative and positive control sections were included. As positive controls, tumours were used with significant amounts of hypoxia that in previous studies have consistently demonstrated positivity for the respective

markers. These were included in each staining procedure to assure that the antibodies were working properly. Three different tumour tissues were used for this: biopsy material from a T3N2cM0 squamous cell carcinoma of the larynx, a resected liver metastasis from a colon carcinoma and the FaDu tumour line which is a human head and neck squamous cell carcinoma transplanted in nude mice. Timing and mode of administration of pimonidazole and IdUrd were similar as for the salivary gland tumours except for the administration of pimonidazole in the metastatic colon carcinoma patient which was done 12 h prior to surgery. The positive controls were not intended to be used for comparison of staining levels. From the tissue samples, sections of 5 μ m were cut and mounted on poly-L-lysine coated slides and stored at -80°C. Prior to staining the sections were fixed in acetone of 4°C for 10 min and rehydrated in phosphate buffered saline (PBS) twice for 2 min. Between all consecutive steps of the staining procedure, sections were rinsed in PBS three times for 5 min. The staining combination of CA-IX, pimonidazole and vessels was performed on two different sections whereas the other stainings were done on a single section from each of the tumour samples.

1) CA-IX, pimonidazole and vessels

During 30 min an incubation was done at 37 °C with mouse-anti-CA-IX (E. Oosterwijk, Dept. of urology UMCN, Nijmegen, the Netherlands) 1:100 in PAD ((primary antibody diluent) Genetex, Cambridge, UK). A second incubation was done with goat-anti-mouse Cy3 (Jackson ImmunoResearch Laboratories, West Grove, PA, USA) 1:600, 30 min at 37 °C, followed by donkey-anti-goat Cy3 (Jackson ImmunoResearch Laboratories) during 30 min at 37 °C. Next the sections were incubated with rabbit-anti-pimonidazole (J.A. Raleigh, Dept. of Radiation Oncology and Toxicology, University of North Carolina, Chapel Hill, North Carolina, USA) 1:1000 in PAD during 30 min at 37 °C. Then the sections were incubated with donkey-anti-rabbit Alexa 488 (Molecular Probes, Leiden, The Netherlands) 1:400, 30 min at 37 °C. Finally, the vessels were stained by PAL-E (Euro Diagnostica BV, Arnhem, the Netherlands) 1:10 during 30 min at 37 °C, followed by goat-anti-mouse Cy5 (Jackson ImmunoResearch Laboratories) 1:200 in PBS during 60 min at 37 °C. After the staining procedure, the sections were mounted in fluorostab (Euro Diagnostica BV).

2) Pimonidazole, IdUrd and vessels

For this combination we started with the PAL-E staining as described above followed by the pimonidazole staining. Both the vascular signal and the hypoxia signal were then scanned under the microscope. Next, the sections were taken

back to the lab and DNA was denaturated during 10 min with 2N HCL, followed by 10 min in 0.1 M Borax to neutralize the pH. Then the sections were incubated overnight with mouse-anti-IdUrd (Caltag laboratories, Burlingame, CA, USA) 1:1000 in PAD at 4 °C, followed by goat-anti-mouse Cy3 (Jackson ImmunoResearch Laboratories) 1:600 in PBS for 30 min at 37°C. Finally, all nuclei were stained by Hoechst 33342 (Sigma, St. Louis, MO, USA) 0.5 µg/ml in PBS during 2 min.

3,4,5) Glut-1, Glut-3, HIF-1 α and vessels

These stainings were done at an overnight incubation with either rabbit-anti-Glut-1 (Chemicon international, Temecula, CA, USA) 1:50 in PAD at 4 °C, rabbit-anti-Glut-3 (Chemicon international) 1:100, or with rabbit-anti-HIF-1 α (Santa Cruz Biotechnology, Santa Cruz, CA, USA) 1:50. The first step was followed by 30 min incubation at 37 °C with goat-anti-rabbit Cy3 (Jackson ImmunoResearch Laboratories) 1:600 in PBS and a third incubation of 30 min at 37 °C with donkey-anti-goat Cy3 1:600. Finally, vasculature was stained by PAL-E, but this time the second antibody was chicken-anti-mouse-Alexa 647 (Molecular Probes) 1:100 in PBS for 30 min.

6) EGFR, pimonidazole and vessels

The final staining was done by an overnight incubation with goat-anti-EGFR (Santa Cruz Biotechnology) 1:50 in PAD at 4 °C, followed by donkey-anti-goat Cy3 1:600 in PBS during 30 min at 37 °C. Pimonidazole was stained as previously described. For the vessels we used again Pal-E 1:10 followed by chicken-anti-mouse-Alexa 647 1:100 in PBS for 30 min.

Image acquisition

The sections were scanned at 100x magnification using a high-resolution intensified solid-state camera on a fluorescence microscope (Axioskop, Zeiss, Göttingen, Germany). Each tumour section was scanned for each immunohistochemical signal separately yielding gray scale images of the corresponding signal. From these images, a composite binary image was created using an interactive threshold operation. Signal intensity levels were graphically displayed on a linear scale and the threshold was set at values twice the intensity level of the background where the signal started to show a steep increase. After completion of the scanning procedure the composite images showing the various combinations of markers were superimposed as previously described by Rijken et al.⁹ The scanning procedure was followed by a delineation of the tumour area

excluding necrosis, artifacts, and non-tumour tissue. This delineation was done with use of a haematoxylin-eosin staining of a consecutive tumour section and was supervised by a pathologist.

Image analysis

Computerized image analysis was performed for the entire delineated tumour section. The vascular density was defined as the number of vascular structures per mm² of tumour surface. Hereto, the number of objects in the binary image containing the vascular structures was divided by the total tumour area (converted to mm²) in the binary image containing the delineated tumour area. The IdUrd labelling index was determined as the area of IdUrd positively stained nuclei relative to the total area of nuclei (Hoechst). To quantify EGFR expression we estimated the percentage of positively labelled cells relative to the total tumour area and categorized the tumours into 4 groups: ≤10%, 10 - 30%, 30 - 50% and ≥50%.

Statistics

Correlations between marker expression were assessed by the Spearman test (two-tailed) using the SPSS 12.0.1 software package.

Results

Patients

Tumour material was collected from 12 patients. Samples from two patients contained no viable tumour tissue and one tumour was too small to properly be examined. One tumour was contaminated by an infection and therefore the tumour was not easily recognizable. All patients underwent primary surgery and were not previously treated for this tumour. Except for one they all received postoperative radiotherapy. Patient and tumour characteristics are shown in table 1. The mean follow-up was 27 months with a range from 6 to 60 months.

Immunohistochemical stainings

The positive controls stained strongly for pimonidazole, partially co-localizing with CA-IX (Figure 1). However, none of the salivary gland tumours showed detectable staining of pimonidazole or CA-IX (Figures 1 and 2). Because this was somewhat unexpected, the combined staining for CA-IX, pimonidazole and vessels was repeated on different tumour sections with the same result. Also, Glut-1, Glut-3,

and HIF-1 α expression could not be demonstrated in any of the salivary gland tumours while the metastatic colon carcinoma showed strong positivity for both glucose transporters and the FaDu tumour line demonstrated extensive nuclear expression of HIF-1 α .

Table 1. Patient and tumour characteristics

Number	Age	Localisation	Histology	Clinical follow up	Duration of follow up
1	66	oral cavity	mucoepidermoid carcinoma, low grade	alive, no evidence of disease	60 months
2	81	parotid gland	oncocytic carcinoma	dead, no evidence of disease	6 months
3	83	parotid gland	adenocarcinoma	died with local relapse	9 months
4	28	parotid gland	oncocytic carcinoma	alive with distant metastases	40 months
5	52	parotid gland	adenosquamous carcinoma	dead with distant metastases	6 months
6	72	parotid gland	mucoepidermoid carcinoma, high grade	dead with distant metastases	32 months
7	43	parotid gland	adenoidcystic carcinoma	alive, no evidence of disease	42 months
8	65	parotid gland	acinic cell carcinoma	alive, no evidence of disease	24 months

The IdUrd staining was bright and reproducible as shown in figures 1 and 2. The proliferative activity varied widely between the tumours with an IdUrd labelling index ranging from <0.1% to 12.2% with a median of 2.2% (Table 2). Whereas squamous cell carcinomas often show active proliferation in close proximity to the blood vessels, the salivary gland tumours mostly showed a more random pattern of proliferation.

All salivary gland tumours exhibited a dense vascular network. Vascular densities ranged from 209 mm⁻² to 546 mm⁻² with a median value of 285 mm⁻² (Table 2). In some of the tumours, areas with lower vascular density were observed which contained mainly stromal elements (Figure 1D-F). There were hardly any necrotic parts.

EGFR expression was found in all tumours but in only four this was a typical membranous staining pattern. The other tumours showed predominantly nuclear expression (Figure 3). In one tumour to a lesser extent both expression patterns were found. EGFR positivity varied from <10% of viable tumour area involved to >50% (Table 2). There was no correlation between IdUrd labelling index and EGFR expression ($p = 0.32$).

Table 2. EGFR expression, vascular density and IdUrd labelling index.

Number	EGFR expression pattern	EGFR relative area positive (%)	Vascular density (mm ⁻²)	IdUrd labelling index (%)
1	membranous	30-50	283	2.1
2	nuclear	10-30	298	5.9
3	nuclear	30-50	275	12.2
4	nuclear	30-50	546	0.1
5	membranous	<10	232	10.5
6	nuclear and membranous	30-50	308	--*
7	membranous	<10	209	2.2
8	membranous	>50	288	<0.1

* No IdUrd administered

Discussion

Salivary gland tumours are generally considered to be of low radiosensitivity. However, the basis for this assumption goes back to few, mainly older studies.¹⁰ It has been suggested that hypoxia might be a causative factor related to this alleged radiotherapy resistance.¹¹ In this context it is of interest to note that for inoperable, incompletely resected or recurrent salivary gland tumours, a significant advantage for radiotherapy with fast neutrons was recognized relative to conventional radiotherapy with high energy photons with 10-year locoregional control rates of 56% and 17%, respectively.¹² Fast neutrons were the first of the non-conventional radiation qualities used in clinical radiation therapy. Neutrons are of high Linear Energy Transfer (LET) quality, characterized by dense energy deposits along the radiation track whereas photons (low LET) produce smaller and more variable energy deposits. High LET radiation is less dependent on tissue oxygenation and thus more effective in hypoxic tumours as compared to low LET photon irradiation. The success of neutrons in salivary gland tumours supported the suggestion of clinically relevant hypoxia in these tumours.¹³ With the re-introduction of high LET particle radiotherapy in several centers around the

world it is likely that the argument of hypoxia will be used again for selection of patients with salivary gland tumours.

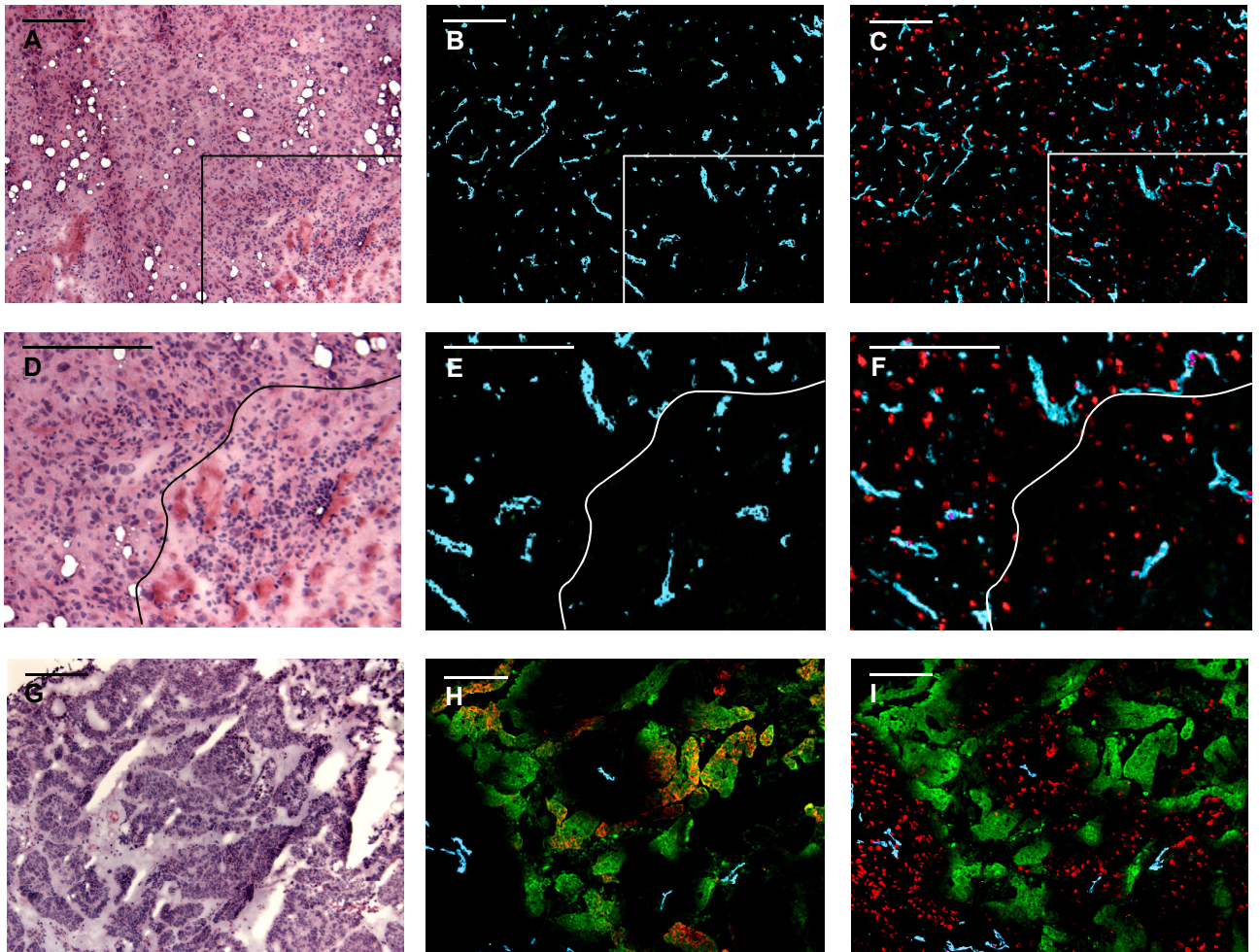


Figure 1. Microscopic images of salivary gland carcinoma (#5) (upper panels) and squamous cell carcinoma of the head and neck (lower panels). A and D: hematoxylin and eosin staining. B and E: immunofluorescent images showing blood vessels (blue), pimonidazole (green) and CA-IX (red). Co-localization of pimonidazole and CA-IX shows as yellow. Note absence of pimonidazole and CA-IX in salivary gland carcinoma but higher vascular density compared to squamous cell carcinoma. C and F: immunofluorescent images showing blood vessels (blue), pimonidazole (green) and iododeoxyuridine (red). Active proliferation in both tumours.

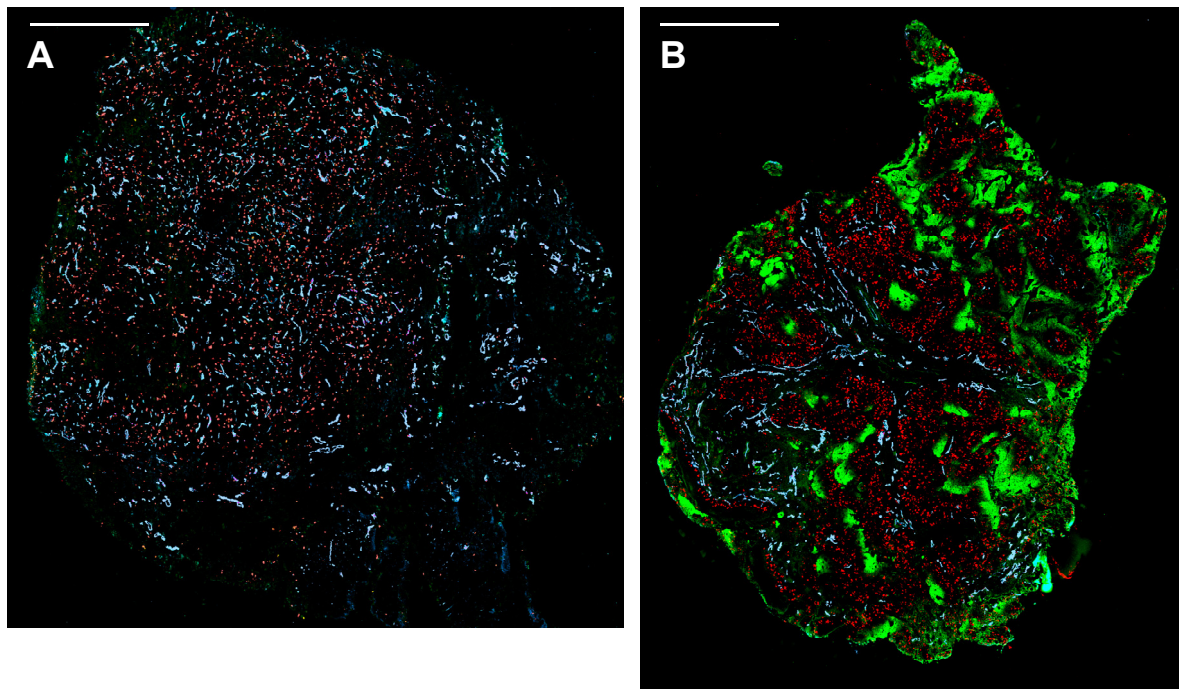


Figure 2. Composite binary images of complete tumour samples showing blood vessels (blue), pimonidazole (green), iododeoxyuridine (red), A: salivary gland carcinoma (#5). B: head and neck squamous cell carcinoma. High vascular density and absence of detectable hypoxia in salivary gland tumour. Active proliferation in both tumours. Scale bars represent 1 mm.

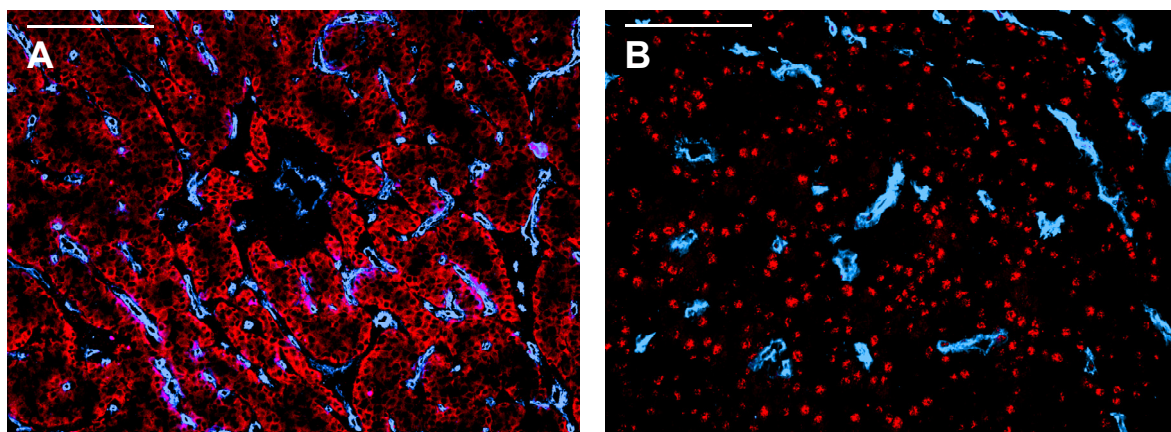


Figure 3. Immunofluorescent images of different salivary gland carcinomas showing blood vessels (blue) and EGFR (red). A: tumour #1 showing membranous EGFR expression pattern. B: tumour #4 showing nuclear EGFR expression. Scale bars represent 100 µm.

However, to our knowledge, the oxygenation status of human salivary gland tumours has not been previously investigated. The current study is the first to provide actual data on oxygenation status and fails to demonstrate any significant hypoxia in salivary gland tumours. The number of tumours examined in this study is relatively small but given the fact that none of them demonstrated detectable levels of pimonidazole binding, it is unlikely that hypoxia is a relevant factor in this tumour type. The pimonidazole binding assay is a robust and widely used method for assessment of tissue hypoxia.¹⁴ In a previous study we analyzed 43 head and neck squamous carcinomas all of which showed some degree of pimonidazole binding with hypoxic fractions varying from 0.3% to 17.2% and a mean of 6.0%.¹⁵ High pimonidazole binding levels were associated with poor locoregional control and disease-free survival. It can be argued that the pimonidazole binding assay can yield false negative results if a tumour does not express sufficient levels of the nitroreductase enzymes that are required for binding of pimonidazole under hypoxic conditions. On the other hand, in all tumour types that have been investigated for hypoxia by this method thus far, pimonidazole binding was observed in a significant proportion of the tumours. This includes a wide range of histologies such as squamous cell carcinomas (head and neck, uterine cervix), adenocarcinomas (colorectal, breast, prostate), urothelial cell carcinomas (bladder), gliomas and sarcomas.¹⁶⁻¹⁹ This might indicate that nitroreductase deficiency, if it is a relevant limitation of the pimonidazole assay, is probably not so much linked to a specific histological tumour type.

The observation that pimonidazole negativity is accompanied by absence of CA-IX, glucose transporters and HIF-1 α supports the conclusion that hypoxia is an uncommon phenomenon in salivary gland tumours. As a survival response to hypoxia, tumour cells up-regulate CA-IX and glucose transporters.^{20,21} The switch from oxidative phosphorylation to anaerobic glycolysis in hypoxic tumour cells is accompanied by an increase in glucose requirements and transport which is mediated by the glucose transporters. CA-IX protects cells from intracellular acidification, thereby producing an acidic extracellular environment which is known to be associated with tissue hypoxia.²² The glucose transporters and CA-IX are under transcriptional control of HIF-1 α . It should be noted however, that they are not very specific markers of hypoxia because they also can be up-regulated by non-hypoxic stimuli. Also, tumours may lack the capacity for upregulation of these hypoxia-related proteins.

In vitro studies using salivary gland carcinoma cell lines have demonstrated that incubation under hypoxic conditions enhances the expression of HIF-1 α and VEGF in these cell lines.^{11,23} Consequently, it was suggested that hypoxia is a

driving force for angiogenesis and metastasis formation in salivary gland tumours. Our observations of absence of HIF-1 α in clinical tumour material, however, dispute the role of hypoxia as an important factor in the malignant progression of these tumours.

Salivary gland tumours are relatively rare and there exist many histological subtypes with different clinical behavior. Before strong and general conclusions can be drawn a larger series will need to be investigated. Nevertheless, the absence of detectable levels of both exogenous and endogenous hypoxia markers in all the tumours examined in the current study does not support the generic presence of hypoxia as observed in several other tumour types.

One possible explanation for the good oxygenation status might be the relatively slow growth rate that is characteristic not only for the low grade tumours but also for some of the high grade types. Under these circumstances angiogenesis can keep up with tumour expansion and the tumour is less likely to outgrow its vasculature. This is consistent with our observation of a much higher vascular density in the salivary gland tumours (median 285 mm⁻², range 209-546 mm⁻²) as compared to our measurements in squamous cell carcinomas (median 55 mm⁻², range 19-89 mm⁻²).²⁴ As a likely consequence, salivary gland tumours rarely exhibit necrosis.

An additional aim of this study was to investigate the relation between the proliferative activity of tumour cells and their oxygenation status. In previous work we have demonstrated that in squamous cell carcinomas of the head and neck a critical subpopulation of cells exists with clonogenic capacity under conditions of intermediate hypoxia.²⁵ These therapy resistant cells can be responsible for tumour regrowth and treatment failure. We questioned whether such a population of cells could be found in salivary gland tumours as well. Intermediate hypoxia is characterized by CA-IX positivity and pimonidazole negativity as pimonidazole binding occurs at pO₂ levels below 10 mmHg²⁶ whereas up-regulation of CA-IX may occur already at pO₂ levels from 20 mmHg and downward.²⁷ To identify proliferating cells we used the S-phase marker IdUrd. In addition we stained for EGFR because this membrane receptor has been linked to several critical components of mitogenic signalling pathways and has been demonstrated to be of prognostic significance in head and neck cancers.²⁸ We found varying levels of IdUrd labelling between the tumours and mostly moderate to high EGFR expression in absence of detectable levels of hypoxia. An interesting observation was the nuclear expression of EGFR in half of the tumour samples. Larger studies confirm the high rate of EGFR expression in malignant salivary gland tumours but have not described this nuclear expression pattern.^{29,30} Nuclear EGFR is

associated with increased treatment resistance and poor prognosis in oropharyngeal squamous cell carcinoma and breast cancer.^{31,32} It has been demonstrated that nuclear EGFR may function as a transcription factor activating genes required for cell proliferation and as a regulator of proliferating cell nuclear antigen (PCNA), an essential protein for DNA replication and damage repair.^{33,34} Furthermore, nuclear EGFR transport was linked with DNA-dependent protein kinase (DNA-PK) complex formation and activation, thus stimulating DNA damage repair after ionizing irradiation.³⁵ These observations might open a new field of research into the radiosensitivity properties of salivary gland tumours.

Conclusion

This is the first report in the literature on the oxygenation status of human salivary gland tumours. Absence of detectable pimonidazole binding, a robust and widely used method for assessment of tissue hypoxia, indicates that these tumours are generally well oxygenated. This is supported by lack of expression of the hypoxia-related proteins CA-IX, Glut-1, Glut-3 and HIF-1 α . Given these observations, it is unlikely that hypoxia is a clinically relevant factor in the aggressive behaviour and treatment resistance of malignant salivary gland tumours.

Acknowledgements

This study was supported by Dutch Cancer Society Grant KUN 98-1814.

References

1. Harris AL. Hypoxia--a key regulatory factor in tumour growth. *Nat Rev Cancer* 2002;2:38-47.
2. Le QT, Denko NC, Giaccia AJ. Hypoxic gene expression and metastasis. *Cancer Metastasis Rev* 2004;23:293-310.
3. Graeber TG, Osmanian C, Jacks T, *et al.* Hypoxia-mediated selection of cells with diminished apoptotic potential in solid tumours. *Nature* 1996;379:88-91.
4. Hoogsteen IJ, Marres HA, van der Kogel AJ, *et al.* The hypoxic tumour microenvironment, patient selection and hypoxia-modifying treatments. *Clin Oncol (R Coll Radiol)* 2007;19:385-396.
5. Vaupel P, Mayer A, Hockel M. Tumor hypoxia and malignant progression. *Methods Enzymol* 2004;381:335-354.
6. Vaupel P, Mayer A. Hypoxia in cancer: significance and impact on clinical outcome. *Cancer Metastasis Rev* 2007;26:225-239.
7. Kaanders JH, Bussink J, van der Kogel AJ. Clinical studies of hypoxia modification in radiotherapy. *Semin Radiat Oncol* 2004;14:233-240.
8. Schlingemann RO, Dingjan GM, Emeis JJ, *et al.* Monoclonal antibody PAL-E specific for endothelium. *Lab Invest* 1985;52:71-76.
9. Rijken PF, Bernsen HJ, van der Kogel AJ. Application of an image analysis system to the quantitation of tumor perfusion and vascularity in human glioma xenografts. *Microvasc Res* 1995;50:141-153.
10. Jakobsson PA, Eneroth CM. Variations in radiosensitivity of various types of malignant salivary-gland tumour. *Acta Otolaryngol Suppl* 1969;263:186-188.
11. Hara S, Nakashiro K, Klosek SK, *et al.* Hypoxia enhances c-Met/HGF receptor expression and signaling by activating HIF-1alpha in human salivary gland cancer cells. *Oral Oncol* 2006;42:593-598.
12. Lindsley KL, Cho P, Stelzer KJ, *et al.* Clinical trials of neutron radiotherapy in the United States. *Bull Cancer Radiother* 1996;83 Suppl:78s-86s.
13. Wambersie A, Hendry J, Gueulette J, *et al.* Radiobiological rationale and patient selection for high-LET radiation in cancer therapy. *Radiother Oncol* 2004;73 Suppl 2:S1-14.
14. Kleiter MM, Thrall DE, Malarkey DE, *et al.* A comparison of oral and intravenous pimonidazole in canine tumors using intravenous CCI-103F as a control hypoxia marker. *Int J Radiat Oncol Biol Phys* 2006;64:592-602.
15. Kaanders JH, Wijffels KI, Marres HA, *et al.* Pimonidazole binding and tumor vascularity predict for treatment outcome in head and neck cancer. *Cancer Res* 2002;62:7066-7074.
16. Hoskin PJ, Sibtain A, Daley FM, *et al.* The immunohistochemical assessment of hypoxia, vascularity and proliferation in bladder carcinoma. *Radiother Oncol* 2004;72:159-168.
17. Arcasoy MO, Amin K, Karayal AF, *et al.* Functional significance of erythropoietin receptor expression in breast cancer. *Lab Invest* 2002;82:911-918.
18. Rijken PF, Peters JP, Van der Kogel AJ. Quantitative analysis of varying profiles of hypoxia in relation to functional vessels in different human glioma xenograft lines. *Radiat Res* 2002;157:626-632.
19. Yuan H, Schroeder T, Bowsher JE, *et al.* Intertumoral differences in hypoxia selectivity of the PET imaging agent ⁶⁴Cu(II)-diacetyl-bis(N4-methylthiosemicarbazone). *J Nucl Med* 2006;47:989-998.
20. Lal A, Peters H, St Croix B, *et al.* Transcriptional response to hypoxia in human tumors. *J Natl Cancer Inst* 2001;93:1337-1343.
21. Zhang JZ, Behrooz A, Ismail-Beigi F. Regulation of glucose transport by hypoxia. *Am J Kidney Dis* 1999;34:189-202.
22. Sly WS, Hu PY. Human carbonic anhydrases and carbonic anhydrase deficiencies. *Annu Rev Biochem* 1995;64:375-401.
23. Ishibashi H, Shiratuchi T, Nakagawa K, *et al.* Hypoxia-induced angiogenesis of cultured human salivary gland carcinoma cells enhances vascular endothelial growth factor production and basic fibroblast growth factor release. *Oral Oncol* 2001;37:77-83.
24. Wijffels KI, Marres HA, Peters JP, *et al.* Tumour cell proliferation under hypoxic conditions in human head and neck squamous cell carcinomas. *Oral Oncol* 2008;44:335-344.
25. Hoogsteen IJ, Marres HA, Wijffels KI, *et al.* Colocalization of carbonic anhydrase 9 expression and cell proliferation in human head and neck squamous cell carcinoma. *Clin Cancer Res* 2005;11:97-106.
26. Raleigh JA, Zeman EM, Calkins DP, *et al.* Distribution of hypoxia and proliferation associated markers in spontaneous canine tumors. *Acta Oncol* 1995;34:345-349.

27. Wykoff CC, Beasley NJ, Watson PH, *et al.* Hypoxia-inducible expression of tumor-associated carbonic anhydrases. *Cancer Res* 2000;60:7075-7083.
28. Ang KK, Berkey BA, Tu X, *et al.* Impact of epidermal growth factor receptor expression on survival and pattern of relapse in patients with advanced head and neck carcinoma. *Cancer Res* 2002;62:7350-7356.
29. Vered M, Braunstein E, Buchner A. Immunohistochemical study of epidermal growth factor receptor in adenoid cystic carcinoma of salivary gland origin. *Head Neck* 2002;24:632-636.
30. Agulnik M, Cohen EW, Cohen RB, *et al.* Phase II study of lapatinib in recurrent or metastatic epidermal growth factor receptor and/or erbB2 expressing adenoid cystic carcinoma and non adenoid cystic carcinoma malignant tumors of the salivary glands. *J Clin Oncol* 2007;25:3978-3984.
31. Psyrri A, Yu Z, Weinberger PM, *et al.* Quantitative determination of nuclear and cytoplasmic epidermal growth factor receptor expression in oropharyngeal squamous cell cancer by using automated quantitative analysis. *Clin Cancer Res* 2005;11:5856-5862.
32. Lo HW, Xia W, Wei Y, *et al.* Novel prognostic value of nuclear epidermal growth factor receptor in breast cancer. *Cancer Res* 2005;65:338-348.
33. Lin SY, Makino K, Xia W, *et al.* Nuclear localization of EGF receptor and its potential new role as a transcription factor. *Nat Cell Biol* 2001;3:802-808.
34. Wang SC, Nakajima Y, Yu YL, *et al.* Tyrosine phosphorylation controls PCNA function through protein stability. *Nat Cell Biol* 2006;8:1359-1368.
35. Dittmann K, Mayer C, Kehlbach R, *et al.* The radioprotector Bowman-Birk proteinase inhibitor stimulates DNA repair via epidermal growth factor receptor phosphorylation and nuclear transport. *Radiother Oncol* 2008;86:375-382.

Chapter 8

General discussion

The aim of this study was to visualize and quantify biologic tumour characteristics relevant for radiation therapy resistance in head and neck cancer. We performed immunohistochemical staining of multiple endogenous and exogenous markers in a same tissue section. Visualization of these marker with preservation of the tissue architecture has improved our understanding of some of the pathophysiological aspects of the microenvironment of these tumours.¹⁻³

The method of computerized image analysis of immunohistochemical stainings provides an objective and quantitative assessment of marker expression and also allows quantitation of co-expression of multiple markers. This is an important step forward compared to the semiquantitative visual scoring that is most often used in this type of studies and which is subjective and prone to inter- and intra-observer variations. In addition, advanced quantitative analysis provides much more information than the mere expression level of markers.

We correlated these characteristics with patient outcome after radiation with the aim to explore their predictive potential. Predictive assays need to be distinguished conceptually from “prognostic factors”. The latter have been determined empirically and although they can be powerful predictors of treatment outcome, they simply indicate favorable or unfavorable response but they offer no basis for selecting possibly superior alternative treatments. A predictive assay on the other hand is mechanistically based, thereby offering the possibility of rational early interventions to improve therapeutic outcome. We demonstrated proof of principle of this in a pilot series of head and neck cancer patients.

Markers of hypoxia

As markers of hypoxia we used the exogenous marker pimonidazole and various endogenous markers such as CA-IX, HIF-1, Glut-1 and Glut-3. These markers demonstrated different expression patterns and also different associations with outcome. There are several reasons for this.

Pimonidazole hydrochloride was the only exogenous hypoxia marker used, it has a high water solubility and can be easily administered intravenously. It distributes rapidly into the tissues and the intracellular binding properties rise steeply at $pO_2 < 10$ mm Hg. The pimonidazole binding assay is a robust and widely used method for assessment of tissue hypoxia.⁴ These properties and the absence of any adverse effect make this agent attractive for clinical use.⁵⁻⁷ Pimonidazole binding was demonstrated in clinical tumours of various histologies such as squamous cell carcinomas (head and neck, uterine cervix), adenocarcinomas (colorectal, breast, prostate), urothelial cell carcinomas (bladder), gliomas and sarcomas.⁸⁻¹¹

The intravenous administration, the inability to investigate archived material and the cost of exogenous hypoxia markers are, however, limiting factors for their widespread application in the clinic. Attractive alternatives are therefore hypoxia-related proteins as potential endogenous markers. HIF-1 is the key regulator of oxygen homeostasis and in response to low oxygen conditions, it is known to transactivate more than 70 genes whose protein products function either to increase O₂ availability or to mediate metabolic adaptation to O₂ deprivation.¹²

Some studies demonstrated strong induction of HIF-1 α by hypoxia, but HIF-1 α induction is also shown to be dependent on other microenvironmental conditions such as glucose availability.^{13,14} Studies using immunohistochemistry and flow cytometry to compare HIF-1 α expression to pimonidazole binding in head and neck squamous cell carcinomas demonstrated no correlation between HIF-1 α expression and pimonidazole positive cells.^{14,15} Given the association between HIF-1 α expression and outcome, it is likely that HIF-1 α indicates tumour aggressiveness.^{16,17} It is however debatable whether it is also a reliable marker of tumour hypoxia.

Experiments with graded hypoxia in one cell line demonstrated CA-IX induction from pO₂ levels of approximately 20 mmHg and downward.¹⁸ Relative to pimonidazole binding, CA-IX expression was often observed at shorter distances from the vessels suggesting that CA-IX upregulation occurs at pO₂ levels higher than required for pimonidazole binding. This indicates that CA-IX expression identifies low tissue oxygenation levels as well as intermediate levels. Furthermore, the duration of hypoxia plays a role with the use of the various markers. The presence of pimonidazole for a period of 30 min is sufficient to stain all hypoxic areas¹⁹ whereas the upregulation of CA-IX requires at least several hours.²⁰ CA-IX is involved in intra- and extracellular pH homeostasis of tumour cells and thus, changes in the acid/base balance may provide additional stimuli for CA-IX expression.²¹

Also the glucose transporters are under transcriptional control of HIF-1. Their expression pattern is often described as “perinecrotic” indicating that they are associated with chronic hypoxia.^{22,23} However, expression of Glut-1 and Glut-3 not related to tissue hypoxia can also be observed as we demonstrated in Chapter 4. Up-regulation of glucose transporters is not specifically under hypoxic conditions and can also be the consequence of glucose starvation and reflecting the high, though inefficient, glucose metabolism in malignant tumours,

Because they are not exclusively regulated by hypoxia, these endogenous proteins are better called “hypoxia-associated” markers. We and others found different associations between these hypoxia-associated proteins and treatment

outcome and most probably their potential usefulness will be as prognosticators of tumour aggressiveness and less as predictors for response to oxygenation modifying treatments such as ARCON.

Clearly, pimonidazole is a more specific and robust marker of hypoxia and for that reason more likely to be an indicator of hypoxic radioresistance. This is supported by our observation that the pimonidazole assay was able to identify the patients that are most likely to profit from ARCON. If confirmed in a larger clinical study this would be an important step forward towards treatment customization.

The presence of hypoxia has been demonstrated in a variety of tumour types and all the squamous cell head and neck carcinomas investigated in this study showed at least some degree of pimonidazole binding indicating hypoxia. Interestingly, no hypoxia could be demonstrated in a less frequent type of head and neck cancers, i.e. salivary gland tumours. This information may be of relevance for the selection of future treatment strategies for this entity.

Vasculature

With our automated image processing system we analyzed complete tissue sections and the average number of vascular structures was calculated per mm² tumour area. This is different from “hot spot counting” where vessel counting is restricted to selected areas of high vascularity yielding what is general referred to as “microvascular density” (MVD). Measures of vascular density have been suggested as surrogate markers for tumour blood flow and/or oxygenation. Obviously there are important limitations to this because the organisation of the tumour vasculature is usually chaotic and functionally deficient.²⁴ This implicates that not all tumour blood vessels visualized by immunohistochemical endothelial markers are perfused. In addition, *if* the vessels are perfused oxygen exchange is not always optimal. This may explain why we found no correlations between the hypoxic fraction based on pimonidazole binding and vascular density (Chapter 3). Nevertheless we did find correlations with outcome and, as for hypoxic fraction, there was an indication that vascular density can predict response to ARCON. The underlying mechanism of this phenomenon remains to be elucidated.

Proliferation

Tumour cell proliferation is another important mechanism of radiotherapy resistance in head and neck cancer. Measurements of proliferative activity in tumours by single proliferation markers, endogenous (Ki-67, PCNA) or exogenous (iododeoxyuridine, bromodeoxyuridine), however, do not demonstrate consistent correlations with outcome.²⁵ Also here it is important to notice that markers have

different characteristics. We used the exogenous marker Iododeoxyuridine and the endogenous marker Ki-67. Iododeoxyuridine is a thymidine analogue and label only those cells that are actively synthesizing DNA. Ki-67, a nuclear antigen is expressed in all phases of the cell cycle except G₀.²⁶ A study by Wilson et al. demonstrated that not so much the proliferation index but the proliferative organization might be relevant for tumour behaviour and response to treatment.²⁷ They found the best local tumour control with proliferation patterns of the marginal type (proliferation in close relation with the vessels) while the outcome was progressively worse for the intermediate, mixed and random patterns. They gave as explanation that this might be due to differences in growth fraction, cell cycle time and cell loss rate. We were able to categorize a series of 50 head and neck tumours before and after transplantation in nude mice according to these proliferation patterns. An important observation was that the probability of growth after xenotransplantation was higher for tumours with high proliferative activity and high vascularity. Half of the tumours retained their proliferation patterns after transplantation. This clearly demonstrates that selection occurs when human tumours are xenotransplanted for preclinical research. It is likely that further selection will occur with subsequent passages. This raises concerns about the widely used experimental tumour lines that are often cultured in labs over many years. It can be questioned to what extent they are still representative for the clinical situation. In addition, if only one or few tumour lines are used in preclinical research this may not represent the variety of tumour characteristics encountered in the clinic. These considerations are of particular importance in settings of translational research where results from preclinical research should be transportable to clinical studies.

Co-registration of hypoxia and proliferative activity may identify an important subpopulation of tumour cells that is resistant to therapy while retaining clonogenic potential. These cells can escape cytotoxic treatment and give rise to tumour recurrence. In chapter 6 we therefore investigated the magnitude and clinical relevance of this population in a cohort of patients with head and neck carcinomas. Quantitative analysis of dual labelling by IdUrd and pimonidazole revealed that active DNA synthesis as measured by IdUrd labelling occurs only sporadically under hypoxic conditions. Also, no association was observed between the magnitude of this small cell population and outcome. However, Hoogsteen et al.²⁸ found that when dual staining with CA-IX and IdUrd was performed a larger population of cells could be identified which did show a significant correlation with the disease-free survival rate. This indicates that

indeed a critical subpopulation of cells may exist under conditions of intermediate hypoxia.

Future considerations

We demonstrated that our system of multiparameter analysis of tumour microenvironmental characteristics has potential as a predictive tool for the selection of patients for customized treatment. This must now be confirmed in a larger prospective clinical study. Not only single marker expression should be subject of investigation but especially marker combinations to provide a better understanding of interactions between treatment resistance mechanisms. This work is now ongoing at the department of Radiotherapy of the Radboud University Nijmegen Medical Centre using biopsy material from larynx cancer patients that have been treated in a randomized trial comparing ARCON against radiotherapy alone.

A limitation of this methodology is that it requires an advanced system for image processing and a certain level of expertise that is not available in all routine pathology labs. Another disadvantage is that only biopsies are examined, and not the complete tumour. Non-invasive techniques with repetitive capacity that image the whole tumour like PET scan or MRI are therefore very attractive. A limitation of these methods is that they are not able to show the relations between different biological features at the microregional level. Also, before they are introduced into clinical routine proper validation of these methods is required. In a collaboration between the departments of Radiotherapy and Nuclear Medicine preclinical and clinical studies are ongoing to validate PET tracers for hypoxia (^{18}F -fluoromisonidazole) and proliferation (^{18}F -fluorothymidine) against histopathology using the immunohistochemical markers pimonidazole and iododeoxyuridine.²⁹⁻³¹ It can be expected that the role of these imaging techniques will increase in future clinical studies.

Another field of research that is rapidly developing is gene expression profiling. This is another approach that may facilitate early detection of aggressive tumours and customization of therapeutic interventions.^{32,33} An important future direction of research will be to correlate gene expression patterns with the micro-environmental phenotypic features of tumours.

The more we learn about the diversity of tumours the more obvious it becomes that there is much to gain if we can categorize patients based on biological tumour characteristics to choose the appropriate treatment for them. Treatments for malignant diseases are continuously improving leading to higher cure rates and longer survival of cancer patients. However, these new approaches are often

accompanied by increased short- and long-term side effects. To provide the best attainable quality of life for individual patients and the cancer patient population as a whole, it is of increasing importance that tools be developed that allow a better selection of patients for these intensified treatments.

References

1. Rijken PF, Bernsen HJ, van der Kogel AJ. Application of an image analysis system to the quantitation of tumor perfusion and vascularity in human glioma xenografts. *Microvasc Res* 1995;50:141-153.
2. Bussink J, Kaanders JH, Rijken PF, *et al.* Multiparameter analysis of vasculature, perfusion and proliferation in human tumour xenografts. *Br J Cancer* 1998;77:57-64.
3. Bussink J, Kaanders JH, Rijken PF, *et al.* Vascular architecture and microenvironmental parameters in human squamous cell carcinoma xenografts: effects of carbogen and nicotinamide. *Radiother Oncol* 1999;50:173-184.
4. Kleiter MM, Thrall DE, Malarkey DE, *et al.* A comparison of oral and intravenous pimonidazole in canine tumors using intravenous CCI-103F as a control hypoxia marker. *Int J Radiat Oncol Biol Phys* 2006;64:592-602.
5. Kennedy AS, Raleigh JA, Perez GM, *et al.* Proliferation and hypoxia in human squamous cell carcinoma of the cervix: first report of combined immunohistochemical assays. *Int J Radiat Oncol Biol Phys* 1997;37:897-905.
6. Raleigh JA, Calkins-Adams DP, Rinker LH, *et al.* Hypoxia and vascular endothelial growth factor expression in human squamous cell carcinomas using pimonidazole as a hypoxia marker. *Cancer Res* 1998;58:3765-3768.
7. Varia MA, Calkins-Adams DP, Rinker LH, *et al.* Pimonidazole: a novel hypoxia marker for complementary study of tumor hypoxia and cell proliferation in cervical carcinoma. *Gynecol Oncol* 1998;71:270-277.
8. Hoskin PJ, Sibtain A, Daley FM, *et al.* The immunohistochemical assessment of hypoxia, vascularity and proliferation in bladder carcinoma. *Radiother Oncol* 2004;72:159-168.
9. Arcasoy MO, Amin K, Karayal AF, *et al.* Functional significance of erythropoietin receptor expression in breast cancer. *Lab Invest* 2002;82:911-918.
10. Rijken PF, Peters JP, Van der Kogel AJ. Quantitative analysis of varying profiles of hypoxia in relation to functional vessels in different human glioma xenograft lines. *Radiat Res* 2002;157:626-632.
11. Yuan H, Schroeder T, Bowsher JE, *et al.* Intertumoral differences in hypoxia selectivity of the PET imaging agent $^{64}\text{Cu}(\text{II})$ -diacetyl-bis(N4-methylthiosemicarbazone). *J Nucl Med* 2006;47:989-998.
12. Belozarov VE, Van Meir EG. Hypoxia inducible factor-1: a novel target for cancer therapy. *Anticancer Drugs* 2005;16:901-909.
13. Beasley NJ, Leek R, Alam M, *et al.* Hypoxia-inducible factors HIF-1 α and HIF-2 α in head and neck cancer: relationship to tumor biology and treatment outcome in surgically resected patients. *Cancer Res* 2002;62:2493-2497.
14. Vordermark D, Kraft P, Katzer A, *et al.* Glucose requirement for hypoxic accumulation of hypoxia-inducible factor-1 α (HIF-1 α). *Cancer Lett* 2005;230:122-133.
15. Janssen HL, Haustermans KM, Sprong D, *et al.* HIF-1A, pimonidazole, and iododeoxyuridine to estimate hypoxia and perfusion in human head-and-neck tumors. *Int J Radiat Oncol Biol Phys* 2002;54:1537-1549.
16. Aebbersold DM, Burri P, Beer KT, *et al.* Expression of hypoxia-inducible factor-1 α : a novel predictive and prognostic parameter in the radiotherapy of oropharyngeal cancer. *Cancer Res* 2001;61:2911-2916.
17. Koukourakis MI, Giatromanolaki A, Sivridis E, *et al.* Hypoxia-inducible factor (HIF1A and HIF2A), angiogenesis, and chemoradiotherapy outcome of squamous cell head-and-neck cancer. *Int J Radiat Oncol Biol Phys* 2002;53:1192-1202.
18. Wykoff CC, Beasley NJ, Watson PH, *et al.* Hypoxia-inducible expression of tumor-associated carbonic anhydrases. *Cancer Res* 2000;60:7075-7083.
19. Ljungkvist AS, Bussink J, Rijken PF, *et al.* Changes in tumor hypoxia measured with a double hypoxic marker technique. *Int J Radiat Oncol Biol Phys* 2000;48:1529-1538.
20. Lal A, Peters H, St Croix B, *et al.* Transcriptional response to hypoxia in human tumors. *J Natl Cancer Inst* 2001;93:1337-1343.
21. Ivanov S, Liao SY, Ivanova A, *et al.* Expression of hypoxia-inducible cell-surface transmembrane carbonic anhydrases in human cancer. *Am J Pathol* 2001;158:905-919.
22. Baer S, Casaubon L, Schwartz MR, *et al.* Glut3 expression in biopsy specimens of laryngeal carcinoma is associated with poor survival. *Laryngoscope* 2002;112:393-396.
23. Oliver RJ, Woodward RT, Sloan P, *et al.* Prognostic value of facilitative glucose transporter Glut-1 in oral squamous cell carcinomas treated by surgical resection; results of EORTC Translational Research Fund studies. *Eur J Cancer* 2004;40:503-507.

24. Vaupel P, Mayer A, Hockel M. Tumor hypoxia and malignant progression. *Methods Enzymol* 2004;381:335-354.
25. Wijffels KI, Kaanders JH, Marres HA, *et al.* Patterns of proliferation related to vasculature in human head-and-neck carcinomas before and after transplantation in nude mice. *Int J Radiat Oncol Biol Phys* 2001;51:1346-1353.
26. Gerdes J, Lemke H, Baisch H, *et al.* Cell cycle analysis of a cell proliferation-associated human nuclear antigen defined by the monoclonal antibody Ki-67. *J Immunol* 1984;133:1710-1715.
27. Wilson GD, Dische S, Saunders MI. Studies with bromodeoxyuridine in head and neck cancer and accelerated radiotherapy. *Radiother Oncol* 1995;36:189-197.
28. Hoogsteen IJ, Marres HA, Wijffels KI, *et al.* Colocalization of carbonic anhydrase 9 expression and cell proliferation in human head and neck squamous cell carcinoma. *Clin Cancer Res* 2005;11:97-106.
29. Troost EG, Laverman P, Kaanders JH, *et al.* Imaging hypoxia after oxygenation-modification: comparing [18F]FMISO autoradiography with pimonidazole immunohistochemistry in human xenograft tumors. *Radiother Oncol* 2006;80:157-164.
30. Troost EG, Vogel WV, Merks MA, *et al.* 18F-FLT PET does not discriminate between reactive and metastatic lymph nodes in primary head and neck cancer patients. *J Nucl Med* 2007;48:726-735.
31. Troost EG, Laverman P, Philippens ME, *et al.* Correlation of [(18)F]FMISO autoradiography and pimonidazole immunohistochemistry in human head and neck carcinoma xenografts. *Eur J Nucl Med Mol Imaging* 2008;35:1803-1811.
32. Schmalbach CE, Chepeha DB, Giordano TJ, *et al.* Molecular profiling and the identification of genes associated with metastatic oral cavity/pharynx squamous cell carcinoma. *Arch Otolaryngol Head Neck Surg* 2004;130:295-302.
33. Gorogh T, Weise JB, Holtmeier C, *et al.* Selective upregulation and amplification of the lysyl oxidase like-4 (LOXL4) gene in head and neck squamous cell carcinoma. *J Pathol* 2007; 212:74-82.

Chapter 9

Summary
Samenvatting
Dankwoord
Curriculum Vitae

Summary

Many efforts have been made to improve treatment outcome of patients with head and neck carcinomas. Important factors determining treatment response after radiation are hypoxia and proliferation.

Chapter 1 is an introductory chapter and briefly describes the history of the oxygen effect and the pathophysiology of tumour hypoxia. Two different types of hypoxia (perfusion-limited and diffusion-limited) are recognized. Endogenous and exogenous immunohistochemical hypoxia markers are discussed as well as non-invasive techniques to visualize and quantify hypoxia. Next, the relevance of tumour cell proliferation and immunohistochemical markers of proliferation are discussed. An outline of the thesis is provided, describing the general aims and outlines of the subsequent chapters.

Chapter 2 describes our first experience with the hypoxia marker pimonidazole in human tumour material. Twenty-one head and neck cancer patients were injected with pimonidazole. Frozen sections of twenty-two biopsies were stained for vessels and hypoxia and subsequently scanned and analyzed. The hypoxic fractions varied from 0.02-0.29 and were independent from other patient and tumour characteristics. Three different hypoxia patterns were described. The first type contained large viable hypoxic areas at large ($> 200 \mu\text{m}$) distance from the vessels. The second category showed a band-like distribution of hypoxia at an intermediate distance 50-200 μm . The third category showed hypoxia within 50 μm from the vessels, indicating acute hypoxia. We demonstrated the clinical feasibility of this quantitative method for multiparameter analysis of vascularity and hypoxia in head and neck tumours.

In *chapter 3* we analyzed forty-three tumour biopsies from patients with head and neck tumours. All patients were potential candidates for a phase II trial with accelerated radiotherapy combined with carbogen and nicotinamide (ARCON). Tissues were stained for blood vessels, pimonidazole and CA-IX. The distribution patterns of both hypoxia markers were similar, although the CA-IX signal was generally observed at shorter distance from the vessels. There was a weak but significant correlation between the relative tumour areas positive for pimonidazole binding and areas with CA-IX expression. The 2-year locoregional control rates were 48 versus 87% for tumours with high and low pimonidazole binding levels ($p=0.01$) and 48 and 88% for tumours with low and high vascular density ($p=0.01$). These associations disappeared in the subgroup of patients treated with ARCON. The level of CA-IX expression had no relationship with treatment outcome. We concluded that pimonidazole binding and vascular density are predictors of

treatment outcome in head and neck carcinomas. Pimonidazole and CA-IX demonstrate concordant staining patterns, however, CA-IX is less specific for hypoxia.

Chapter 4 describes the prognostic value of different endogenous hypoxia-related markers CA-IX, Glut-1 and Glut-3 in patients treated with ARCON. We examined tumour biopsies of 58 patients with head and neck carcinomas treated with ARCON. All sections were stained for CA-IX, Glut-1 and Glut-3. CD-34 was used as an endothelial marker to assess microvascular density. Sections were scored for relative tumour area stained by the markers (CA-IX and Glut-3) and for the intensity of the staining (Glut-1 and Glut-3). Both CA-IX and Glut-3 were observed at some distance from vessels and adjacent to necrosis. Glut-1 staining was more diffuse. Patients with a high CA-IX positivity (>25% of tumour area) had a significantly better locoregional control ($p=0.04$) and freedom of distant metastases ($p=0.02$). High Glut-3 expression was associated with a better locoregional control ($p=0.04$). Higher Glut-1 intensity was associated with an increased rate of distant metastases ($p=0.0005$) and a worse overall survival ($p=0.001$). We concluded that the inconsistent associations with outcome of CA-IX and the glucose transporters indicates that different factors play a role in up-regulation of these markers.

Chapter 5 describes different proliferation patterns in human tumour samples and quantitative categorization based on these patterns. Also, it was examined whether these characteristics were retained after xeno-transplantation. Fifty tumour samples from head and neck cancer patients were immunohistochemically stained for Ki-67 and vessels. Also, parts of the samples were transplanted into nude mice. Vascular and proliferation patterns were analyzed using an image processing system. The 50 tumours were categorized into four patterns of proliferation by visual assessment: marginal (6), intermediate (10), random (21) and mixed (12). One tumour could not be classified. These patterns were quantified by calculating the Ki-67 labelling index in distinct zones at increasing distance from vessels yielding good discrimination and significant differences between patterns. We found that the probability of growth after xeno-transplantation was significantly higher for tumours with a labelling index and vascular density above the median value compared to tumours with both parameters below the median (82% vs. 35%). Fifty percent of the tumours retained their proliferation patterns after xeno-transplantation. We concluded that the combination of quantitative and architectural information of multiple microenvironmental parameters adds a new dimension to the study of treatment resistance mechanisms. Tumour models representative of the various patterns

can therefore be used to further investigate the relevance of these architectural patterns.

In *chapter 6* we examined a subpopulation of tumour cells in human head and neck cancers that retain clonogenic potential under hypoxic conditions. The markers iododeoxyuridine and pimonidazole were administered intravenously prior to biopsy taking in patients with stage II-IV squamous cell carcinoma of the head and neck. Triple immunohistochemical staining of blood vessels, IdUrd and pimonidazole was performed and co-localization of IdUrd and pimonidazole was quantitatively assessed by computerized image analysis. The results were related with treatment outcome. Thirty-nine biopsies were analyzed. Tumours exhibited different patterns of proliferation and hypoxia but generally the IdUrd signal was found in proximity to blood vessels whereas pimonidazole binding was predominantly at a distance from vessels. Overall, no correlations were found between proliferative activity and oxygenation status. The fraction of IdUrd-labelled cells positive for pimonidazole ranged from 0% to 16.7% with a mean of 2.4% indicating that proliferative activity was low in hypoxic areas and occurring mainly in the well-oxygenated tumour compartments. IdUrd positive cells in hypoxic areas made up only 0.09% of the total viable tumour cell mass. There were no associations between the magnitude of this cell population and local tumour control or survival.

Chapter 7 deals with salivary gland tumours. Twelve patients planned for surgical resection of a salivary gland tumour were preoperatively injected with pimonidazole and iododeoxyuridine. Tissue samples of the dissected tumour were immunohistochemically stained for blood vessels, pimonidazole, carbonic anhydrase-IX, the glucose transporters-1 and -3, hypoxia-inducible factor-1 α , IdUrd and for the epidermal growth factor receptor. Tissue material from 8 patients was of sufficient quality for quantitative analysis. All tumours were negative for pimonidazole binding as well as for CA-IX, Glut-1, Glut-3 and HIF-1 α . Vascular density was high with a median value of 285 mm⁻² (range 209 – 546 mm⁻²). IdUrd labelling index varied from <0.1% to 12.2% with a median of 2.2%. EGFR expression levels were mostly moderate to high. In half of the cases nuclear expression of EGFR was observed. We concluded that the absence of detectable pimonidazole binding, as well as the lack of expression of hypoxia-associated proteins in all analyzed tumours indicates that malignant salivary gland tumours are generally well oxygenated. It is therefore unlikely that hypoxia is a relevant factor for their clinical behavior and treatment responsiveness.

Samenvatting

De laatste jaren is veel moeite gedaan om de behandelingsuitkomst van patiënten met een hoofd-hals tumor te verbeteren. Belangrijke factoren die het resultaat van een bestraling beïnvloeden zijn een tekort aan zuurstof (hypoxie) en de mate van celdeling (proliferatie).

Hoofdstuk 1 is een inleidend hoofdstuk, en geeft een beknopte beschrijving van het zuurstof effect en de pathofysiologie van tumor hypoxie. Twee verschillende soorten van hypoxie (perfusie-gelimiteerd en diffusie-gelimiteerd) worden onderscheiden. Endogene en exogene immunohistochemische hypoxiemarkers worden besproken, evenals de verschillende niet-invasieve methoden om hypoxie aan te tonen en te kwantificeren. Vervolgens wordt de relevantie van tumor cel proliferatie en immunohistochemische proliferatie markers besproken. Hierna wordt kort het doel en de studie opzet per hoofdstuk vermeld.

Hoofdstuk 2 beschrijft de eerste studie die we hebben verricht met de hypoxie marker pimonidazol in humaan tumor weefsel. Eenentwintig patiënten met een hoofd-hals tumor werden geïnjecteerd met pimonidazol. Vriescoupes van tweeëntwintig bipten werden gekleurd voor vaten en hypoxie en vervolgens gescand en geanalyseerd. De hypoxische fracties varieerden van 0.02-0.29 en waren onafhankelijk van andere patiënt- en tumor karakteristieken. Drie verschillende patronen van hypoxie werden beschreven. Het eerste type bevatte grote vitale hypoxische gebieden op ruime afstand van de vaten (>200 μm). De tweede categorie toonde een lijnvormige verdeling van hypoxie op een middelgrote afstand van de vaten (50-200 μm). De laatste categorie toonde hypoxie binnen 50 μm van de vaten, duidend op acute hypoxie. We toonden de klinische toepasbaarheid van deze kwantitatieve methode aan voor multi-parameter analyse van vasculariteit en hypoxie in hoofd-hals tumoren.

In *hoofdstuk 3* hebben we 43 tumor bipten van patiënten met een hoofd-hals tumor onderzocht. Alle patiënten waren potentiële kandidaten voor een fase 2 onderzoek waarbij versnelde bestraling met carbogeen en nicotinamide werd gecombineerd (ARCON). De bipten werden gekleurd voor vaten, pimonidazol en CA-IX. De verdelingspatronen van beide hypoxische markers was vergelijkbaar, hoewel het CA-IX signaal meestal dicht bij de vaten lag. Er was een kleine, maar significante correlatie tussen de relatieve tumor oppervlakten positief voor pimonidazol en de gebieden met CA-IX aankleuring. De locoregionale tumor vrije controle na 2 jaar bedroeg 48 versus 87% voor tumoren met een hoge danwel lage pimonidazol aankleuring ($p=0.01$) en 48 en 88% voor tumoren met een lage en hoge vaatdichtheid ($p=0.01$). Deze verschillen verdwenen in de groep

patiënten die behandeld was met ARCON. De mate van de CA-IX kleuring had geen relatie met de behandelingsuitkomst. We concludeerden dat pimonidazol binding en vaatdichtheid een voorspellende waarde hebben in de behandelingsuitkomst bij patiënten met een hoofd-hals tumor. Pimonidazol en CA-IX tonen vergelijkbare kleuringspatronen, hoewel CA-IX minder specifiek hypoxie aankleurt.

Hoofdstuk 4 beschrijft de voorspellende waarde van verschillende endogene hypoxie gerelateerde markers CA-IX, Glut-1 en Glut-3 in met ARCON behandelde patiënten. We onderzochten 58 tumorbipten van patiënten met hoofd-hals tumoren die met ARCON behandeld waren. Alle coupes werden gekleurd met CA-IX, Glut-1 en Glut-3. Voor de vaatdichtheid werd CD-34 als endotheelmarker gebruikt. Tevens werd gekeken naar het door de markers aangekleurde relatieve tumor oppervlakte (CA-IX en Glut-3) en naar de intensiteit van de kleuring (Glut-1 en Glut-3). Zowel CA-IX als Glut-3 werden voornamelijk gezien op grote afstand van de vaten en dicht bij necrose. De Glut-1 kleuring was meer diffuus verspreid. Patiënten met meer CA-IX aankleuring ($> 25\%$ van de tumoroppervlakte) hadden een significant betere locoregionale controle ($p=0.04$) en afwezigheid van afstandsmetastasen ($p=0.02$). Een hogere expressie van Glut-3 was eveneens geassocieerd met een betere locoregionale controle ($p=0.04$). Een sterke Glut-1 intensiteit was geassocieerd met toename van afstandsmetastasen ($p=0.0005$) en een slechte overleving ($p=0.001$). We concludeerden dat de verschillende uitkomsten voor CA-IX en glucose transporters in relatie met tumor controle impliceren dat er meerdere factoren een rol spelen in de op-regulatie van deze markers.

Hoofdstuk 5 beschrijft verschillende proliferatiepatronen in humane tumoren, alsmede de kwantitatieve categorisatie gebaseerd op deze patronen. We onderzochten in hoeverre deze karakteristieken bewaard bleven na xeno-transplantatie. Vijftig tumor bipten van patiënten met een hoofd-hals tumor werden immuno-histochemisch gekleurd voor Ki-67 en vaten. Van de bipten werd een deel in naakte muizen geïmplanteerd. Tumoren werden gecategoriseerd in 4 proliferatiepatronen. De verschillende vaat- en proliferatiepatronen werden geanalyseerd gebruik makend van een beeldverwerkingsysteem. De vier verschillende proliferatiepatronen waren: marginaal (6), intermediair (10), diffuus (21) en gemengd (12). Eén tumor kon niet worden geclassificeerd. Deze patronen werden gekwantificeerd door de Ki-67 labeling index te berekenen per zone op toenemende afstand van de vaten. Hierbij vonden we een goed onderscheid en significante verschillen tussen de patronen. De kans op groei na implantatie in de muis was significant hoger voor tumoren met een labeling index en vaatdichtheid

boven de mediaan in vergelijking met tumoren waarbij deze waarden onder de mediaan lagen (82-35%). Vijftig procent van de tumoren behield het proliferatiepatroon na xeno-transplantatie. We concludeerden dat de combinatie van kwantitatieve en architectonische informatie over vaten en proliferatie een bijdrage kan leveren in het onderzoek naar bestralingsreacties. Het belang van de verschillende patronen moet nog nader onderzocht worden.

Hoofdstuk 6 beschrijft een studie naar een subpopulatie van tumor cellen in hoofd-hals kanker, die de mogelijkheid tot celdeling onder hypoxische omstandigheden behouden. Hiervoor werden bij patiënten met een stadium II-IV hoofd-hals plaveiselcelcarcinoom de markers iododeoxyuridine en pimonidazol intraveneus toegediend. Negenendertig bipten werden gekleurd op vaten, IdUrd en pimonidazol. Vervolgens werd co-lokalisatie van IdUrd en pimonidazole met behulp van de computer gekwantificeerd. Het resultaat hiervan werd aan de behandeluitkomst gerelateerd. De tumoren toonden verschillende patronen van proliferatie en hypoxie, maar IdUrd labeling werd vooral gevonden in de buurt van de vaten, terwijl pimonidazol binding zich voornamelijk op afstand van de vaten bevond. Over het algemeen was er geen correlatie tussen proliferatieve activiteit en de oxygenatie-toestand van een tumor. De fractie IdUrd gelabelde cellen positief voor pimonidazol varieerde van 0% tot 16.7% met een gemiddelde van 2.4%. De proliferatieve activiteit was laag in hypoxische gebieden en kwam voornamelijk voor in de goed geoxigeneerde tumor velden. IdUrd positieve cellen in hypoxische gebieden bedroegen slechts 0.09% van het totale aantal vitale tumorcellen. Er was geen verband tussen de hoogte van deze celpopulatie en lokale tumor controle of overleving.

Hoofdstuk 7 beschrijft een studie bij speekselkliertumoren. Twaalf patiënten met een geplande resectie van een speekselkliertumor werden preoperatief geïnjecteerd met pimonidazol en iododeoxyuridine. Weefselstukjes van de verwijderde tumor werden immunohistochemisch gekleurd op bloedvaten, pimonidazol, carbon anhydrase-IX, glucose transporters-1 en -3, hypoxia-inducible factor-1 α , IdUrd en voor epidermale groei factor receptor. Weefsel van 8 patiënten was van voldoende kwaliteit voor verdere analyse. Geen van de tumoren toonde aankleuring voor pimonidazol, CA-IX, Glut-1, Glut-3 en HIF-1 α . De vaatdichtheid was hoog met een mediaan van 285 mm⁻² (spreiding 209-546 mm⁻²). IdUrd labeling index varieerde van <0.1% tot 12.2% met een mediaan van 2.2%. De EGFR expressie was voornamelijk gemiddeld tot hoog. In de helft van de gevallen werd een kernkleuring waargenomen. We concludeerden dat de afwezigheid van aantoonbare pimonidazol binding, evenals het ontbreken van aan hypoxie gerelateerde eiwitten in alle onderzochte tumoren, aantoont dat maligne

speekselkliertumoren over het algemeen goed geoxygeneerd zijn. Het is daarom onwaarschijnlijk dat hypoxie bij speekselkliertumoren een relevante rol speelt in het klinisch gedrag en behandeluitkomst.

Dankwoord

Een wetenschapper ben ik van huis uit niet, dat dit onderzoek uiteindelijk toch heeft geresulteerd in een proefschrift, is zeker niet alleen voor mij een verrassing. Hierbij wil ik alle patiënten bedanken voor hun medewerking. Daarnaast wil ik iedereen bedanken die de afgelopen jaren tot steun is geweest, in wetenschappelijk of sociaal opzicht. Enkele personen wil ik echter nadrukkelijk bedanken.

Prof. Dr. J.H.A.M. Kaanders, beste Hans. Zonder jou, geen proefschrift. Het is ongeloofelijk wat jij uit zo'n scherp geslepen potloodje kunt toveren. Bedankt voor je vertrouwen en je geduld. Ook in diplomatiek oogpunt kan ik veel van je leren.

Prof. Dr. H.A.M. Marres, beste Henri. Jij zei tegen mij: "Er is meer in het leven dan promoveren". Bedankt dat ik de kans kreeg om deze promotie af te ronden zonder "de rest van het leven" tekort te doen. Bij de volgende SNK drinken we er samen een borrel op.

Prof. Dr. A.J. van der Kogel, beste Bert. Ik bewonder je enthousiasme voor de wetenschap en je geduld waarmee je de biologische raadsels van menselijke tumoren probeert op te lossen. Helaas is geduld niet een van mijn sterkste eigenschappen.

Hans, Ankie, Jasper en Wendy, bedankt voor jullie tips en trics in de immunohistochemie. Jullie hulp in het lab was altijd laagdrempelig en accuraat. Ankie, bedankt voor al je gezelligheid en relativeringsvermogen.

Paul, zonder jouw beeldverwerking, geen data. Fijn dat ik al die keren ad hoc je computertechnische ondersteuning heb gekregen. Bedankt voor je hulp.

Prof. Dr. K. Graamans, beste Kees. Ik wil je bedanken voor al je inzet om de opleiding tot KNO-arts up to date te maken. Er is veel ten goede veranderd.

Prof. Dr. C.W.R.J. Cremers. Ik zat niet in uw trein. Ik wil u echter bedanken voor al uw trouwe reacties. Bij ieder huwelijk, geboorte, ziekte van een van de arts-assistenten was u er altijd als eerste bij.

Overige opleiders, ik heb veel geleerd, en gelachen. Bedankt voor de leuke tijd in het Radboud, CWZ en in het Rijnstate.

(Oud) arts-assistenten, wat was het heerlijk om tijdens de experimenten door even op de KNO te koepelen. Bedankt voor de gezelligheid. Het spreekwoord gedeelde smart is halve smart geldt bij de KNO wat betreft promoveren zeker.

KNO-vakgroep Deventer, wat heb ik een geluk dat ik samen met jullie in de maatschap zit. Wat super dat jullie mij de kans hebben gegeven mijn promotie af te ronden. Mijn/onze tent is top!

Carin en Joost, wat een mazzel dat ik zulke fijne schoonouders heb! Wat super dat jullie altijd klaar staan om ons te helpen, wanneer nodig.

Pappie en mammië, ik bof met zulke ouders! Bedankt voor al jullie onvoorwaardelijke liefde en hulp voor mij en mijn gezin. Bedankt ook voor al die jaren dat jullie mij hebben gesteund in mijn plannen en wensen. Wat ze in d'r kop heeft.....

Geerte, Joep en Tom, lieverdjes, jullie mogen nu eindelijk op mamma's computer K3- en Bob de Bouwer spelletjes spelen. Ik geniet enorm van jullie drieën.

Lieve Nils, mijn steun en toeverlaat! Je bent een supervent, een heerlijke man en fantastische vader. Je weet als geen ander hoe druk soms een gezin, baan en promotie kan zijn. Ik hoop dat ik jou hierin net zoveel kan steunen zoals jij de afgelopen tijd voor mij hebt gedaan. Op naar Zermatterhof!

Karien Irène Eugenie Marie Wijffels werd geboren op 6 september 1970 in Nijmegen. Het VWO-diploma werd behaald aan het Mencia de Mendoza lyceum te Breda in 1989. In hetzelfde jaar startte zij met de studie geneeskunde aan de Rijksuniversiteit van Leiden. Het artsexamen werd in 1997 cum-laude behaald. Er volgde een kortstondige aanstelling als AGNIO heekunde in het LUMC. In 1998 werd bij de afdeling radiotherapie in het Radboud ziekenhuis aangevangen met het onderzoek dat ten grondslag ligt aan dit proefschrift. In maart 2000 werd in Nijmegen gestart met de opleiding tot keel, neus en oor-arts, waarop in 2005 haar registratie tot KNO-arts volgde. Zij is gevestigd KNO-arts in het Deventer ziekenhuis.

Karien Wijffels is getrouwd met Nils Vogtländer, samen hebben ze drie kinderen Geerte (2002), Joep (2004) en Tom (2006).

Publication of this thesis was financially supported by:
Alk-Abelló, Artu, Atos medical, Beter horen, Ed Dellink, Entemed, Glaxo Smith Kline,
Meditop, Ooms allergie, Raadgevers Kuijkhoven, Schering-Plough, Schoonenberg,
Specsavers, Stallergenes, Stegeman hoortechniek, Tefa-portanje, NSvG

